

https://dspace.org/

A comparison of performance and emissions characteristics of an engine fuelled on DME and on diesel with particular interest on injection characteristics

Lopes, Renato

2010-02-02T08:17:52Z
http://hdl.handle.net/10539/7494

Downloaded from a DSpace repository. https://dspace.org/

Declaration

I declare that this report is my own, unaided work, except where otherwise acknowledged. It is being submitted in partial fulfillment of the requirements for the degree M.Sc. (Mech. Eng.) in the University of the Witwatersrand, Johannesburg. It has not been submitted for any degree or examination at any other University.

Signed this day _____ of _____ 2009

_____

Renato Lopes

Abstract

This report contains the results of tests conducted on a compression ignition engine which was fuelled on both DME and diesel. The results compare the performance and emissions characteristics of the two fuels. As an addition to the existing test cell setup, an injector lift sensor was added in order for the injection characteristics to be monitored. It was established that the engine requires more fuel when running on DME than on diesel in order to obtain the same power output. This is because DME has a lower heating value as well as density than diesel. DME CO_2 emissions were higher than diesel, while DME CO emissions were lower than diesel. The NOx emissions for DME were higher than diesel at lower engine speeds, and then lower than diesel at higher engine speeds. It is suspected that the DME emissions are negatively affected by later injection of DME than diesel injection as well as longer duration of injection for DME than for diesel as this may result in incomplete combustion of fuel.

Acknowledgements

I would like to thank Dr. D Cipolat for his help and instruction during the course of this project.

Contents

Declaration i
Abstract ii
Acknowledgements iii
Contents iv
List of Figures vii
List of Tables ix
1. Introduction 11
1.1. The Internal Combustion Engine 11
1.2. Motivation behind Alternate Fuels Research 11
1.2.1. What are Greenhouse Gases? 12
1.2.2. What is the Greenhouse Effect? 13
1.3. Exhaust Emissions Standards 15
2. Literature Review 16
2.1. DME as an Alternative to diesel 16
2.2. Previous Studies on DME as an Alternative to Diesel 18
2.3. Mechanisms Controlling Diesel Combustion 19
2.3.1. Fuel Injection Systems 19
2.4. Injection Characteristics 21
2.4.1. Fuel Mass Flow Rate 21
2.4.2. Fuel Spray Behaviour 22
2.5. Pollutant Formation and Control 29
2.5.1. The Combustion Process 29
2.5.2. Nitrogen Based Emissions 29
2.5.3. Carbon Based Emissions 30
3. Objectives 31
4. Experimental Facilities 32
4.1. The Compression Ignition Engine 32
4.2. The Dynamometer 34
4.3. Fuel System 35
4.3.1. Fuel Supply System 35
4.3.2. Fuel Pumps and Injectors 36
4.4. Low Pressure DME Rig 36

4.4.1. Controller 38
4.5. Engine Cooling 40
4.6. Instrumentation 41
4.6.1. Cylinder Pressure 41
4.6.2. Ambient Pressure 41
4.6.3. Fuel Line Pressure 41
4.6.4. Air Flowrate 42
4.6.5. Fuel Flowrate 42
4.6.6. Exhaust Temperature 42
4.6.7. Crank Angle and Speed 42
4.6.8. Injector Needle Lift 42
4.7. Gas Analyser 43
5. Experimentation 44
5.1. Approach 44
5.2. Procedure 44
5.2.1. Pre-Testing Procedure 44
5.2.2. Testing Procedure 45
5.3. Precautions 46
5.3.1. Equipment Precautions 46
5.3.2. Testing Procedure Precautions 47
6. Results and Discussion 48
6.1. Engine Performance 48
6.1.1. Introduction 48
6.1.2. Analysis 48
6.2. Injection Characteristics 51
6.2.1. Introduction 51
6.2.2. Error Analysis 55
6.2.3. Analysis 56
6.3. Emissions 73
6.3.1. Introduction 73
6.3.2. Analysis 74
7. Conclusions 77
8. Recommendations 78
9. References 79
A Appendix – Calibration 81

A.1 Fuel Flow Calibration 81
A.2 Dynamometer Calibration 82
A.3 Speed Calibration 84
A.4 Air Flow Calibration 84
A.5 Ambient Air Thermocouple Calibration 85
A.6 Air Intake Thermocouple Calibration 86
A.7 Injector Needle Lift Sensor Calibration 88
A.8 Equipment Specification 89
B Appendix – Signal Gas Analyser Procedure 91
B.1 Start up Procedure 91
B.2 Analyser Requirements and Gas Cylinder Contents 92
B.3 Calibration Procedure 92
B.4 Variable Ranges For Each Analyser 94
B.5 Notes 96
B.6 Problems With Calibration 97
B.7 Shut Down 97
C Appendix - Data Acquisition Procedure 99
C.1 Performance Data Set-up 99
C.2 Emissions Data Set-up 101
D Appendix – Low Pressure DME Rig Procedure 102
E Appendix – Program Flow Diagram 103
F Appendix – Raw Data 104
F.1 DME Data 104
F.2 Injector Lift Data 105
F.3 Injector Pressure Data 108
F.4 Performance Data 111
F.5 Specific Fuel Flow Data 115
F.6 Low Pressure DME 116
F.7 High Pressure DME 119
F.8 Diesel 122

List of Figures

Figure 1: The Carbon Cycle; all values have units of gigatons of carbon [4] 14
Figure 2: EU Emission Standards for Passenger Cars (Category M_1*), g/km [5] 15
Figure 3: Dimethyl Ether Molecular Structure [18] 16
Figure 4: Diesel Fuel Spray [1] 22
Figure 5: Variation of Droplet Characteristics [1] 24
Figure 6: Engine Test Cell Schematic [17] 32
Figure 7: Lister Petter Engine 33
Figure 8: Dynamometer 34
Figure 9: Low Pressure DME Rig 35
Figure 10: Low Pressure DME Rig Schematic [16] 38
Figure 11: Control PC Screenshot 39
Figure 12: Instrumentation Wiring Diagram [19] 40
Figure 13: Signal Gas Analyser 43
Figure 14: Pressure trace 49
Figure 15: Energy Released vs. Crank Angle 50
Figure 16: Rate of Heat Transfer vs. Crank Angle 51
Figure 17: Injector Lift vs. Crank Angle 56
Figure 18: Injection Duration vs. Engine Speed 57
Figure 19: Injector Lift vs. Engine Speed 58
Figure 20: Oscillations of injector needle 59
Figure 21: Angle of Start of Injection vs. Engine speed 62
Figure 22: Fuel Line Pressure vs. Crank Angle 63
Figure 23: Fuel Line Pressure Change vs. Engine Speed 64
Figure 24: Specific Fuel Flow vs. Engine Speed at 25 Nm 70
Figure 25: Specific Fuel Flow vs. Engine Speed at 35 Nm 71
Figure 26: Specific Fuel Flow vs. Engine Speed at 45 Nm 72
Figure 27: Specific NOx vs Engine Speed 74
Figure 28: Specific CO_2 vs Engine Speed 75
Figure 29: Specific CO vs Engine Speed 76
Figure 30: Fuel Flow Calibration 82
Figure 31: Dynamometer Calibration Curve 83
Figure 32: Airflow Calibration Curve 85

Figure 33: Ambient Air Thermocouple Calibration Curve 86
Figure 34: Air Intake Thermocouple Calibration Curve 87
Figure 35: Injector Needle Lift Sensor Calibration Curve 89
Figure 36: Controller program flow diagram 103

List of Tables

Table 1: The Automotive Urban-Air Pollution Problem [1] 13
Table 2: DME and Diesel fuel properties [9] 17
Table 3: Examples of Formulation Constants 25
Table 4: Engine Specifications 33
Table 5: Dynamometer Specifications 34
Table 6: Fuel Flow Calibration Data 81
Table 7: Dynamometer Calibration data 83
Table 8: Speed Calibration Data 84
Table 9: Airflow Calibration Data 84
Table 10: Ambient Air Thermocouple Calibration Data 85
Table 11: Air Intake Thermocouple Calibration Data 86
Table 12: Injector Needle Lift Sensor Calibration Data 88
Table 13: Thermocouple Specifications 89
Table 14: Pressure Transducer Specification 90
Table 15: Rotameter Specifications 90
Table 16: Gas Cylinder Contents 92
Table 17 - Variable Ranges for CO_2 Analyser 94
Table 18 - Variable Ranges for CO Analyser 94
Table 19 - Variable Ranges for THC Analyser 95
Table 20 - Variable Ranges for NOx Analyser 95
Table 21 - Fuel Type Coding Description 100
Table 22: DME Physical Properties at a Low Pressure and Varying Temperature Range 104
Table 23: DME Physical Properties at a High Pressure and Varying Temperature Range 104
Table 24: DME Physical Properties at Increasing Pressure 105
Table 25: Injector Lift Data for diesel at 25 N.m 105
Table 26: Injector Lift Data for diesel at 35 N.m 106
Table 27: Injector Lift Data for DME at 25 N.m 106
Table 28: Injector Lift Data for DME at 35 N.m 106
Table 29: Percentage Differences in Injector Needle Lift Duration and Start of Injector Needle Lift at 25 N.m for the two fuels 107

Table 30: Percentage Differences in Injector Needle Lift Duration and Start of Injector Needle Lift at 35 N.m for the two fuels 107
Table 31: Percentage Differences in Injector Needle Lift for the same fuel at different torques 107
Table 32: Injector Pressure Data for diesel at 25 N.m 108
Table 33: Injector Pressure Data for diesel at 35 N.m 108
Table 34: Injector Pressure Data for DME at 25 N.m 109
Table 35: Injector Pressure Data for DME at 35 N.m 109
Table 36: Percentage Differences in the Injector Pressure Difference and Start of Injector Pressurisation at 25 N.m for the two fuels 109
Table 37: Percentage Differences in the Injector Pressure Difference and Start of Injector Pressurisation at 35 N.m for the two fuels 110
Table 38: Overall Performance Data for diesel at 25 N.m 111
Table 39: Overall Performance Data for diesel at 35 N.m 112
Table 40: Overall Performance Data for DME at 25 N.m 113
Table 41: Overall Performance Data for DME at 35 N.m 114
Table 42: Average Specific Fuel Flow and Ratio between Averages 115
Table 43: Overall Results for 25 Nm LP DME 116
Table 44: Overall Results for 35 Nm LP DME 117
Table 45: Overall Results for 45 Nm LP DME 118
Table 46: Overall Results for 25 Nm HP DME 119
Table 47: Overall Results for 35 Nm HP DME 120
Table 48: Overall Results for 45 Nm HP DME 121
Table 49: Overall Results for 25 Nm diesel 122
Table 50: Overall Results for 35 Nm diesel 123
Table 51: Overall Results for 45 Nm diesel 124

1. Introduction

1.1. The Internal Combustion Engine

The purpose of internal combustion engines is the production of mechanical power by harnessing the chemical energy contained in a fuel. In internal combustion engines, as is distinct from external combustion engines, this energy is released by burning or oxidising the fuel inside the engine [1].

There exist two types of internal combustion engines, namely the spark ignition engine (also known as the Otto engine), and the compression ignition engine (also known as the diesel engine), both of which are reciprocating type engines. The existence of the spark ignition engine dates back to 1876 when Nicolaus Otto developed it, while the compression ignition engine dates back to 1892 when it was invented by Rudolf diesel [1].

1.2. Motivation behind Alternate Fuels Research

Engines have come a long way from the inefficient fuel guzzlers which Otto and diesel developed in the late 1800's. The advances made over the years in the refining of fuel allowed for the production of fuels with better and better antiknock properties, and as a result, engine compression ratios steadily increased, and thus the power and efficiency of engines improved. The latest explosive growth in engine research and development is due to the issues of air pollution, rising fuel cost and market competitiveness.

The largest percentage of fuels used to power IC engines is fossil fuels. When fossil fuels are burned, numerous gases are released as byproducts. It did not take long, after the popularity of automobiles increased, for it to become clear that automobiles were a major contributor to hydrocarbon and oxides of nitrogen emissions, as well as the prime cause of high carbon monoxide levels in urban areas. Diesel engines, which are predominantly used in trucks, are a significant source of small soot or smoke particles, as well as hydrocarbons and oxides of nitrogen [1].

Some of these emitted gases are often referred to as greenhouse gases and can be harmful to the environment and to humans.

One way of considerably reducing the amount of greenhouse gases that humans add to the atmosphere, is to reduce the amount of petrol and diesel used in the powering of motor vehicles and their IC engines. This can be achieved by replacing petrol and diesel with alternate fuels that have significantly less impact on the environment.

Increasing demand for fossil fuels drives the price of this commodity higher and higher each year. Limited availability also contributes to price increases due to uncertainty in future supply. In future fossil fuels will become harder to access from the earths surface and thus more sophisticated methods will be needed to extract them also resulting in increased prices.

Due to continued rising fuel costs and heightened concern for the environment, there is considerable effort being made in the research of alternate fuels as a replacement for petrol and diesel. Such attention may result in the discovery of fuels which are not harmful to the environment, are less expensive to produce than petrol and diesel, and are able to yield the same performance from engines as petrol and diesel are.

1.2.1. What are Greenhouse Gases?

Some greenhouse gases occur naturally in the atmosphere, while others result from human activities. Naturally occurring greenhouse gases include water vapour, carbon dioxide, methane, nitrous oxide, and ozone. Certain human activities however, add to the levels of most of these naturally occurring gases. The contribution by automotives is shown in Table 1 below.

Carbon dioxide is released to the atmosphere when solid waste, fossil fuels (oil, natural gas, and coal), and wood and wood products are burned. Methane is emitted during the production and transportation of coal, natural gas, and oil. Methane emissions also result from the decomposition of organic wastes in municipal solid waste landfills, and the raising of livestock. Nitrous oxide is emitted during agricultural and industrial activities, as well as during combustion of solid waste and fossil fuels. Water vapour is overall the most abundant and dominant greenhouse gas in the atmosphere; however human activities are not

believed to directly affect the average global concentration of water vapour.

Very powerful greenhouse gases that are not naturally occurring include hydrofluorocarbons (HFC's), perfluorocarbons (PFC's), and sulphur hexafluoride (SF6), which are generated in a variety of industrial processes [2].

Table 1: The Automotive Urban-Air Pollution Problem [1]

			Automobile Emissions		Truck Emissions	
Pollutant	Impact	Mobil Source Emissions as % of Total	Uncontrolled Vehicles (g/km)	Reduction In New Vehicles (%)	SI Engines	Diesel
Oxides of Nitrogen	Reactant in Photochemical smog; NO2 is toxic.	40 - 60	2.5	75	7	12
Carbon Monoxide	Toxic	90	65	95	150	17
Unburned Hydrocarbons	Reactant in Photochemical smog	60 - 80	10	90	17	3
Particulates	Reduces visibility; Some compounds mutagenic		0.5	40	negligible	0.5

1.2.2. What is the Greenhouse Effect?

This is the term given for the role that the atmosphere plays in helping warm the earth's surface. The atmosphere is largely transparent to incoming short-wave solar radiation, which is absorbed by the earth's surface. Much of this radiation is then re-emitted as infrared wavelengths. Greenhouse gases such as carbon dioxide, methane, nitrous oxide, halocarbons, and ozone in the atmosphere, absorb and re-radiate this outgoing radiation, effectively storing some of the heat in the atmosphere, thus producing a net warming of the surface. The question is whether the measurably increasing levels of carbon dioxide in the atmosphere over the last century, will lead to elevated global temperatures. Consequences of global warming include:

- serious implications for agricultural productivity,
- warmer temperatures,
- increase in number of droughts and wildfires,
- more intense rainstorms,
- deadly heat waves,
- increased spread of disease,
- melting of glaciers and early ice thaw resulting in sea-level rise and ecosystem shifts which could cause species extinction [3].

By arresting and reversing the upward trend in greenhouse gas emissions that started in developed countries 150 years ago, the Kyoto Protocol promises to move the international community one step closer to achieving the Convention's ultimate objective of preventing "dangerous man-made interference with the climate system".

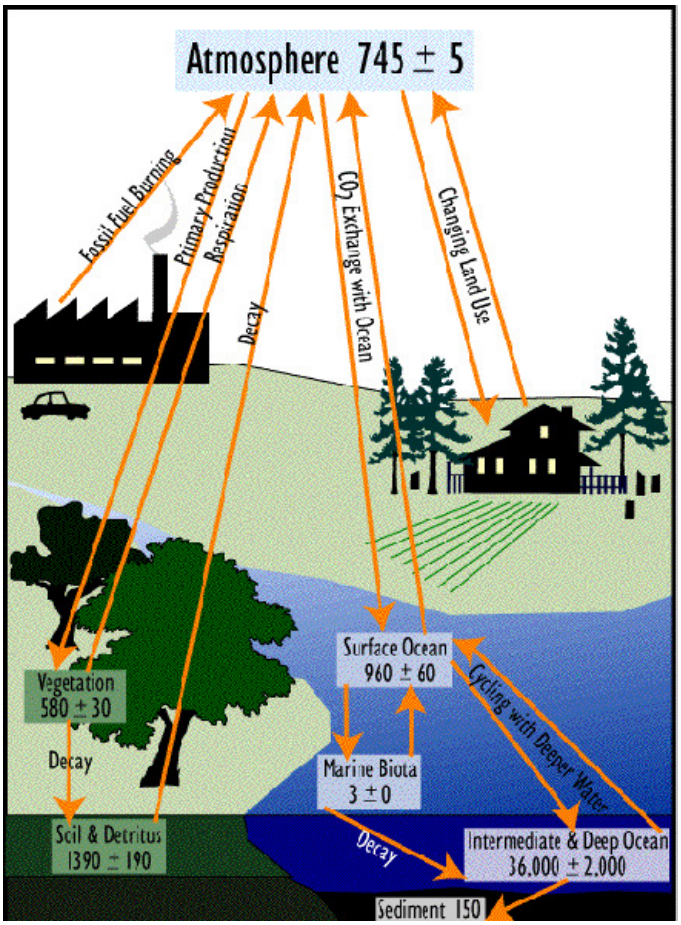


Figure 1: The Carbon Cycle; all values have units of gigatons of carbon [4]

It can be seen from Figure 1 that all carbon produced through the burning of fossil fuels remains in the atmosphere i.e. there is no natural way for the atmosphere to rid itself of this excess carbon.

1.3. Exhaust Emissions Standards

Due to the major concerns raised by the impact of the burning of fossil fuels on the environment, many countries have joined forces (mainly through the efforts of the Kyoto Protocol) in an attempt to kerb the impact of emissions from vehicles. These countries have set standards which specify minimum allowable emissions for particular types of "greenhouse gases". The figure below illustrates these values.

Tier	Date	CO	HC	HC+NOx	NOx	PM
diesel						
Euro 1†	1992.07	2.72 (3.16)	-	0.97 (1.13)	-	0.14 (0.18)
Euro 2, IDI	1996.01	1.0	-	0.7	-	0.08
Euro 2, DI	1996.01[a]	1.0	-	0.9	-	0.10
Euro 3	2000.01	0.64	-	0.56	0.50	0.05
Euro 4	2005.01	0.50	-	0.30	0.25	0.025
Euro 5	2009.09[b]	0.50	-	0.23	0.18	0.005[e]
Euro 6	2014.09	0.50	-	0.17	0.08	0.005[e]
Petrol (Gasoline)						
Euro 1†	1992.07	2.72 (3.16)	-	0.97 (1.13)	-	-
Euro 2	1996.01	2.2	-	0.5	-	-
Euro 3	2000.01	2.30	0.20	-	0.15	-
Euro 4	2005.01	1.0	0.10	-	0.08	-
Euro 5	2009.09[b]	1.0	0.10[c]	-	0.06	0.005[d,e]
Euro 6	2014.09	1.0	0.10[c]	-	0.06	0.005[d,e]

* At the Euro 1..4 stages, passenger vehicles > 2,500 kg were type approved as Category N_1 vehicles

† Values in brackets are conformity of production (COP) limits

a - until 1999.09.30 (after that date DI engines must meet the IDI limits)

b - 2011.01 for all models

c - and NMHC = 0.068 g/km

d - applicable only to vehicles using DI engines

e - proposed to be changed to 0.003 g/km using the PMP measurement procedure

Figure 2: EU Emission Standards for Passenger Cars (Category M_1*), g/km [5]

2. Literature Review

2.1. DME as an Alternative to diesel

Dimethyl Ether (DME) is the simplest ether with the chemical formula CH_3OCH_3. At ambient temperature and pressure DME is a colourless gas. A toxicity study of DME has confirmed that its toxicity is very low and it does not corrode any metals [14].

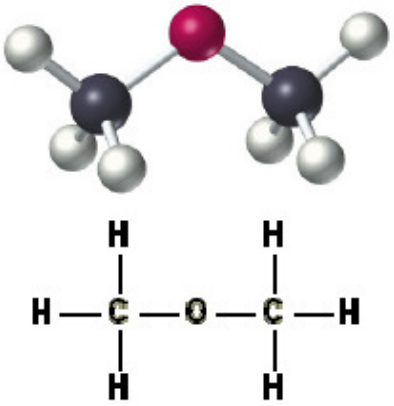


Figure 3: Dimethyl Ether Molecular Structure [18]

However, some artificial rubbers swell in liquid DME but, for example, NBR (Nitric rubber) or PTFE is durable and can be used with DME in liquid and gas conditions [18].

DME can be manufactured from natural gas, coal or biomass etc. Currently, DME is produced using the catalytic dehydration of methanol. The reaction is described as follows [15]:

$$2\ CH_3OH \leftrightarrow CH_3OCH_3 + H_2O$$

The physical and chemical properties of a fuel have an impact on the combustion process of the engine as well as on the injection system and fuel spray characteristics. Lubrication of moving parts in contact with the fuel is also affected by the viscosity of the fuel. In Table 2 below, some of these characteristics are shown for both diesel and DME. These characteristics, when compared, will highlight the strengths and weaknesses of each fuel,

and thus the advantages and disadvantages of using DME as an alternative to diesel will become clear.

DME is a favourable alternative to diesel as it contains oxygen, about 34.8%, and it has no carbon-carbon bond. This means that when it is burned, less soot and particulate matter will be emitted as compared to diesel fuel. Since most fuels are liquid at atmospheric conditions, like diesel, the fuel pumps are designed to pump liquid to the injector nozzle. Since DME is gaseous at atmospheric conditions, the DME must be pressurised and/or cooled in order to keep the DME in its liquid state until it reaches the injector pumps. The differences in the densities of the fuels will have an impact on the fuel spray behaviour, since a number of spray characteristics are dependant on fuel density, as is illustrated by the equations shown in Section 2.4.

Table 2: DME and Diesel fuel properties [9]

Property	**DME**	**Diesel**
Chemical formula	C_2H_6O	$C_{14.4}H_{24.9}$
Mole weight (g)	46	>100
Boiling Point (^oC)	-24.9	180 – 350
Vapour Pressure @ 25^OC (bar)	5.1	<0.01
Liquid Density (kg/m^3)	668	840
Liquid Viscosity (cP)	0.15	4.4 – 5.4
Low Heat Value (MJ/kg)	28.43	42.5
Explosion Limit in air (vol %)	3.4 - 17	0.6 – 6.5
Ignition Temperature (^oC)	235	250
Cetane Number	55 - 60	40 - 55
%wt of Carbon	52.2	86
%wt of Hydrogen	13.0	14
%wt of Oxygen	34.8	0

The liquid viscosity of DME is far lower than that of diesel fuel, thus the lubricating capabilities of DME are less than that of diesel, resulting in more wear of moving parts when using DME than when using diesel. Since the heating value of DME is less than that of diesel, it can be expected that for the same mass of fuel, the power output for DME will be less than for diesel. Since DME has a higher cetane number than diesel, the DME has a higher ignition quality than diesel which is desirable for cold starting. A higher cetane

number means a shorter ignition delay, thus resulting in smoother engine operation. The modulus of elasticity, when inverted, determines the compressibility of a fuel. As a result, because the modulus of elasticity of DME is lower than that of diesel, DME is more compressible than diesel. Since fuel is compressible there is a time lag between the beginning of delivery by the pump and the beginning of discharge from the nozzle, and the rate of delivery from the pump is not identical to the rate of discharge from the nozzle [7]. These effects will become more pronounced the more compressible the fuel is.

2.2. Previous Studies on DME as an Alternative to Diesel

A paper published by Huang, Wang, Chen, Zhou and Jiang (1999) from the X'ian Jiatong University in China conducted tests on a light-duty direct-injection diesel engine operating on dimethyl ether (DME). The results were then compared to another identical engine running on diesel. The results show that:

- The DME engine has a longer delay of injection and duration of injection.
- A lower maximum cylinder pressure and rate of pressure rise.
- A shorter ignition delay.
- The DME engine has a low mechanical load and combustion noise, a fast rate of diffusion combustion and shorter combustion duration than that of a diesel engine.
- It has the ideal pattern of compression ignition engine heat release.

Sorensen and Mikkelson (1995) did similar experiments on a small naturally aspirated diesel engine with the following results:

- Equivalent thermal efficiency.
- Near-zero smoke.
- NOx emissions reduced by approximately 75%; a 90% reduction was achieved with the use of EGR.
- Lower engine noise.
- The diesel fuel injection pump could operate on DME for more than 500 hours.

2.3. Mechanisms Controlling Diesel Combustion

Fuel is injected into the engine cylinder towards the end of the compression stroke just before the desired start of combustion via a fuel injection system. Because the liquid fuel is injected at a high velocity, and due to the nature of the injector, the fuel atomises into small droplets inside the combustion chamber. The fuel then vaporises and mixes with the high-temperature high-pressure air in the cylinder. Because the temperature and pressure of the air is higher than the ignition point of the fuel, portions of the fuel-air mixture ignite after a delay period of a few crank angle degrees. As this initial combustion occurs, the pressure in the cylinder increases, which causes combustion of the remaining fuel-air mixture to occur more rapidly. The fuel continually being injected into the cylinder also vaporises more rapidly. Atomisation, vaporisation, fuel-air mixing and combustion occur for the rest of the fuel that is injected into the cylinder.

It is clear that the major factors affecting the combustion process are the fuel injection system, the nature of the combustion chamber, and the properties of the fuel. Due to the nature of an engine, very little flexibility is offered in improving the combustion process through the altering of the combustion chamber. However it is possible to modify the combustion process by modifying the injection system or varying the type of fuel used.

2.3.1. Fuel Injection Systems

The fuel injection system consists of an injector pump, delivery pipes and injector nozzles. There are a number of different variations to the kinds of pumps and nozzles that are used.

Pumps can be single barrel type, where there is an individual plunger pump for each cylinder, or all of the pumps for each cylinder could be grouped together in a single unit. The fuel could also be accumulated at a constant pressure in a manifold before being distributed to the nozzles, as is done for a common rail system. In the common rail accumulator injection system, the generation of the injection pressure is separate from the injection itself. A high-pressure pump generates a pressure of 1,600 bar and higher in the rail [20].

Nozzles can vary by the way that they are actuated, and by the number of holes and the orientation of the holes through which the fuel sprays into the combustion chamber. Some nozzles can be mechanically actuated, whereby a spring-loaded valve is opened when the pressure of the fuel acting on some of the surface of the valve overcomes the spring force and opens the valve. By varying the spring force, the injection pressure can be altered.

Modern technology allows for valves to be electronically actuated by solenoids, allowing for increased flexibility in injection control and fuel metering. The latest injectors are actuated by piezo crystals. Piezo crystals have the special characteristic of expanding rapidly when an electric field is applied to them [20].

The common rail injection system is equipped with a control unit that has the ability to control extremely precisely all the injection parameters – such as the pressure in the rail and the timing and duration of injection – as well as performing other engine functions [20].

2.4. Injection Characteristics

2.4.1. Fuel Mass Flow Rate

The amount of fuel delivered to the combustion chamber is an important injection characteristic, as the amount of fuel consumed will determine the amount of power developed by the engine. However the fuel conversion efficiency also impacts the power output, so it is important to have the fuel mix well with the air in the combustion chamber to ensure that as little of the fuel as possible goes to waste. An estimate of the fuel mass flow rate through an injector nozzle can be made using equation 1 shown below [1]:

$$\dot{m} = C_d A_n \sqrt{2\rho_f dP}$$

Where:

$\dot{m}$ = Fuel mass flow rate (kg/s)
C_d = Discharge coefficient
A_n = Nozzle minimum area (m^2)
ρ_f = Fuel density (kg/m^3)
dP = Pressure drop across the nozzle (Pa)

$$dP = P_i - P_f$$

$$A_n = n\pi\left(\frac{d_n}{2}\right)^2$$

Where:

P_f = Combustion chamber pressure at injection (Pa)
P_i = Injection pressure (Pa)
n = Number of nozzle holes
d_n = Nozzle hole diameter (m)

2.4.2. Fuel Spray Behaviour

Figure 4 below illustrates a typical diesel fuel spray, with some of the injection spray characteristics shown.

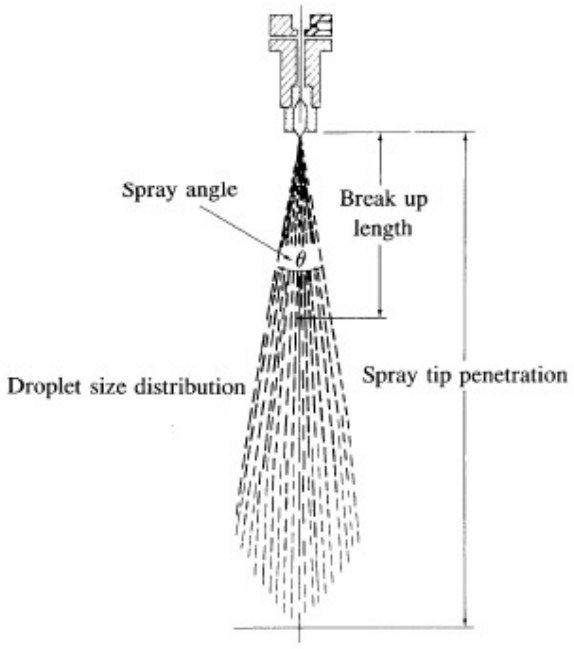


Figure 4: Diesel Fuel Spray [1]

Under diesel engine injection conditions, as the fuel exits the nozzle, the fuel spray diverges into a cone shape and breaks up into small droplets which are very much smaller than the nozzle hole diameter. This behaviour is known as the atomisation break up regime.

The angle of the cone is illustrated in Figure 4, and the equation used to model this angle is illustrated below [1]:

$$\tan\frac{\theta}{2} = \frac{1}{A} 4\pi \left(\frac{\rho_g}{\rho_f}\right)^{1/2} \frac{\sqrt{3}}{6} = Z$$

$$\theta = \frac{\arctan Z}{2}$$

Where:

θ = Injection spray angle (°)
A = Nozzle geometry constant
ρ_g = Combustion chamber air density (kg/m^3)

$$A = 3 + 0.28\frac{L_n}{d_n}$$

Where:

L_n = Nozzle hole length (m)

The droplets formed during atomisation must evaporate before the fuel can mix with the air and then combust. The history of the droplet in the combustion chamber is determined by the following three conditions [1]:

1. Deceleration of the drop due to aerodynamic drag.
2. Heat transfer to the drop from the air
3. Mass transfer of vaporised fuel away from the drop.

As the droplet temperature increases due to heat transfer, the fuel vapour pressure increases and the evaporation rate increases. As the mass transfer rate of vapour away from the drop increases, so the fraction of the heat transferred to the drop surface which is available to increase further the drop temperature decreases. As the drop velocity decreases, the convective heat transfer coefficient between the air and the drop decreases [1]. The combined effect of these factors will change the characteristics of a droplet in the way illustrated in the figure below.

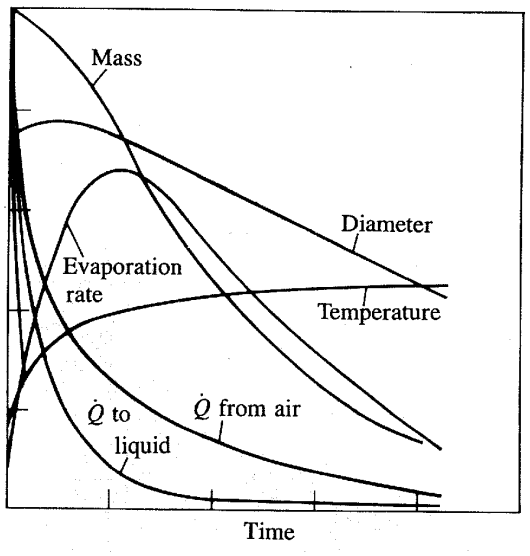


Figure 5: Variation of Droplet Characteristics [1]

Since evaporation occurs when heat is transferred to the droplets from the air, the diameter of a droplet will affect the amount of time that it takes to evaporate that droplet. If evaporation of the fuel does not occur rapidly, when combustion begins the fuel that has not evaporated will remain unburnt thus resulting in an increase of emissions of unburned and partially burned species as well as poor fuel conversion efficiency. Thus the definition of mean drop diameter is desirable for characterising the spray. An appropriate and commonly used mean diameter is the Sauter mean diameter (SMD). A correlation developed by Hiroyasu and Kadota (1974) for defining SMD is shown in equation 9 below [8]:

$$SMD = 2.33\times10^{3}\left(dP\right)^{-0.135}\left(\rho_{g}\right)^{0.121}\left(V\right)^{0.131}$$

Where:

SMD = Sauter mean diameter (microns)
V = Injection fuel volume (m^3)

$$V = \frac{\dot{m}}{\rho_{f}} t_{inj}$$

Where:

t_{inj} = Injection duration (ms)

Upon atomisation, under steady-state conditions, the vaporisation time of a single droplet is given by the following equation [8]:

$$t_v = \frac{d_o^{\,2}}{4\beta}$$

Where:

t_v = Vaporisation time (ms)
d_o = Initial droplet diameter (μm)
β = Vaporisation constant

Table 3: Examples of Formulation Constants

C_d =	0.1
P_i (MPa) =	3
n =	3
d_n (m) =	0.00026
ρ_g (kg/m^3) =	25
L_n (m) =	0.00098
t_{inj} (s) =	0.0019
T_{inj} (K) =	291

Air utilization and fuel-air mixing rates are both dependant on the speed and extent to which the fuel spray penetrates the combustion chamber. In multispray, DI, diesel combustion systems overpenetration of the spray will cause liquid fuel to come into contact with cool surfaces which will lower mixing rates and increase emissions of unburned and partially burned species. Underpenetration of the spray will cause poor air utilization due to the fact that the air on the periphery of the cylinder does not mix with the fuel [1]. A correlation developed by Hiroyasu et al. (1980) allows for the modelling

of the spray tip penetration as a function of time after start of injection. This model shows that initially, before jet breakup, the spray tip penetration is linearly proportional to time. After jet breakup however, the spray tip penetration is proportional to the square root of time. The jet breakup length is the length of spray during which the liquid fuel leaving the nozzle disintegrates into drops of varying diameters. The equations for this model are shown below [1]:

$$\underline{t < t_{break}} : S = 0.39\left(\frac{2dP}{\rho_f}\right)^{1/2} t$$

$$\underline{t > t_{break}} : S = 2.95\left(\frac{dP}{\rho_g}\right)^{1/4} (d_n t)^{1/2}$$

$$t_{break} = \frac{29\rho_f d_n}{(\rho_g dP)^{1/2}}$$

Where:

S = Spray tip penetration (m)
t = Time after start of injection (ms)
t_{break} = Time to jet breakup (ms)

Injection duration is defined as the time that the injector stays open for. A model for the injection duration is shown by the following transformed equation [7]:

$$\theta_{dur.} = 0.0016\frac{VN_{pump}}{A_n C_d}\sqrt{\frac{\lambda}{(P_i - P_f)}}$$

Where:

$\theta_{dur.}$ = Duration of injection (cam degrees)

N_{pump} = Pump speed (rpm)
λ = fuel specific gravity

The time delay that exists between the beginning of fuel delivery from the pump and the start of spray from the nozzle is known as injection lag. Two distinct periods exist in describing the injection lag; these are as follows [7]:

1. The time required for the first pressure wave to travel from the pump to the nozzle,
2. The time that elapses between arrival of the first wave at the nozzle and the lifting of the valve off its seat.

Since pressure waves travel through the tubing with the velocity of sound in the fuel, the injection lag will increase with the increase of tubing length. Retracting type delivery valves are known to increase injection lag because of lower residual pressures. Lower residual pressures lower the acoustic velocity of the fuel particularly if residual pressure drops below atmospheric [7].

As injection pressure increases, injection lag decreases and a shorter injection lag can be achieved by decreasing the pressure difference between the residual pressure and the nozzle opening pressure. It should also be noted that the discharge tubing for each cylinder should be equal to insure the same injection timing to each cylinder [7].

The acoustic velocity is defined by the following equation:

$$V_s \approx \sqrt{\frac{K \times g}{\rho_f}}$$

Where:

V_s = Acoustic Velocity (m/s)
K = Bulk Modulus of Elasticity (MPa)

As is shown by the equation, the acoustic velocity is dependant on the modulus of elasticity of the fuel and density of the fuel. Both characteristics are influenced by the temperature and pressure that the fuel is stored at. The

density and modulus of elasticity of DME as a function of pressure (P_i) and temperature (T_{inj}) was found using a computer program called "REFPROP". This program was developed by the National Institute of Standards and Technology (NIST), the property formulations and fluid data files were programmed by:

Eric W. Lemmon, Marcia L. Huber, and Mark O. McLinden

Physical and Chemical Properties Division
National Institute of Standards and Technology
Boulder, CO 80305
ericl@boulder.nist.gov
markm@boulder.nist.gov
huber@boulder.nist.gov

The user interface was written by Eric W. Lemmon.

The peak injection pressure developed by the injection system can be modelled by the equation shown below:

$$P \approx \sqrt{\frac{K \times \rho_f}{g}} \times \left(\frac{D}{d}\right)^2 \times v_p$$

Where:

P = Peak Pressure (MPa)
D = Plunger Diameter (mm)
d = Tubing Bore (mm)
v_p = Plunger Velocity (m/s)

2.5. Pollutant Formation and Control

2.5.1. The Combustion Process

Petrol and diesel fuels are known as hydrocarbon fuels. A hydrocarbon fuel is described by its structure or bonding between the hydrogen and carbon atoms in it. “Perfect" combustion of a hydrocarbon fuel would mean that the reaction between the oxygen in the air and the fuel would convert all the hydrogen in the fuel to water in the form of water vapour and all the carbon in the fuel to carbon dioxide. Nitrogen and other gases in the air should remain unaffected. In reality, the combustion process cannot be "perfect," and automotive engines emit several types of pollutants [13].

"Perfect" combustion results in the following by-products:

Fuel (hydrocarbons) + Air (oxygen and apparent nitrogen) → Carbon Dioxide + water + unaffected apparent nitrogen;

Realistically typical engine combustion results in the following by-products:

Fuel (hydrocarbons) + Air (oxygen and apparent nitrogen) → Unburned Hydrocarbons + Nitrogen Oxides + Carbon Monoxide + Carbon Dioxide + water.

2.5.2. Nitrogen Based Emissions

The principle source of NO is the oxidation of atmospheric nitrogen [1]. As a result more air means more NOx. High temperatures and high oxygen concentrations result in high NO formation rates. At this point it should be noted that the injection temperature increases with engine speed while the volumetric efficiency decreases with engine speed.

2.5.3. Carbon Based Emissions

The principle source of carbon based emissions is the fuel, thus the amount of carbon present in the fuel should determine the amount of carbon based emissions produced.

Carbon monoxide is usually present when there is a deficiency of air. The CO concentration is primarily a function of air/fuel ratio and is essentially unchanged by load or speed. It is formed when there is insufficient oxygen to convert all the carbon in the fuel to carbon dioxide [21]. Theoretically CO formation should correspond to the chemical equilibrium equation that follows [22].

$$H_2O + CO \leftrightarrow H_2 + CO_2$$

At maximum flame temperatures, combustion yields insignificant quantities of CO relative to CO_2, but as the combustion gases become cooler, the equilibrium shifts in a direction favouring oxidation of CO to CO_2.

3. Objectives

The objectives of this research were to fuel a compression ignition engine on diesel and Dimethyl Ether (DME) and record the results. The two fuels were compared in terms of the following engine characteristics:

- Performance.
- Injection.
- Emissions.

Particular interest was given to the injection characteristics and their effect on the performance and emissions, in particular, injection duration, injector lift, angle of start of injection, fuel line pressure and rate of change of fuel line pressure were considered.

4. Experimental Facilities

Testing was conducted in one of the engine test cells located within the Mechanical, Aeronautical and Industrial Engineering Laboratory in the North West Engineering Building. Figure 6 below shows a schematic of the test equipment used during the experimentation. The individual components will be discussed in more detail in this section.

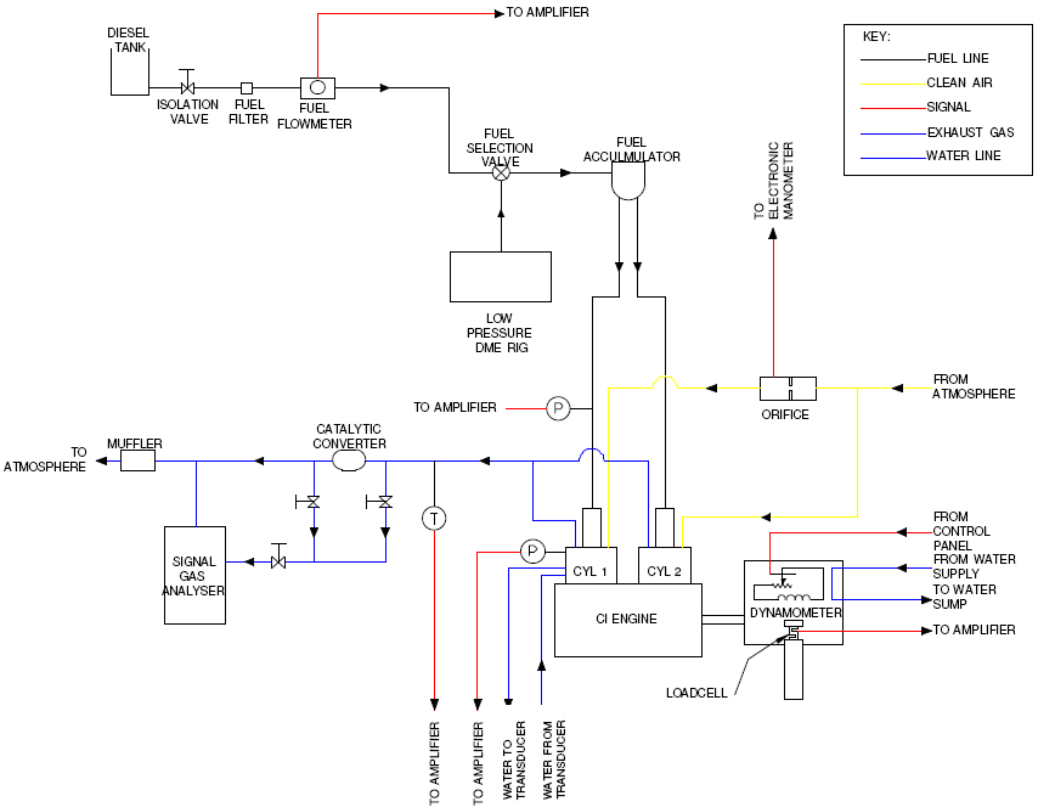


Figure 6: Engine Test Cell Schematic [17]

4.1. The Compression Ignition Engine

A four stroke Lister Petter direct injection compression ignition engine was used as the test engine. It is shown in Figure 7 below mounted onto a fixed steel structure which is secured to the concrete foundation. The engine specifications are shown in Table 4 below.



Figure 7: Lister Petter Engine

Table 4: Engine Specifications

Description	
Manufacturer	Lister Petter
Model	R V19 PH2 40 9602
Displacement	1330cc
No. of Cylinders	2
Bore	87.74mm
Stroke	110.0mm
Maximum Power	13.4 kW @ 2200 rpm
Maximum Torque	59.4 Nm @ 2200 rpm
Compression Ratio	16.5 : 1
Fuel Injection Pressure:	
900 rpm – 1099 rpm	137 / 152 bar
1100 rpm – 2000 rpm	197 / 217 bar
Fuel Injection Timing:	
0 – 1650 rpm	24° BTDC
1651 – 2000 rpm	28° BTDC
Valve Timing:	
Inlet valve open	13.5° BTDC
Inlet valve closed	38.5° ABDC
Outlet valve open	38.5° BBDC
Outlet valve closed	13.5° ATDC

4.2. The Dynamometer

A water cooled eddy current Borghi & Saveri dynamometer which is coupled to the Lister Petter engine is used to put the engine under load. Figure 8 below illustrates how it is fixed to a similar steel structure and then secured to the same concrete foundation as the engine. The control of the dynamometer is such that the user can keep either the torque constant or the speed constant.



Figure 8: Dynamometer

Table 5 below shows the specifications for the dynamometer.

Table 5: Dynamometer Specifications

Manufacturer	Borghi & Saveri
Model	FE 150 S
Maximum Speed	13000 rpm
Maximum Torque	280 Nm
Maximum Power	110 kW
Accuracy	0.1 rpm and 0.1 Nm

The load cell output signal is amplified and sent through the Borghi & Saveri control box to the data acquisition PC situated in the control room. The load applied to the engine is controlled by sending a signal from the control box to

the dynamometer which would cause a change in voltage applied to the stator and thus control the torque applied to the rotor.

4.3. Fuel System

4.3.1. Fuel Supply System

The fuel supply is controlled by a three-way valve to allow the selection of either DME or diesel fuel. An accumulator exists between the valve and the injector pumps to ensure constant fuel supply to the engine.

Diesel is gravity fed to the three-way valve via a fuel header tank mounted above the engine. An isolation valve, fuel filter and fuel flow monitor are mounted upstream of the three-way valve.

The DME is supplied to the three-way valve via a Low Pressure DME Rig designed and built as part of a postgraduate research programme [18]. The rig maintains the DME in a liquid state before it enters the injector pumps by pressurising and cooling the DME. Figure 9 below is a photograph of the system. The specifications and operation of the Low Pressure DME Rig is covered in greater detail in Section 4.4 below.



Figure 9: Low Pressure DME Rig

4.3.2. Fuel Pumps and Injectors

The injectors used were of the three-hole type and were set to 210 bar injection pressure. Each injector has its own dedicated fuel pump and fuel line. The fuel pump and injectors are of the manufacturer's specifications; however one of the injectors was fitted with an injector needle lift sensor. This sensor converts the lift into an electrical signal which is fed to the control PC in the control room. The signal is then converted again into lift.

4.4. Low Pressure DME Rig

The Low Pressure DME (LP DME) Rig is based on a modified concept of a vehicle air conditioning unit. The system consists of the following main components:

- A compressor,
- A condenser
- A counter-flow heat exchanger.

The system operates in the following manner. Reference can be made to Figure 10:

1. High pressure DME enters the system from the DME cylinder by first passing through a check valve, then through a solenoid actuated shut-off valve, and finally through a mechanically adjustable needle flow control valve.
2. The DME gas then passes through the outer tube of the counter flow heat exchanger on its way to the compressor. The fluid passing through the inner tube is cooled further.
3. The compressor then pressurises the DME gas with the aim of turning it into a liquid more easily at the condenser. At the compressor the DME mixes with the compressor oil thus the mixture is passed through an oil separator after the compressor to separate the compressor oil from the DME and return the oil to the compressor.
4. Upstream of the compressor, the pressurised DME is passed through a radiator condenser which cools the hot, pressurised DME. Upon

cooling, the DME begins to turn to liquid. A fan mounted on the condenser assists in additional cooling. When the system pressure reaches 13 bar, the fan will turn on.

5. The DME then passes through the inner tube of the counter flow heat exchanger. The high pressure DME entering the system via the outer tube of the heat exchanger cools the DME further. After the heat exchanger the DME is in a liquid state and is suitable for use by the engine.
6. The DME then passes through a rotameter to measure the fuel flow of the system. At this point the DME is at a pressure of between 12 and 13 bar and is roughly 10°C.
7. Fuel consumption by the engine is measured by a second rotameter placed prior to the three-way valve discussed previously.
8. Any surplus DME not consumed by the engine is returned to the main supply via a mechanically adjustable needle expansion valve, returning the DME to between 2 and 3 bar. A pressure relief valve is placed in the line supplying the engine and is set to trigger at approximately 14.5 bar.

With reference to Figure 10 below, the system is monitored by three thermocouples and a pressure transducer. The values obtained by these sensors are fed into the control PC, and according to the programming, control signals are fed back to the system to operate the solenoid valve (DME supply from the cylinder) and the fan (additional cooling).

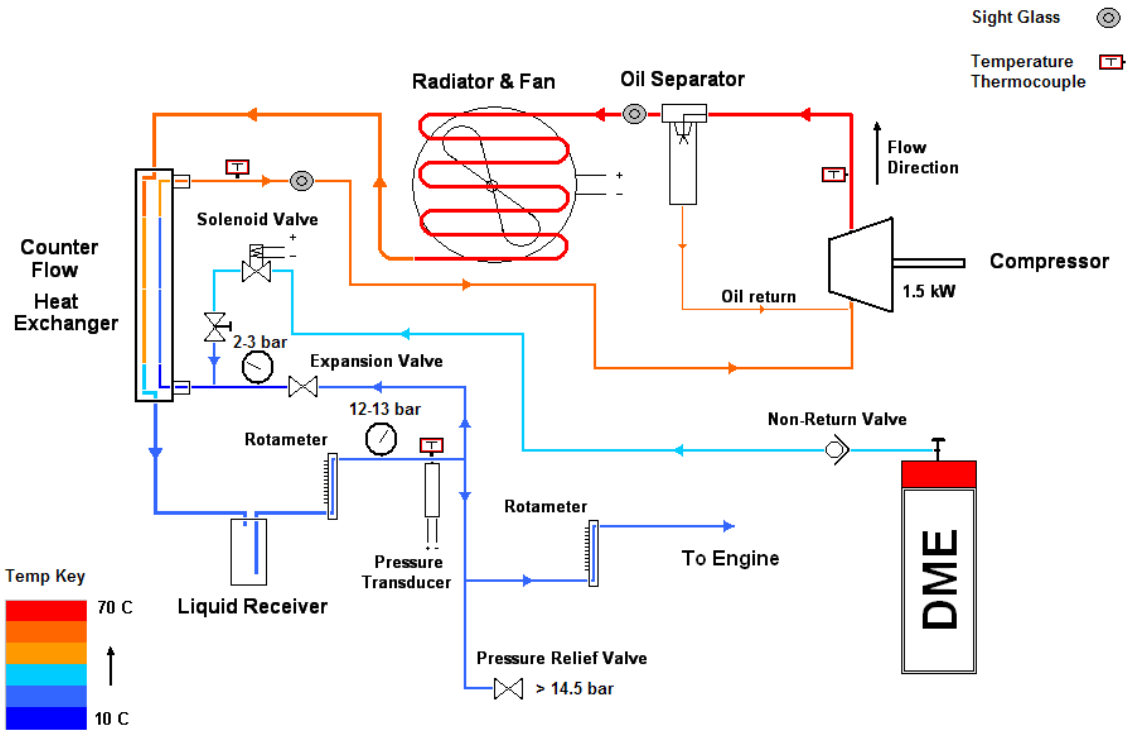


Figure 10: Low Pressure DME Rig Schematic [16]

4.4.1. Controller

A data acquisition and control card located within a PC was used to monitor and control the rig. The logic of the system works as follows:

- When the pressure reaches 13 bar the fan will turn on, and when the system reaches 12 bar the fan will switch off. The additional cooling from the fan at the condenser lowers the pressure in the system.
- The solenoid valve will open and allow more DME into the system when the pressure reads less than 13 bar and the compressor outlet temperature reads greater than 60°C.

Software called Visual Designer was used to develop the code and program the control card. The program is shown in Appendix E.

A snapshot of the user interface is shown in Figure 11 below. This interface screen is used for live monitoring of the system but also allows for set points

and input sample rates to be altered in order to optimise the operation of the system.

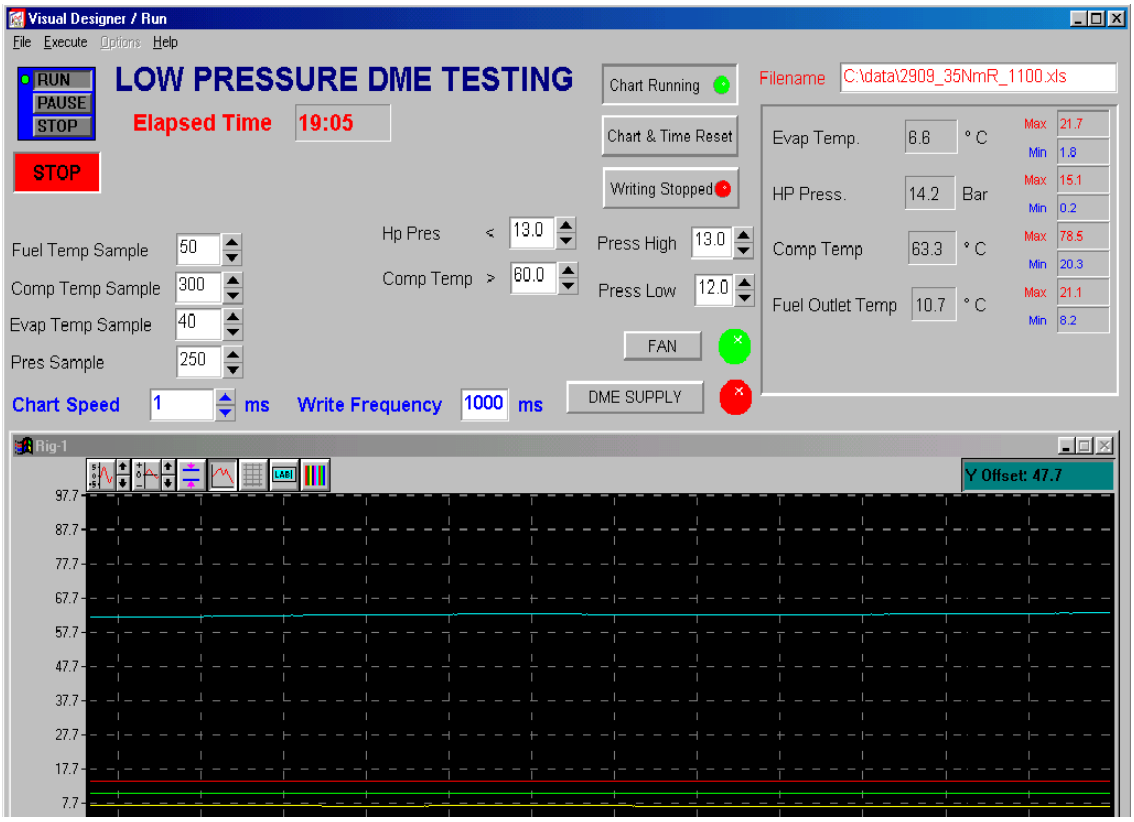


Figure 11: Control PC Screenshot

The Wiring and Termination Panel Connections are illustrated in Figure 12 below.

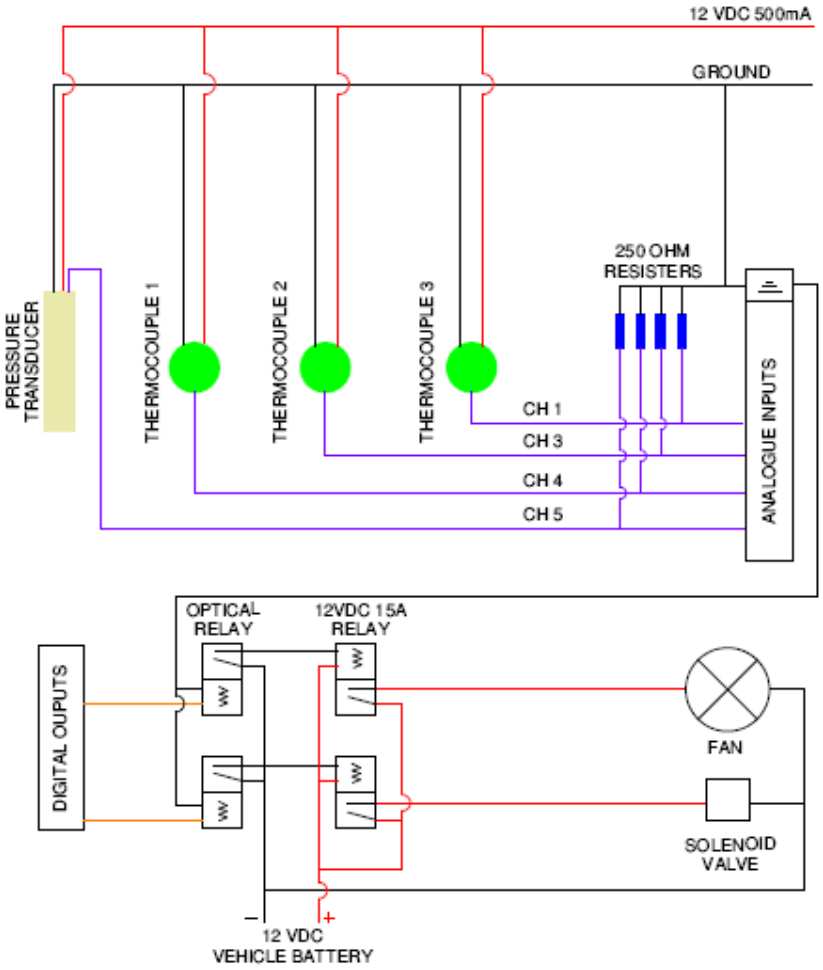


Figure 12: Instrumentation Wiring Diagram [19]

4.5. Engine Cooling

The Lister Petter engine is an air-cooled unit so additional air-flow was generated by using two large blowers placed on either side of the engine, one pointed at each of the engine cylinders. An extractor fan located at the window of the test facility was used to improve the ventilation in the room. A third large blower was used to cool the motor and compressor of the Low pressure DME Rig.

4.6. Instrumentation

A number of sensors are used to generate signals of important information required for calculating the performance characteristics of the engine. These signals are fed into a computer located in the control room where the real-time engine performance is displayed and captured by a program called “Engine Test”. A second program on the computer called “Heat Release and Combustion Analysis (HRCA)” was used to process the captured data and automatically calculate engine performance characteristics and produce performance plots.

The gas analyser located in the test cell takes samples of the emissions. The samples are processed by the analyser and the data is sent to a second computer which uses a program called “Signal” to process and then capture the emissions data.

4.6.1. Cylinder Pressure

A pressure transducer is mounted in a custom made water jacket which screws into a tapped hole above cylinder one in the cylinder head. This hole goes through to the combustion chamber so that the pressure in the combustion chamber can be read. The water jacket cools the transducer as the transducer is exposed to excessive heat from the combustion chamber. The transducer is cleaned regularly in an ultrasonic bath to ensure accurate and consistent readings. The conversion factor used in HRCA is 20 bar/V.

4.6.2. Ambient Pressure

A pressure transducer and amplifier were interfaced with the computer to measure the atmospheric pressure.

4.6.3. Fuel Line Pressure

A transducer was fitted to the fuel line of cylinder one to measure fuel line pressure. The conversion factor used in HRCA is 100 bar/V.

4.6.4. Air Flowrate

An orifice plate is located at the end of an air-line from which the air is supplied to the engine. A pressure tapping is located directly behind the orifice plate where an electronic manometer is connected to read the pressure. The reading from the manometer is referenced to the ambient pressure and the difference is used by the computer to calculate the flowrate using the equation for the orifice and the difference pressure.

4.6.5. Fuel Flowrate

The fuel flowrate of diesel was measured using an electronic fuel flowmeter. To measure the DME flowrate, manual readings are taken from a rotameter located on the DME line. These readings are manually entered into the computer in order for HRCA to calculate the fuel flowrate.

4.6.6. Exhaust Temperature

A thermocouple mounted in the exhaust pipe about 500mm from the engine reads the exhaust temperature.

4.6.7. Crank Angle and Speed

An encoder attached to the crank shaft was used to determine the crank angle position. A pulse is produced by the encoder every 0.2 degrees of crank angle. A second pulse was produced when cylinder 1 was at TDC. Using these two pulses and the time between them, speed and position of the shaft can be calculated.

4.6.8. Injector Needle Lift

An injector needle lift sensor was installed on the injector of cylinder 1. The conversion factor used in HRCA was 0.2656 mm/V.

4.7. Gas Analyser



Figure 13: Signal Gas Analyser

The Signal Gas Analyser used to measure the composition of the exhaust emissions consists of five separate units, namely:

- Signal Series 200 Gas Cooler/Dryer
- Signal 4000 VM Heated Vacuum No_x Analyser
- Signal 7000 GFIR CO_2 Analyser
- Signal 7000 GFIR CO Analyser
- Signal HM Total Hydrocarbons (THC) Analyser

5. Experimentation

5.1. Approach

The approach used to obtain the necessary research results was as follows:

- It was decided to run tests at constant load for ranging engine speeds. Tests were run at loads of 25 Nm and 35 Nm for an engine speed range of 1100 rpm to 1800 rpm in 100 rpm intervals.
- Tests were run at both torques for DME and for diesel.
- Emissions and performance data were captured.
- A comparison of the results was performed.

5.2. Procedure

5.2.1. Pre-Testing Procedure

1. The equipment was calibrated as detailed in Appendix A.
2. All of the units of the Signal Gas Analysers were switched on approximately one hour prior to testing. The equipment was allowed to warm up and stabilise before testing was done in order to insure the quality of the results. Once the analysers were at operating temperature the reference gas cylinders were opened and calibration of each of the units was done as detailed in Appendix B.
3. The copper sulphate crystals in the oxygen analyser were checked. If the crystals were orange they would have to be dried in the oven until they turned blue before being replaced.
4. The cylinder pressure transducer was cleaned in an ultrasonic bath for 20 minutes then reinstalled.
5. The injector was checked to insure that it is set to 210 bar.
6. The computer and electronic equipment were switched on.
7. The performance data acquisition PC was set up as per Appendix C1.
8. The emissions data acquisition PC was set up as per Appendix C2.

5.2.2. Testing Procedure

1. The water supply to the dynamometer was turned on.
2. The water supply to the water jacket of the cylinder pressure transducer was turned on.
3. The engine was cranked over once and special attention was given to the pressure transducer to note if any leaks occurred. If leaks did appear, the pressure transducer would be refitted.
4. The Low Pressure DME Rig was set up, started and allowed to stabilise as per Appendix D.
5. The diesel supply was turned on and the three-way fuel valve turned to diesel.
6. The blowers were placed on either side of the engine, one per cylinder, and another blower facing the LP DME Rig compressor. They were turned on once in position.
7. The extractor fan was turned on.
8. The engine was started with diesel and allowed to run at around 1300 rpm for a few minutes while under a low applied torque.
9. The three-way fuel valve was then turned to the DME supply.
10. The engine was allowed to run for a few minutes before testing commenced in order to ensure that a total fuel cross over took place. When almost no visible exhaust smoke was being emitted, testing began.
11. Once the desired torque was set, the required speed setting was selected using the dynamometer control unit and the throttle on the engine.
12. Readings on both data acquisition PC's were allowed to stabilise.
13. Between four and six sets of data for engine performance and emissions were captured. The following values were recorded manually to confirm consistency of the results:

    a. Load
    b. Speed,
    c. Air flowrate
    d. Emission averages
    e. Fuel flowrate
    f. Fuel overflow from the rotameters.

These last two values do not apply for diesel testing.

14. The speed was then varied and then steps 12 and 13 were repeated.
15. This was done for each interval until the entire speed range was covered; then the torque was altered.
16. Once testing was completed, the DME cylinder was shut-off and the red *STOP* button on the control PC screen was activated. The engine speed and torque were decreased and the engine was allowed to use the remaining fuel in the system.
17. The engine was then switched off.
18. The LP DME Rig was purged of any remaining DME and then the compressor was turned off.
19. The three-way fuel valve was then turned back to diesel.
20. The engine was started again to purge the system of DME and ensure that each engine cylinder was operating on diesel.
21. The performance data was then analysed using HRCA. Emissions data was converted to graphs of specific emissions vs. engine speed.

5.3. Precautions

The following precautions were taken to avoid damage to equipment and erroneous data capturing.

5.3.1. Equipment Precautions

- Battery water levels were checked.
- Engine oil levels were checked.
- Compressor oil levels were checked.
- Batteries on all electronic equipment were checked.
- Injector operating pressures were checked and an even spray distribution from the injectors was confirmed by using an injector test rig equipped with an analogue pressure gauge and clear, glass-walled injection chamber.
- The pressure transducer was inspected to ensure cleanliness and that no blockages were present.
- The copper sulphate crystals were confirmed to be blue in colour.
- The amount of fuel was confirmed to be enough to finish an entire test session. Continuation will result in erroneous data.

5.3.2. Testing Procedure Precautions

- Engine temperatures and emissions were confirmed to be stable before data was recorded.
- Cylinder and injector pressure traces were continuously monitored throughout testing to ensure correct operation of the engine.
- Regular checks were made to ensure that the data files were being correctly recorded in the correct folders and that the filenames correlated to the test being performed.
- Regular checks were made to ensure that the low pressure DME rig was operating within the correct pressure boundaries.
- Regular checks were made to ensure that the LP DME rig compressor was not over heating.

6. Results and Discussion

6.1. Engine Performance

6.1.1. Introduction

This section contains graphs of the following engine performance characteristics:

- Combustion Chamber Pressure.
- Total Apparent Energy Released.
- Rate of Heat Transfer.

All of the graphs are plotted against crank angle. The graphs are generated with the intention of illustrating the difference in behaviour of the engine whilst running on LP DME and on diesel, as well as the difference in behaviour whilst running at 25 Nm load and 35 Nm load. The graphs were generated in HRCA by overlaying one of each of the following tests:

- A 1600 rpm diesel test at 25 Nm,
- A 1600 rpm DME test at 25 Nm,
- A 1600 rpm diesel test at 35 Nm,
- A 1600 rpm DME test at 35 Nm.

Also shown on these plots are the points that HRCA deems when fuel injection occurs and when combustion occurs. These are represented by a triangle and square respectively.

6.1.2. Analysis

Figure 14 below shows the combustion chamber pressure trace at 1600 rpm for loads of 25 Nm and 35 Nm for both diesel and LP DME. It is immediately evident that the pressure developed by the engine when fuelled with DME is less than that of the engine when fuelled on diesel. The maximum pressure of DME is approximately 60% of the maximum pressure of diesel. Since the

cylinder pressure is directly proportional to the power generated by the engine, this lower pressure results in a lower power output. For both DME and diesel, the engine develops a slightly higher pressure at a higher load.

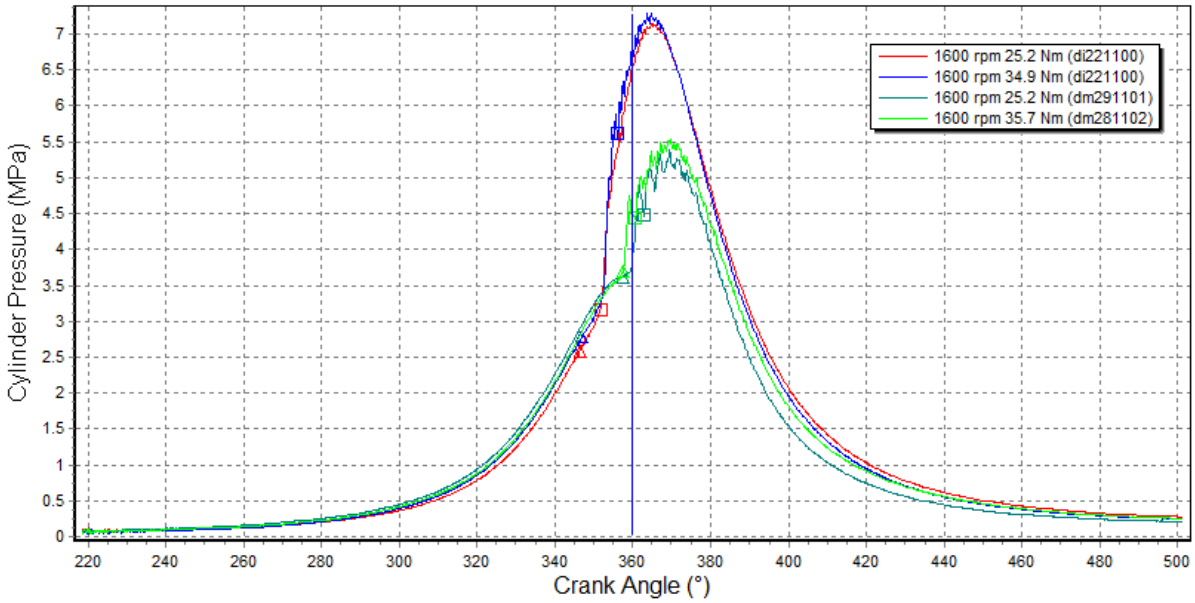


Figure 14: Pressure trace

The irregular spikes and dips in the pressure at the top of the DME pressure traces are attributed to knocking. In compression ignition engines, if too much fuel is injected into the combustion chamber before ignition occurs, engine knock can occur [11]. Engine knock is also said to limit engine efficiency, as it effectively limits the temperature and pressure of the end-gas, thus limiting the engine compression ratio [1].

Figure 14 also illustrates the fact that the ignition of the DME occurs later than that of the diesel, i.e. towards the end of compression. The ignition is illustrated by the sharp increase in combustion chamber pressure. For diesel this occurs at about 8 degrees before TDC whereas for DME this occurs approximately at TDC or about 3 degrees before TDC. Since the cetane number of DME is higher than that of diesel, the ignition delay of DME is shorter than that of diesel. As a result, the cause for the later ignition of the DME must be attributed to a later injection of the fuel.

Figure 15 shows the graph of total apparent energy released vs. crank angle for the above tests. The graph once again highlights the lower amount of energy released by the engine when powered by DME. Also evident is the later release of energy from the DME tests. The energy release curve dips consistently prior to reaching TDC which can be attributed to the heat transfer to the walls as the fuel has not been injected yet. When the fuel is injected the curve dips more rapidly due to the vaporisation of the fuel. Vaporisation occurs approximately 10 degrees before the sudden spike in energy, where there is a small additional dip in the energy curve. This occurs when the fuel is injected into the combustion chamber and the liquid fuel must first be vaporised and heated up from the injection temperature to the typical compression air temperature [1]. The graph for the DME dips to a lower energy value than the diesel test before energy release occurs. This is attributed to the late injection of fuel and the higher latent heat of vaporisation of DME.

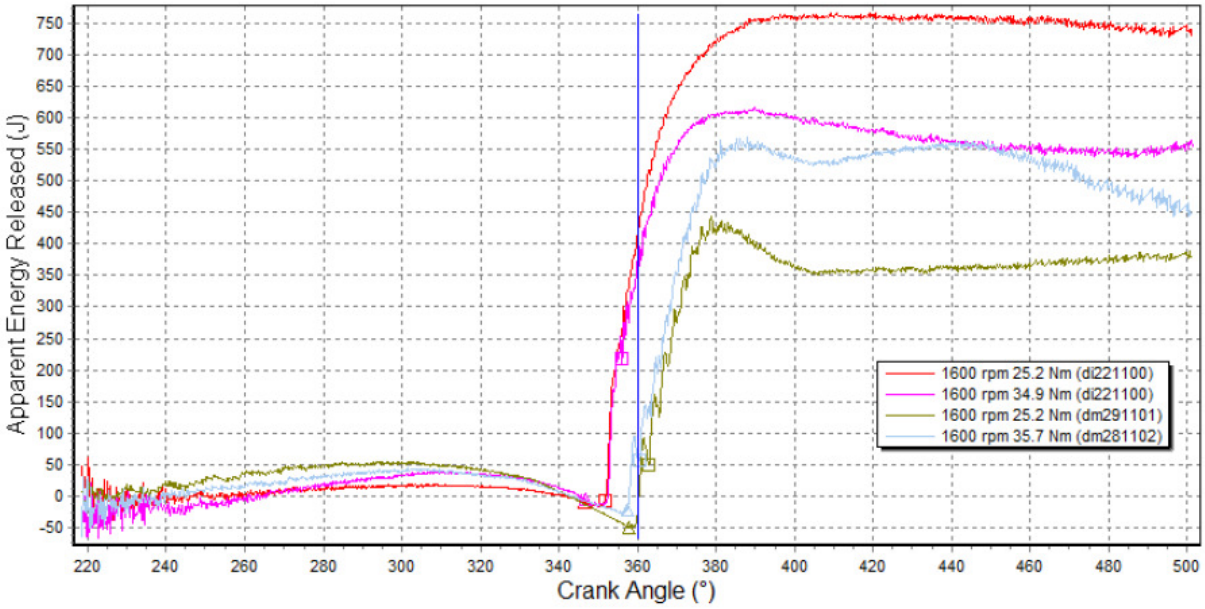


Figure 15: Energy Released vs. Crank Angle

The effects of fuel vaporisation and heating of the fuel are also evident in Figure 16 which is a graph of heat transfer vs. crank angle. Here it is evident that the heat transfer rate decreases towards the end of compression and for DME it flattens out and becomes negative, indicating that heat is absorbed by the fuel. Also evident in Figure 16 is how the fuel continues to burn long after injection is complete.

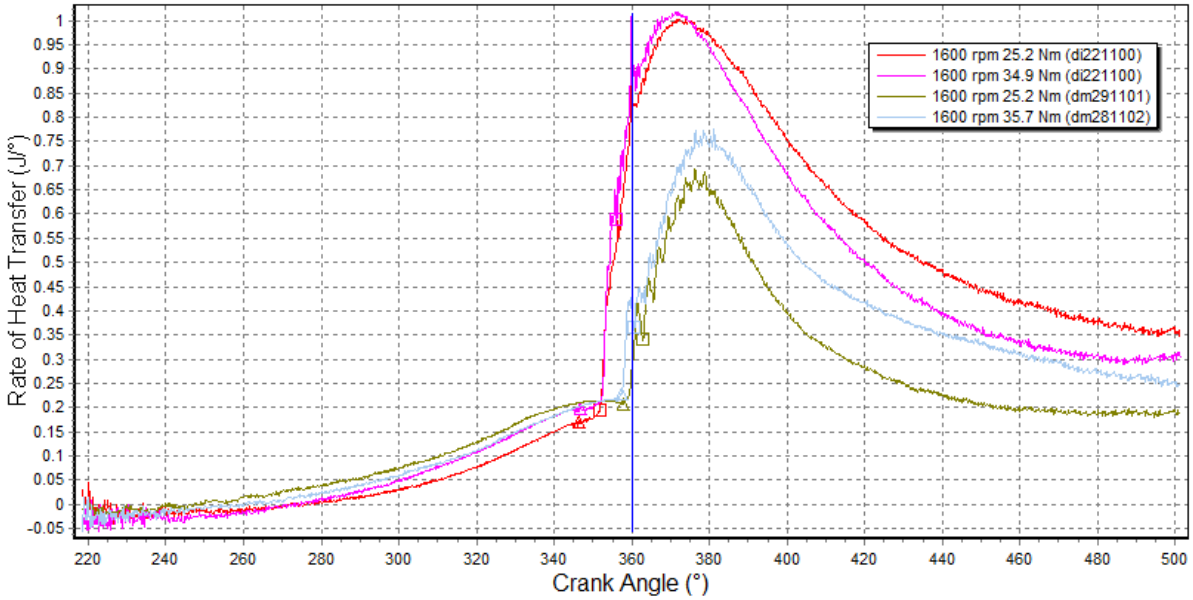


Figure 16: Rate of Heat Transfer vs. Crank Angle

6.2. Injection Characteristics

6.2.1. Introduction

This section begins with the analysis of the injector needle behaviour. A graph of injector needle lift vs. crank angle is shown. The graph was generated in HRCA by overlaying one of each of the following tests:

- A 1600 rpm diesel test at 25 Nm,
- A 1600 rpm DME test at 25 Nm,
- A 1600 rpm diesel test at 35 Nm,
- A 1600 rpm DME test at 35 Nm.

The graph illustrates the differences in behaviour of the injector needle whilst running on LP DME and on diesel, as well as the difference in behaviour whilst running at 25 Nm load and 35 Nm load. Differences occur for the following injection characteristics:

- Injection Duration.
- Injector Lift.
- Angle of Start of Injection.

The need to quantify these differences resulted in the generation of the following graphs:

- Injection duration vs. engine speed.
- Injector lift vs. engine speed.
- Angle of start of injection vs. engine speed.

These were generated in the following way:

1. For every test captured, for LP DME and diesel, at 25 Nm load and 35 Nm load, and at each speed setting the HRCA graph of injector needle lift vs. crank angle was generated.
2. From each graph the following data points were read off and captured:

    - Angle of start of injection.
    - Angle of end of injection.
    - Injector lift at start of injection.
    - Injector lift at peak of injection.

3. Injection duration was then calculated by subtracting angle of end of injection from angle of start of injection.
4. Injector lift was then calculated by subtracting injector lift at start of injection from injector lift at peak of injection.
5. For each engine speed an average was then taken of all the tests in order to find a mean data point for angle of start of injection, injection duration and injector lift.
6. The resulting mean data points were then plotted against engine speed.

Another graph of injector needle lift vs. crank angle illustrates the evidence of injector needle bounce for DME injection.

Next to be discussed is the behaviour of the fuel line pressure. A graph of fuel line pressure vs. crank angle is shown. The graph was generated in HRCA by overlaying one of each of the following tests:

- A 1600 rpm diesel test at 25 Nm,
- A 1600 rpm DME test at 25 Nm,
- A 1600 rpm diesel test at 35 Nm,
- A 1600 rpm DME test at 35 Nm.

The graph illustrates the differing behaviour of LP DME and diesel in the fuel line whilst running at 25 Nm load and 35 Nm load. Differences in the following injection characteristics are noticeable:

- Fuel Line Pressure,
- Rate of Fuel Line Pressure Change.

The need to quantify these differences resulted in the generation of the graph of fuel line pressure change vs. engine speed. The graph was generated in the following way:

1. For every test captured for LP DME and diesel, at 25 Nm load and 35 Nm load at each speed setting the HRCA graph of fuel line pressure vs. crank angle was generated.
2. From each graph the following data points were read off and captured:

    - Crank angle at start of pressure rise.
    - Crank angle at peak of pressure rise.
    - Fuel line pressure at start of pressure rise.
    - Fuel line pressure at peak of pressure rise.

3. Fuel line pressure difference was then calculated by subtracting fuel line pressure at peak of pressure rise from fuel line pressure at start of pressure rise.

4. The change in crank angle degrees between the peak of injection and the start of pressure rise was calculated by subtracting the crank angle at peak of pressure rise from the crank angle at start of pressure rise.
5. For each engine speed an average was then taken of all the tests in order to find a mean data point for fuel line pressure difference.
6. The resulting mean data point was then plotted against engine speed.

To calculate the rate of fuel line pressure rise the average fuel line pressure difference for each speed setting was divided by the change in crank angle degrees between peak fuel line pressure and start of fuel line pressure rise.

Also in this section are three graphs of specific fuel flow vs. engine speed. Each graph comprises an overlay of diesel specific fuel flow, HP DME specific fuel flow and LP DME specific fuel flow. Each graph represents the specific fuel flow of the engine under a specific load. The three loads used were 25 Nm, 35 Nm and 45 Nm. Since the data captured for the purposes of this report was limited to 25 Nm load and 35 Nm load and since for this report no HP DME data was captured, data was taken from the final year research report of Dave Morris (2005), i.e. reference 19, and is shown in Appendix F.

HP DME is an acronym for high pressure DME. This system was the original system used to supply the engine with DME. The difference between the two systems is explained by name, i.e. the HP DME supplies DME at a higher pressure than the LP DME system.

6.2.2. Error Analysis

The method used to generate the graphs for injection duration vs. engine speed, injector lift vs. engine speed and angle of start of injection vs. engine speed would have resulted in some errors.

In order to read the points off of the HRCA graphs, the cursor is used to locate the particular point of interest on the graph and then the coordinates of the cursors position are displayed in the bottom left hand corner of the plot window. However the coordinates that are displayed could have been erroneous by the following amounts:

- Injector lift:
    - Lift (y-axis): ± 0.001 mm
    - Crank angle (x-axis): ± 0.1°

- Injector pressure:
    - Pressure readings (y-axis): ± 0.05 MPa
    - Crank angle (x-axis): ± 0.1°

6.2.3. Analysis

Figure 17 shows a plot of injector lift vs. crank angle. It can again be seen that the injection of DME occurs later than that of diesel. The injection duration is greater for 35 Nm load than for 25 Nm for both LP DME and diesel. The injection duration is greater for DME than for diesel for both 35 Nm load and 25 Nm load. The later injection of DME will be discussed further on in this section. Also visible is that for both fuels injector needle lift is larger at 35 Nm.

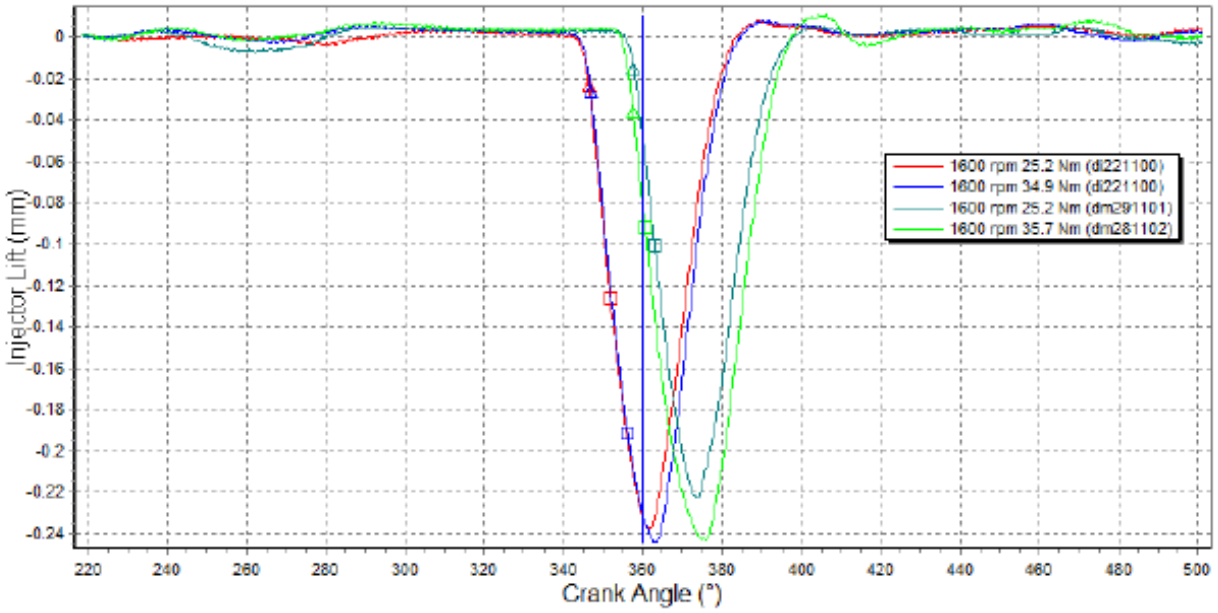


Figure 17: Injector Lift vs. Crank Angle

The injection duration is plotted against engine speed in Figure 18 and linear trend lines are used to illustrate the data pattern. The plot shows that for all of the tests, as the engine speed increases, the injection duration increases. It shows that at 25 Nm the difference in injection duration between DME and diesel is relatively small. By taking a mean of the data points over the speed range for each fuel, it is possible to say that injection duration of DME is on average 3% longer than for diesel. At 35 Nm however the injection duration of DME is on average 15% longer than that of diesel. For both fuels the rate of change of injection duration over the speed range is larger at 25 Nm than at 35 Nm. For both loads, the rate at which the duration increases is larger for DME than for diesel. Therefore the rate at which the duration increases is largest for DME at 25 Nm and smallest for diesel at 35 Nm. Visible in Figure 18 is that injector lift increases as the torque increases for DME.

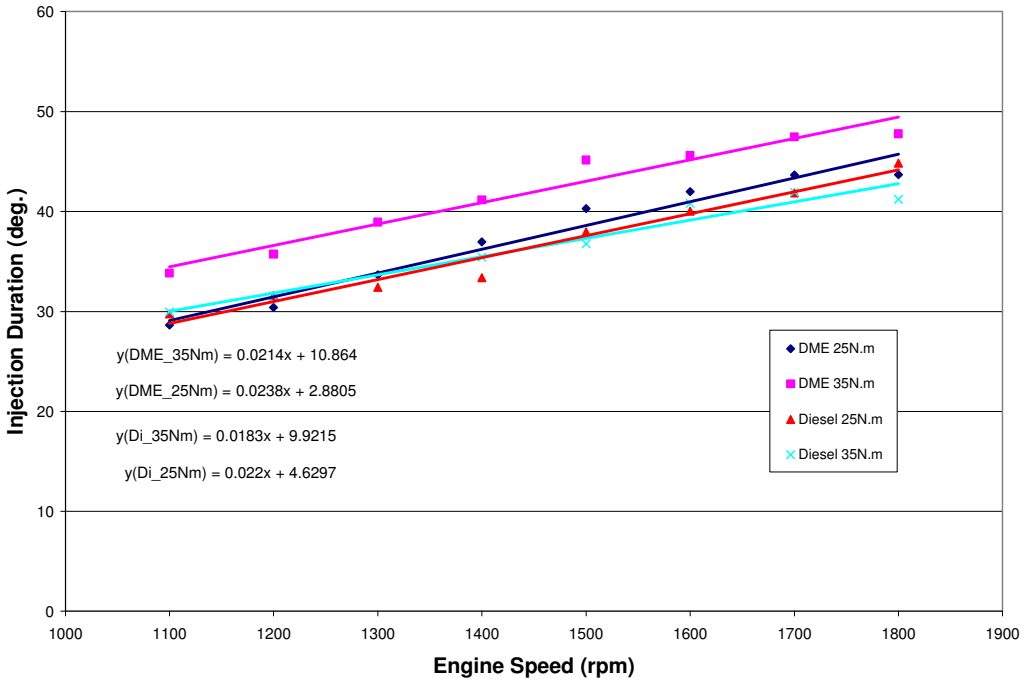


Figure 18: Injection Duration vs. Engine Speed

The relationship between the injector lift and engine speed is shown in Figure 19. Both DME tests closely follow a 2nd degree polynomial relationship with injector lift lowest at lower speeds then increasing to its highest point mid-way through the engine speed and then finally decreasing again. The diesel test data is represented by linear trend lines, both of which have positive gradients with very minimal increases in injector lift as the engine speed increases. For both fuels, injector lift is greatest at the higher torque. By taking a mean of the data points over the speed range for each fuel, it is found that injector lift for diesel is on average 1 % greater at 35 Nm load than for 25 Nm load. Injector lift for DME is on average13 % greater at 35 Nm load than for 25 Nm load.

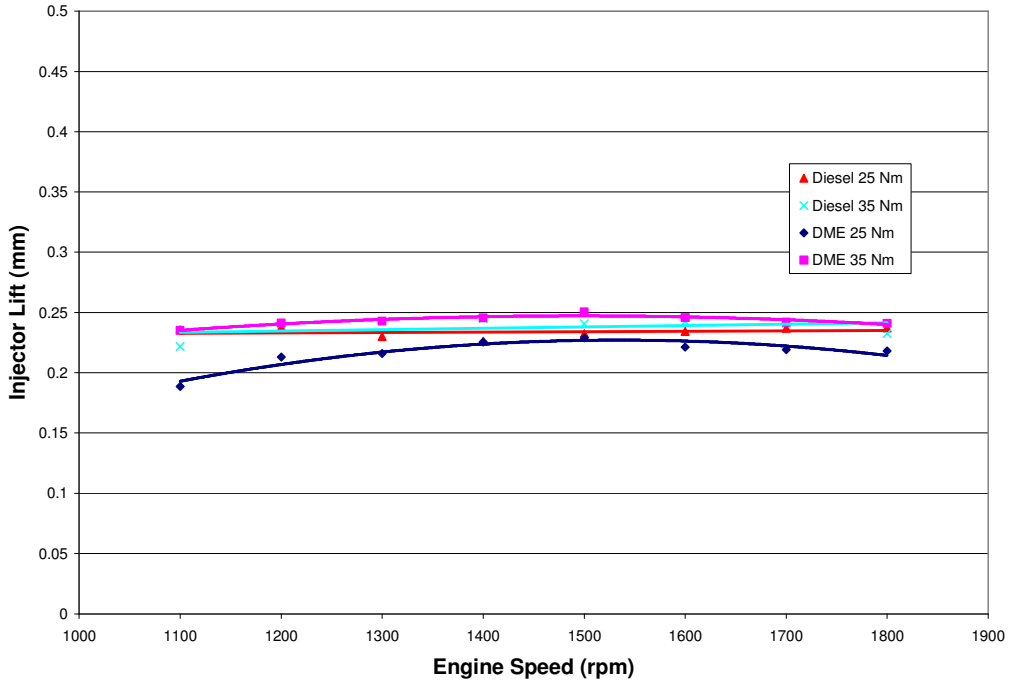


Figure 19: Injector Lift vs. Engine Speed

In Figure 17 the plot of DME at 35 Nm shows an irregular oscillation of the injector needle after injection ends. These oscillations are again shown in Figure 20. This phenomenon is known as injector needle bounce and is most prominent at higher engine speeds for DME. It is thought that inwardly opening injectors are more prone to needle bounce [7]. The reason for the needle bounce being so much more noticeable in DME than in diesel could be because the DME is more compressible and has a lower acoustic velocity. As a result, when the needle is closed, large pressure waves from the pump may still be travelling through the fluid and will only reach the injector a small time later.

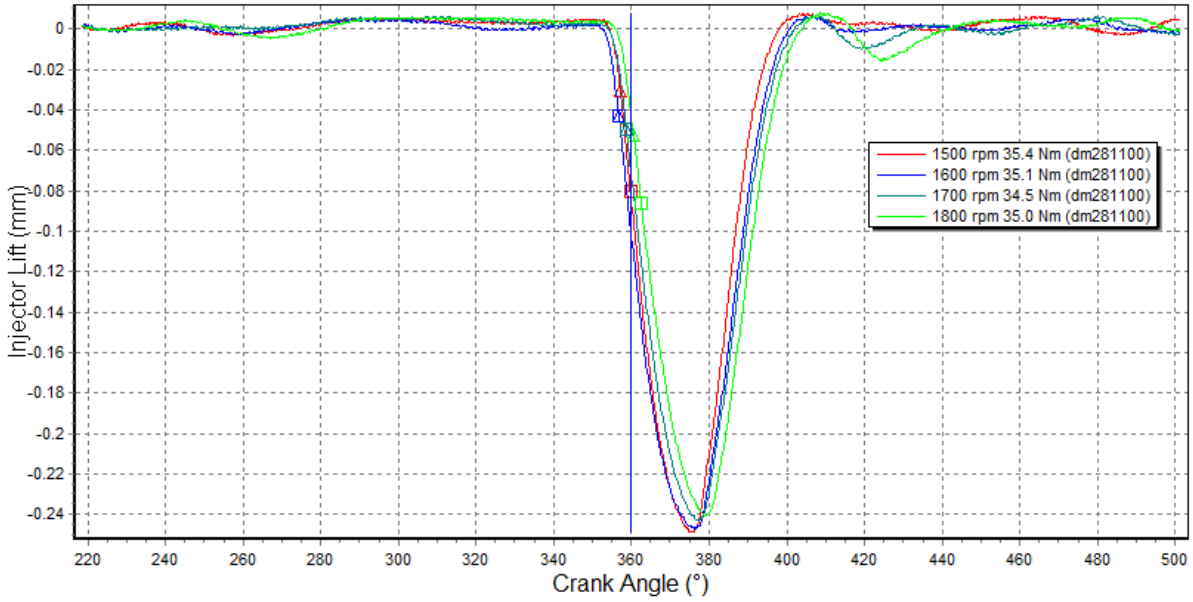


Figure 20: Oscillations of injector needle

The difference between the start of injection of diesel and the start of injection of DME indicates that there is a greater injection lag for DME than for diesel. This means that the time that it takes for the first pressure wave to travel from the pump to the nozzle is longer for DME than for diesel, and as a result the pressure build up is slower for DME than for diesel.

The acoustic velocity of a fluid will determine how quickly a pressure wave will travel through the fluid. It is suspected that the acoustic velocity of diesel is greater than that of DME so pressure waves travel faster through diesel than DME. As a result pressure builds more rapidly in diesel than in DME. Physical

properties that affect acoustic velocity are modulus of elasticity and fluid density. Since the modulus of elasticity and fluid density of both the fluids is known, it is possible to establish theoretically what the difference in acoustic velocity is between diesel and DME.

The relationship between the modulus of elasticity of the two fluids is shown below. Properties of diesel are taken at ambient temperature and pressure, while properties of DME are taken from Table 22 at a temperature of 10℃ and pressure of 12.5 MPa. These are the conditions that the fuels are under when supplied to the engine.

K_{Di} = 1490 MPa;
K_{DME} = 777 MPa.

Where K_{DME} is the modulus of elasticity of DME and K_{Di} is the modulus of elasticity of diesel.

$$\frac{K_{DME}}{K_{Di}} = 0.52$$

I.e. the modulus of elasticity of DME is 52% that of diesel.

The relationship between the densities of the two fluids is as follows:

ρ_{Di} = 840 kg/m^3;
ρ_{DME} = 704 kg/m^3

Where ρ_{DME} is the density of DME and ρ_{Di} is the density of diesel.

$$\frac{\rho_{DME}}{\rho_{Di}} = 0.84$$

I.e. the density of DME is 84% that of diesel.

Theoretically the differences in density and bulk modulus will have the following effect on the acoustic velocity:

$$V_{DME} \approx \sqrt{\frac{K_{DME}}{\rho_{DME}}}$$
$$\approx \sqrt{\frac{0.52K_{Di}}{0.84\rho_{Di}}}$$
$$\approx \sqrt{0.62\frac{K_{Di}}{\rho_{Di}}}$$
$$\approx 0.79\sqrt{\frac{K_{Di}}{\rho_{Di}}}$$
$$\approx 0.79 \times V_{Di}$$

This means that theoretically the acoustic velocity of DME is 79 % that of diesel and therefore pressure waves travelling through DME travel at 79% of the velocity that pressure wave's travel through diesel. As a result, injection lag is longer for DME.

The difference in injection lag over the speed range is evident in Figure 21 which is a plot of angle of start of injection vs. engine speed. The DME tests both follow a 2nd degree polynomial relationship as in both tests the injection is later towards the start and end of the engine speed range and is earlier at the mid-way engine speeds. Towards the end of the speed range, the 25 Nm test shows injection beginning later than the 35 Nm test. It is assumed that both the diesel tests follow a linear relationship. Both tests show a very small but positive gradient indicating that as the engine speed increases the start of injection occurs later. Throughout the speed range, at both torque settings, the DME injection occurs later than the diesel injection. By taking a mean of the data points over the speed range for each fuel, it is possible to say that for the 25 Nm tests, on average, the DME injection begins 3.1% later than the diesel injection, while for the 35 Nm tests, the DME injection begins 2.9% later than the diesel injection.

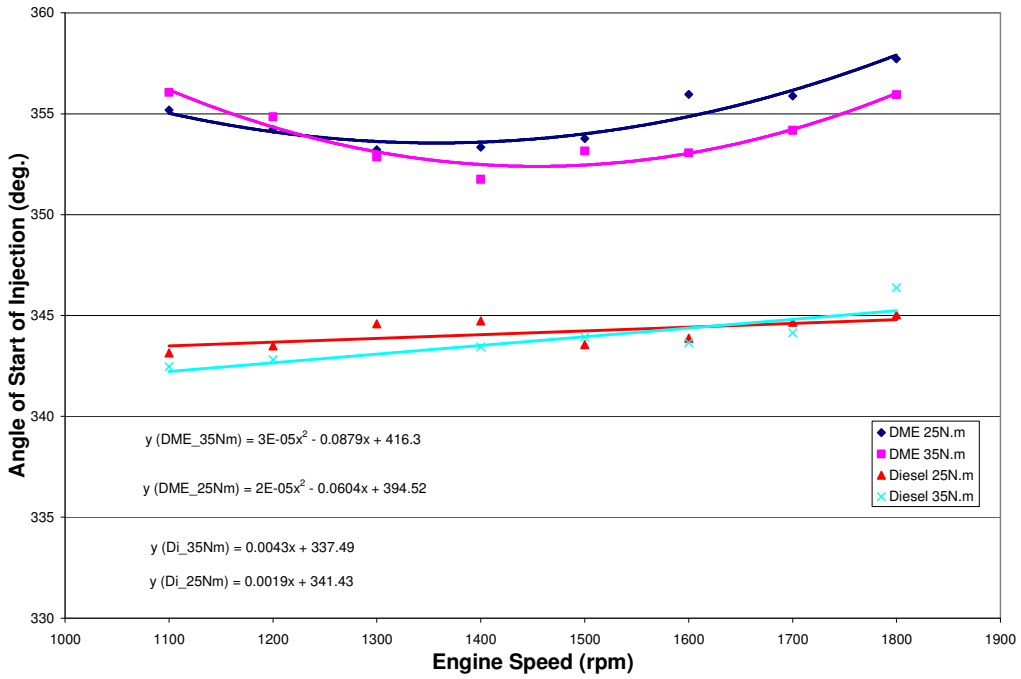


Figure 21: Angle of Start of Injection vs. Engine speed

Figure 22 illustrates fuel line pressure vs. crank angle. It shows that for DME, fuel line pressure begins to build only about 5 degrees of crank angle after that of diesel, and it shows that pressure builds at a much slower rate for DME than for diesel. Also evident is that the fuel line pressure difference (i.e. the difference between the peak pressure and the pressure in the line before pressure begins to rise) is lower for DME than for diesel.

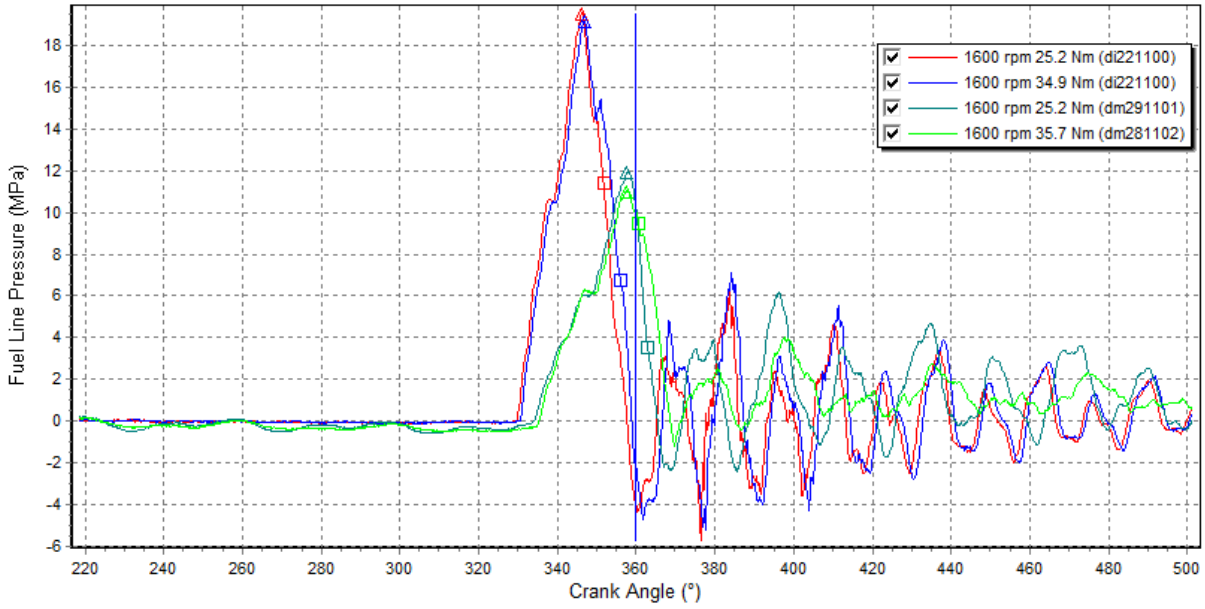


Figure 22: Fuel Line Pressure vs. Crank Angle

Figure 23 is a plot of the fuel line pressure change vs. engine speed. The pressure difference is largest for diesel at 25 Nm while the 35 Nm DME test shows the smallest pressure difference. By taking a mean of the data points over the speed range for each fuel, it is possible to say that, on average, the pressure difference of DME is approximately 60% less than diesel for both 25 Nm and 35 Nm loads. The pressure difference at the lower engine speeds is smaller than at higher engine speeds for all of the tests indicating a positive gradient. The increase in the pressure difference over the speed range is most significant for diesel; this is evident by the larger gradient for the diesel plots than the DME plots.

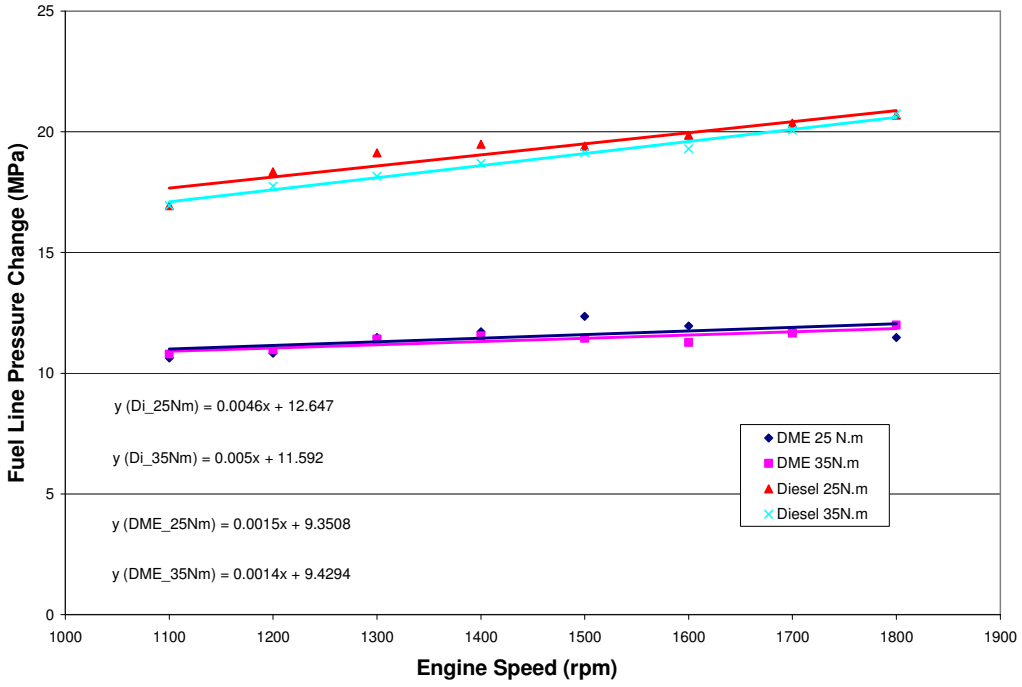


Figure 23: Fuel Line Pressure Change vs. Engine Speed

The amplitude of a pressure wave generated in a hydraulic system is dependant on the velocity that the disturbance is created at, as well as the physical properties of the fuel, namely the density and the bulk modulus. In the situation where DME and then diesel is used, the velocity of the disturbance, namely the pump plunger velocity does not change, therefore only the difference in density and the difference in bulk modulus will affect the pressure wave magnitude. Theoretically the relationship is as follows:

$$P_{DME} \approx \sqrt{K_{DME} \times \rho_{DME}}$$
$$\approx \sqrt{0.52K_{Di} \times 0.84\rho_{Di}}$$
$$\approx 0.66\sqrt{K_{Di} \times \rho_{Di}}$$
$$\approx 0.66P_{Di}$$

I.e. the amplitude of a wave generated in the system while using DME will be 66% of the magnitude of a wave generated in the same system using diesel.

For DME, the peak fuel line pressure, which happens to be the pressure at which injection occurs, is only reached about 15 degrees after the start of pressurisation, whereas for diesel the peak fuel line pressure is reached about 5 degrees after the start of pressurisation. Theoretically the pressure is a function of the crank angle because the plunger velocity is a function of crank angle. This relationship is visible in Figure 23, where the pressure change increases as the engine speed increases. As the plunger velocity increases so does the pressure. If it is considered that the velocity of the plunger increases by an amount v_1, and as a result the pressure of the diesel system increases by an amount P_1, then the pressure increase in the DME system will be $0.59P_1$. Every successive increase of the velocity would result in an increase in the pressure, and every pressure increase developed in the DME system will be 60% of the equivalent increase developed in the diesel system. The result is that the pressure rise of diesel is much steeper than that of DME. The results show an average rate of pressure rise (dP/d(CrankAngle)) for diesel of approximately 1.2 MPa/Crank Angle Degree, while the average rate of pressure rise for DME is about 0.5 MPa/Crank Angle Degree.

Most particularly of concern is the fuel mass flow rate and hence mass of fuel injected, because the mass of fuel injected is directly proportional to the energy produced and hence the power generated by the engine. Also directly affected are the fuel consumption and exhaust emissions. The injected fuel mass is dependant on the injection duration, fuel density and the pressure difference. Theoretically the relationship is as follows:

$$\dot{m} \approx \sqrt{\rho_f \times \Delta P}$$

And,

$$m \approx \dot{m} \times t_{inj}$$
$$\approx \sqrt{\rho_f \times \Delta P} \times t_{inj}$$

Where $\dot{m}$ is the mass flow rate, ρ_f is the fuel density, ΔP is the fuel line pressure change, m is the mass of fuel injected and t_{inj} is the injection duration.

Since theoretically the fuel line pressure difference of the system on DME will be 66% of that of diesel, and the fuel density of DME is 84 % that of diesel, then theoretically the mass flow rate of fuel injected should be affected in the following way:

$$\dot{m}_{DME} \approx \sqrt{\rho_{DME} \times \Delta P_{DME}}$$
$$\approx \sqrt{0.84\rho_{Di} \times 0.66\Delta P_{Di}}$$
$$\approx 0.75\sqrt{\rho_{Di} \times \Delta P_{Di}}$$
$$\approx 0.75\dot{m}_{Di}$$

Since the density of DME is 84% that of diesel, for the same volume of fuel, the mass of DME will be 84% that of diesel. This is indeed the case as the volume of the fuel injector chamber remains unchanged for both fuels. Therefore:

$$\frac{m_{DME}}{m_{Di}} = 0.84$$

In order for the same mass of DME to be injected, the theoretical required duration of injection for DME can be calculated in the following way:

$$\frac{m_{DME}}{m_{Di}} = 1$$

$$\frac{\dot{m}_{DME} \times t_{injDME}}{\dot{m}_{Di} \times t_{injDi}} = 1$$

$$\frac{0.75\dot{m}_{Di} \times t_{injDME}}{\dot{m}_{Di} \times t_{injDi}} = 1$$

$$\frac{t_{injDME}}{t_{injDi}} = \frac{1}{0.75}$$

$$t_{injDME} = 1.33 t_{injDi}$$

I.e. the DME injection duration should be 33% longer than diesel in order to have the same mass of fuel injected.

However, even an increase in injection duration would not alone compensate for the difference in the heating values of the two fuels. Considering the difference in the heating values of the two fuels, the following relationship is obtained.

$Q_{HV.DME}$= 28 MJ/kg
$Q_{HV.Di}$= 42.5 MJ/kg

Where Q_{HV} is the heating value of the fuel.

$$\frac{Q_{HV.DME}}{Q_{HV.Di}} = 0.67$$

I.e. the heating value of DME is 67% of that of diesel.

Theoretically the fuel energy can be compared in the following way when the effects of the heating value and fuel mass are considered.

$$
\begin{aligned}
&E_{DME} \approx m_{DME} \times Q_{HV.DME} \\
&\approx 0.84 m_{Di} \times 0.67 Q_{HV.Di} \\
&\approx 0.56 m_{Di} \times Q_{HV.Di} \\
&\approx 0.56 E_{Di}
\end{aligned}
$$

Where E is the energy in the fuel.

So theoretically the energy in the DME fuel is only 56% of that of diesel.

To obtain the same power output from the engine while running on DME and diesel, the following should happen:

$$\frac{PO_{DME}}{PO_{Di}} = 1$$

Where PO is the power produced.

However power is equal to the energy produced per time period. So since the period of time that the engine operates for is the same for both fuels, the following can be deduced:

$$
\begin{aligned}
&\frac{E_{DME}}{E_{Di}} = 1 \\
&\frac{m_{DME} \times Q_{HV.DME}}{m_{Di} \times Q_{HV.Di}} = 1 \\
&\frac{m_{DME} \times 0.67 Q_{HV.Di}}{m_{Di} \times Q_{HV.Di}} = 1 \\
&\frac{m_{DME}}{m_{Di}} = \frac{1}{0.67} \\
&m_{DME} = 1.49 m_{Di}
\end{aligned}
$$

So theoretically, by considering the effects of heating value, 50% more DME than diesel is required to obtain the same power.

This can be obtained by either increasing the injection duration, as is what currently happens, or by increasing the mass flow rate.

Increasing the injection duration would not be a desirable characteristic since injecting fuel into the combustion chamber once the crank angle has progressed too far past TDC would probably result in incomplete combustion of some of the fuel. As a result improving the fuel mass flow rate will be investigated.

By assuming the injection duration to be the same for both fuels, it is possible to establish the effects of fuel density and fuel line pressure change as follows:

$$\frac{\dot{m}_{DME} \times t_{injDME}}{\dot{m}_{Di} \times t_{injDi}} = \frac{1}{0.67}$$

But the injection duration is the same so:

$$\frac{\dot{m}_{DME}}{\dot{m}_{Di}} = \frac{1}{0.67}$$

$$\frac{\sqrt{\rho_{DME} \times \Delta P_{DME}}}{\sqrt{\rho_{Di} \times \Delta P_{Di}}} = \frac{1}{0.67}$$

$$\frac{\rho_{DME} \times \Delta P_{DME}}{\rho_{Di} \times \Delta P_{Di}} = \left(\frac{1}{0.67}\right)^2$$

$$\frac{\rho_{DME} \times \Delta P_{DME}}{\rho_{Di} \times \Delta P_{Di}} = 2.23$$

$$\rho_{DME} \times \Delta P_{DME} = 2.23\left(\rho_{Di} \times \Delta P_{Di}\right)$$

So in order to get the same power output using DME it is necessary to increase the fuel density and change in injection pressure of DME such that the product of the two increases will result in a factor of 2.23. By increasing the injection pressure, the density of the fuel will also increase. With reference to Table 24, by increasing the injection pressure to 27 MPa the density of DME will increase to approximately 695 kg/m^3. The combination of the density increase and pressure increase results in the following factor increase:

$$\frac{27MPa}{12MPa} \times \frac{695kg/m^3}{676kg/m^3} = 2.250 \times 1.028 = 2.31$$

This is larger than 2.23 and theoretically would be a sufficient increase to obtain the same power output.

Figure 24 shows that for 25 Nm load the HP DME fuel flow is higher than that of diesel fuel flow over the entire speed range. For both the HP DME and diesel plots, the specific fuel flow decreases as the engine speed increases. For the LP DME plot the specific fuel flow increases as the engine speed increases. With reference to Table 42, when averaged over the entire speed range, the specific fuel flow of the LP DME is 88 % of that of HP DME specific fuel flow and 97 % of that of the diesel specific fuel flow.

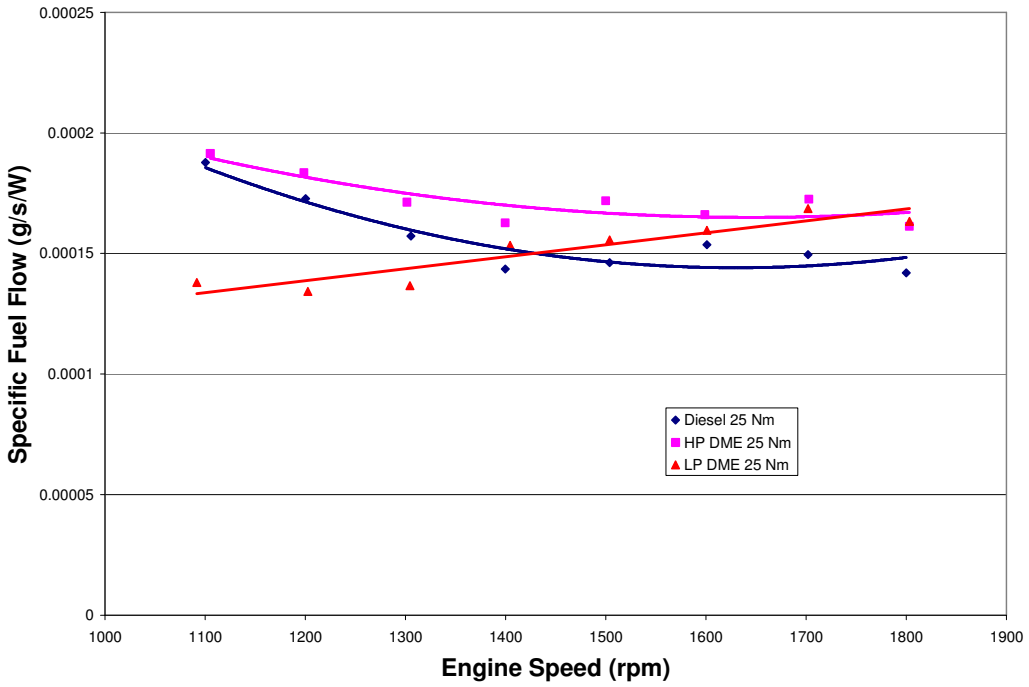


Figure 24: Specific Fuel Flow vs. Engine Speed at 25 Nm

As is shown in Figure 25, at 35 Nm load the diesel specific fuel flow decreases as the engine speed increases. For the LP DME and HP DME, specific fuel flow starts high, decreases as the engine speed increases, then towards the middle of the speed range they begin to increase again until ending at approximately the same specific fuel flow as they started. If averaged over the entire speed range, the specific fuel flow of the LP DME is 17 % more than that of HP DME specific fuel flow and 28 % more than that of the diesel specific fuel flow.

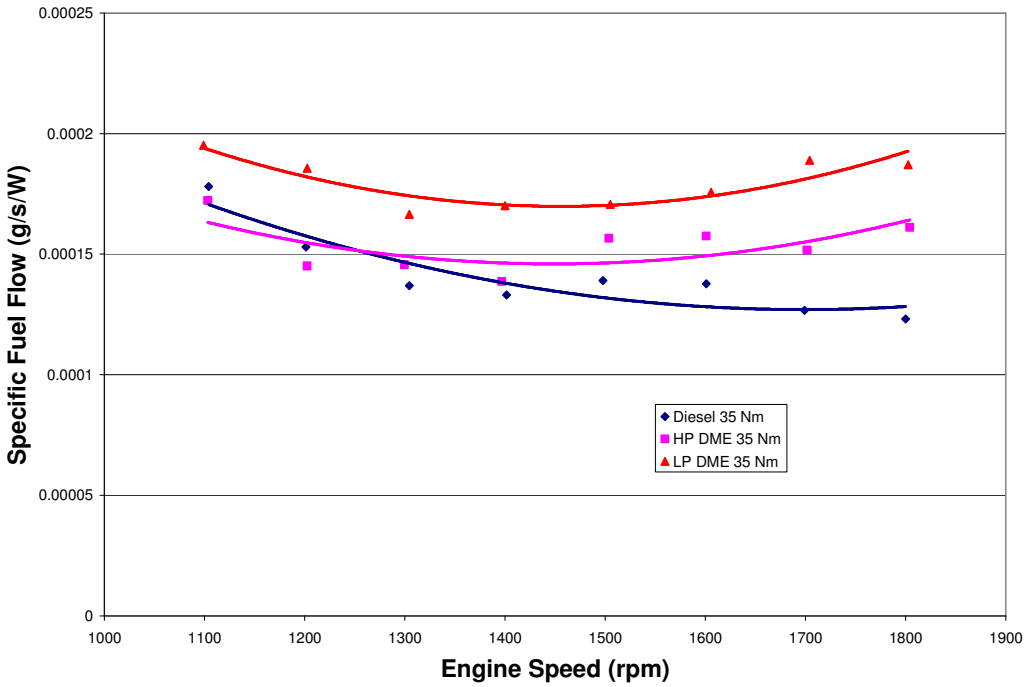


Figure 25: Specific Fuel Flow vs. Engine Speed at 35 Nm

Specific fuel flow at 45 Nm load is shown in Figure 26. Here, for HP DME, the specific fuel flow decreases as the engine speed increases. For the LP DME and diesel, specific fuel flow starts high, decreases as the engine speed increases, then towards the middle of the speed range they begin to increase again until ending slightly higher than the lowest point. When averaged the specific fuel flow of the LP DME is 46 % more than that of HP DME specific fuel flow and 39 % more than that of the diesel specific fuel flow.

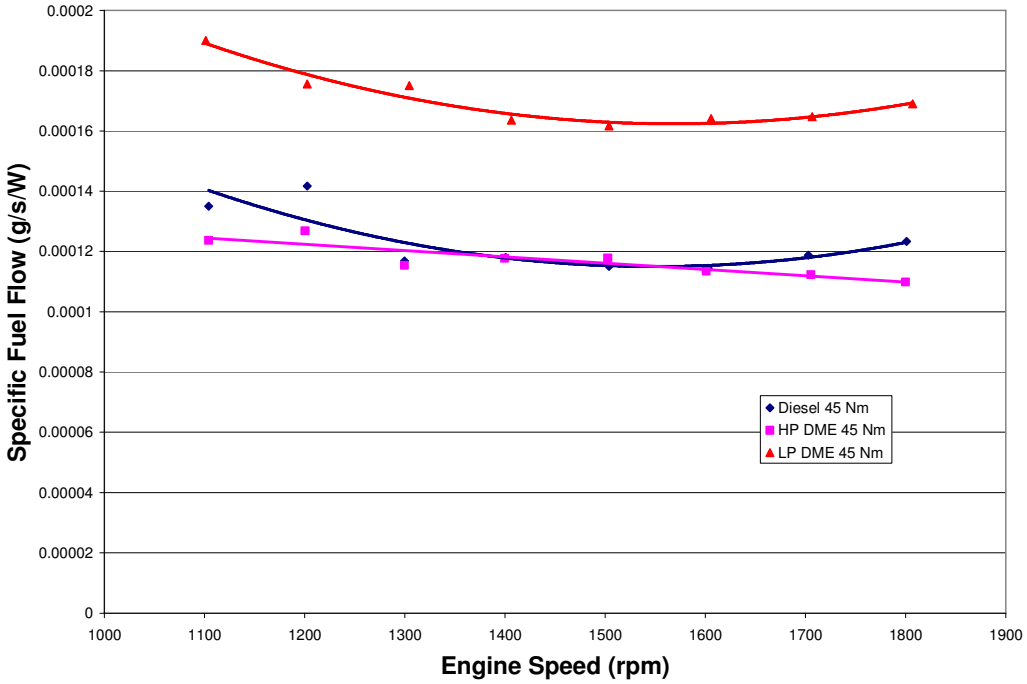


Figure 26: Specific Fuel Flow vs. Engine Speed at 45 Nm

6.3. Emissions

6.3.1. Introduction

This section contains a very brief analysis of the emissions data, as much greater emphasis was placed on the study of the injection characteristics. The section contains three graphs, namely:

- Specific NOx vs. engine speed.
- Specific CO_2 vs. engine speed.
- Specific CO vs. engine speed.

The graphs are generated with the intention of illustrating the difference in emissions characteristics of the engine whilst running on the LP DME fuelling system, the HP DME fuelling system and on diesel. The load and engine speed are kept constant, namely 45 Nm and 1600 rpm respectively. Since no data was captured for 45 Nm load, once again the data from the final year report of Dave Morris (2005) was used. The specific fuel flow was found by dividing the parts per million emissions data by the power; this was done for each speed.

6.3.2. Analysis

Figure 27 shows that specific NOx is higher for HP DME than for LP DME. In both DME cases the specific NOx starts out higher than diesel then becomes less than diesel as the engine speed increases. This indicates that the effect of decreased volumetric efficiency has a far larger effect on NOx formation for DME. The formation of NOx may also be favoured at first due to the 34.8% oxygen content of DME. For diesel, the specific NOx increases up to close to the middle of the speed range at which point it decreases until the end of the speed range. This would indicate that at first NOx formation in diesel is more dependant on temperature and then the effect of the decreasing volumetric efficiency becomes more significant.

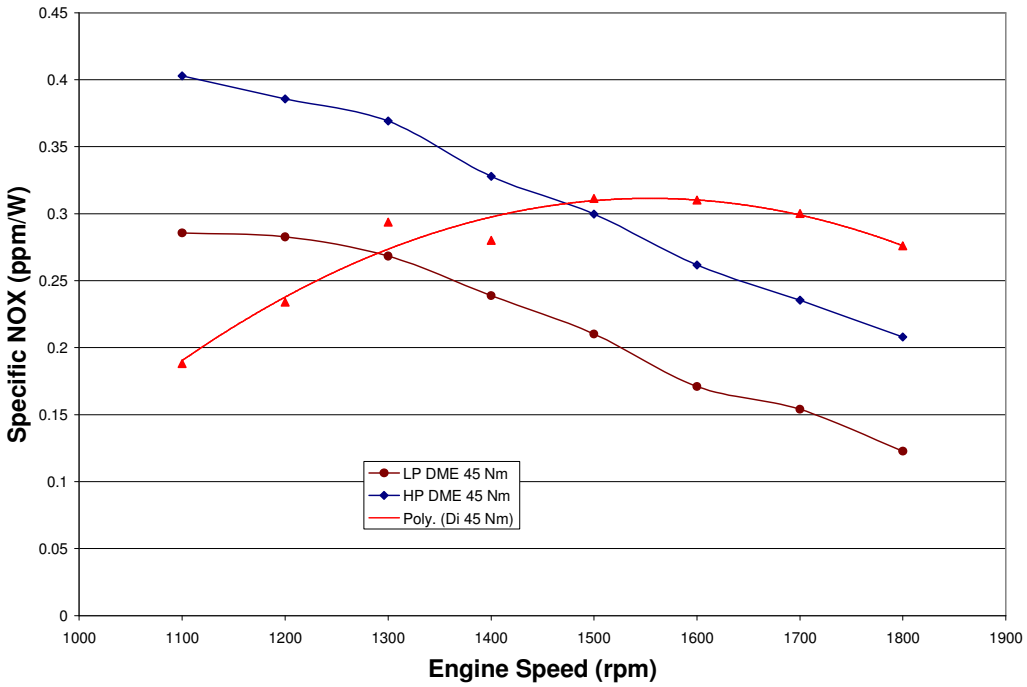


Figure 27: Specific NOx vs Engine Speed

In all of the CO_2 plots shown in Figure 28 the specific CO_2 begins low then increases as the engine speed increases, it then flattens out and finally decreases. The specific CO_2 values are higher for both DME plots than diesel across the speed range with HP DME being the highest of all.

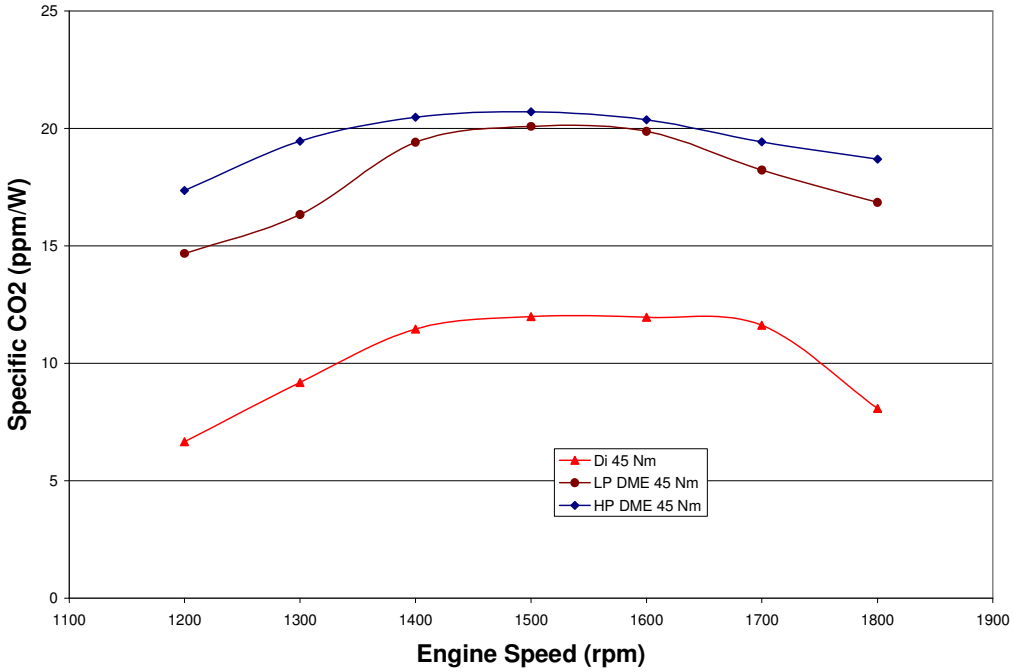


Figure 28: Specific CO_2 vs Engine Speed

In Figure 29 specific CO emissions for diesel and LP DME follow similar trends. The specific CO begins high and then decreases exponentially with engine speed. Diesel specific CO emissions are the highest of the three plots. The specific CO for HP DME is the lowest of the three plots and remains relatively unchanged over the speed range.

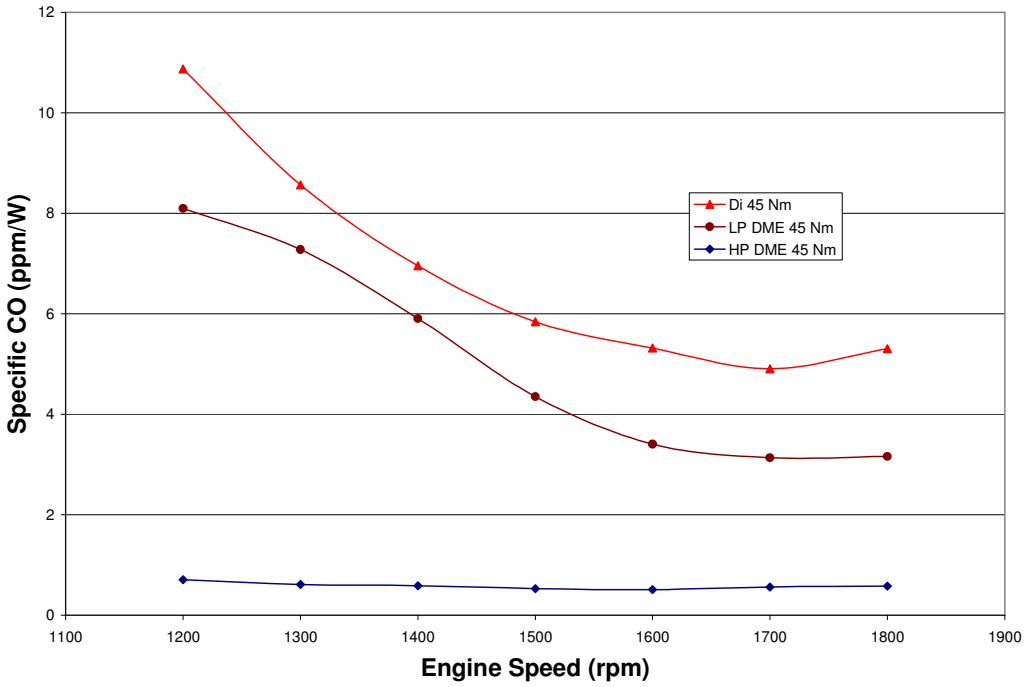


Figure 29: Specific CO vs Engine Speed

Figure 28 and Figure 29 follow the chemical equilibrium equation shown in Section 2.5.3, as for HP DME when specific CO_2 is highest the specific CO is lowest. This may suggest that the flame temperature for HP DME is high thus favouring the production of CO_2 over CO [1]; the opposite is true for diesel. However another reason for such behaviour of diesel could be attributed to the fact that diesel has no oxygen content in its molecular structure whereas DME consists of 34.8% oxygen thus favouring the conversion of the carbon in the fuel into carbon dioxide.

7. Conclusions

From the discussion it is concluded that the engine requires more fuel to achieve the same power output when running on DME as compared to when it runs on diesel. It was established that the start of injection occurs later for DME than for diesel and the injection duration for DME is longer than for diesel. Start of injection begins later as the pressure build up in the fuel line takes longer for DME than for diesel. Fuel line pressure is lower for DME than for diesel when injection occurs. The injection duration is longer for DME than for diesel as the engine requires more fuel to obtain the same power output. It is believed that these characteristics are undesirable as this would result in incomplete combustion of the fuel resulting in poor emissions.

The results and discussion indicate that the specific NOx for both DME cases starts out higher than diesel. It then becomes less than diesel as the engine speed increases. Specific NOx formation is higher for HP DME than for LP DME.

Specific CO_2 formation shows that for both DME cases as well as diesel specific CO_2 begins low then increases as the engine speed increases. It then stabilises and finally decreases. The specific CO_2 values are higher for both DME plots than diesel across the speed range with HP DME being the highest of all.

Specific CO emissions for diesel and LP DME follow similar trends, that is, the specific CO begins high and then decreases exponentially with engine speed. Diesel specific CO emissions are the highest of the three plots. The specific CO for HP DME is the lowest of the three plots and remains relatively stable over the speed range.

8. Recommendations

It is believed that DME should be stored and injected at a higher pressure, as this would result in a higher density for DME and as a result a larger mass of fuel would be injected. However this alone will not solve the problem, the injection of the fuel should occur earlier.

In order to have complete control over the injection system it is recommended that a common rail injection system with solenoid operated injector valves replace the existing injection system. Also necessary would be a control unit which would be used to accurately control and measure the stored pressure of the fuel, the injection pressure, the injection duration and the injection timing by controlling the operation of the common rail pump and the injector valve solenoids. Also necessary from the control unit would be the ability to switch between different programs for different fuels. This would allow the injection pressure, injection duration and injection timing to be programmed for a specific fuel with physical properties which may vary from another fuel to be used in the same system. By using a common rail it is hoped that the same power will be produced with better emissions results as the control afforded will result in improved combustion of the fuel.

9. References

1. Heywood JB, (1988), “Internal Combustion Engine Fundamentals”, McGraw-Hill, New York.
2. United States Environmental Protection Agency, INTERNET: http://epa.gov/climatechange/emissions/index.html, Cited 2 December 2008.
3. Natural Resources Defence Council, INTERNET: http://www.nrdc.org/globalWarming/fcons.asp, Cited 2 December 2008.
4. Kreger C, (2004), Exploring the environment, INTERNET: http://www.cotf.edu/ete/modules/carbon/efcarbon.html, cited 3 April 2006.
5. Copyright Ecopoint Inc, (2007), DieselNet, INTERNET: http://www.dieselnet.com/standards/eu/ld.php, Cited 2 December 2008.
6. Moran MJ and Shapiro HN, (1998) “Fundamentals of Engineering Thermodynamics”, John Wiley & Sons Ltd, West Sussex, England.
7. Burman PG and DeLuca F, (1962), “Fuel Injection & Controls: For Internal Combustion Engines”, Simmons-Boardman Publishing Corporation.
8. Borman GL, Ragland KW, (1998), “Combustion Engineering”, McGraw-Hill.
9. Sorensen SC, Glensvig M, Abata DL, (1998), “Dimethyl Ether in Diesel Fuel Injection Systems”, SAE International Congress and Exposition SAE 981159.
10. Cipolat D, (2005) “Engine Design and Operating Parameters”, MECN 469 Course notes.
11. Cipolat D, (2005), “Thermochemistry of fuel-air mixtures”, MECN 469 Course notes.
12. EPA National Vehicle and Fuel Emissions Laboratory, (2006), Feather River Air Quality Management District, INTERNET: http://www.fraqmd.org/autoemissions.htm, Cited 2 December 2008.
13. Vehicle Emissions: An Overview, http://www.fraqmd.org/autoemissions.htm
14. Ogawa T, Inoue N, Shikada T, Ohno Y, (2003) “Direct Dimethyl Ether Synthesis”, Journal of Natural Gas Chemistry 12 219-227.
15. Production of Dimethyl Ether, West Virginia University's Department of Chemical Engineering, (2002), INTERNET: http://www.che.cemr.wvu.edu/publications/projects/large_proj/dimethyl_ether.PDF, Cited 2 December 2008.
16. Chanka T, (2004), “Optimisation of the Performance of a Compression Ignition Engine Fuelled on Ether Fuel”, 4th Year Research Project for the University of the Witwatersrand.

17. Murray K, (2003), “Optimisation of the Performance of a Compression Ignition Engine Fuelled on Ether Fuel”, 4th Year Research Project for the University of the Witwatersrand.
18. Groess K, (2005), “Fuelling of a Compression Ignition Engine on Low Pressure DME”, MSc Research Project for the University of the Witwatersrand.
19. Morris D, (2005), “Evaluation of a Low Pressure Fuelling System for a Compression Ignition Engine”, 4th Year Research Project for the University of the Witwatersrand.
20. Robert Bosch GmbH, (2004), Swedespeed, INTERNET: http://www.swedespeed.com/news/publish/Features/printer_272.html, cited 3 April 2006.
21. Kaczor MS, (2002), “A Comparative Study of the Combustion and Emissions of a Compression Ignition Engine Fuelled on diesel and Dimethyl Ether”, MSc Research Project for the University of the Witwatersrand.
22. Lopes PMP, (2002), “A Comparative Study of the Combustion and Emissions of a Compression Ignition Engine Fuelled on diesel and Dimethyl Ether”, MSc Research Project for the University of the Witwatersrand.
23. Huang ZH, Wang HW, Chen HY, Zhou LB and Jiang DM, (1999), “Study of combustion characteristics of a compression ignition engine fuelled with dimethyl ether.”, Proceedings Institution of Mechanical Engineers Vol 213 Part D, IMechE.
24. Sorensen SC, Mikkelson SE, (1995), “Performance and Emissions of a 0.273 Litre Direct Injection Diesel Engine Fuelled with Neat Dimethyl Ether.”, SAE International Congress and Exposition, SAE 950064.

A Appendix – Calibration

The equipment used during the research was all previously calibrated unless otherwise stated. The data and procedures from the calibrations are shown below and are referenced from a previous project [17].

A.1 Fuel Flow Calibration

- The fuel is to be bled through the fuel flow meter into a container positioned on an electronic scale.
- While the fuel is running through the meter the input voltage to the data acquisition system is recorded. Due to the sensitivity of the instrument an upper and lower voltage reading are taken and an average is subsequently determined.
- The time taken to collect a certain mass of fuel is noted. From this information the mass flow rate can be calculated.
- The fuel flow is increased for each consecutive reading.
- The results are tabulated and then plotted. A linear curve is fitted to the data so as to determine the calibration constants for the data acquisition system.

Table 6: Fuel Flow Calibration Data

Voltage max (V)	Voltage min (V)	Average Voltage	Fuel mass (g)	Time (s)	Massflow (g/s)	Fuel flow (l/h)
0.026	0.030	0.028	0.0	120	0.000	0.0
0.543	0.545	0.544	40.8	120	0.340	1.0
1.025	1.080	1.052	80.8	120	0.673	2.2
1.541	1.553	1.547	118.4	120	0.986	3.2
1.863	1.883	1.873	144.6	120	1.205	4.0
2.264	2.272	2.268	177.2	120	1.476	5.0
2.274	2.754	2.513	213.4	120	1.778	6.0
3.192	3.209	3.200	248.5	120	2.070	7.0
3.750	3.761	3.755	292.2	120	2.435	8.4
3.990	3.999	3.994	309.7	120	2.580	9.0
4.588	4.599	4.593	352.2	120	2.935	10.4
4.910	4.921	4.915	183.7	60	3.061	11.2

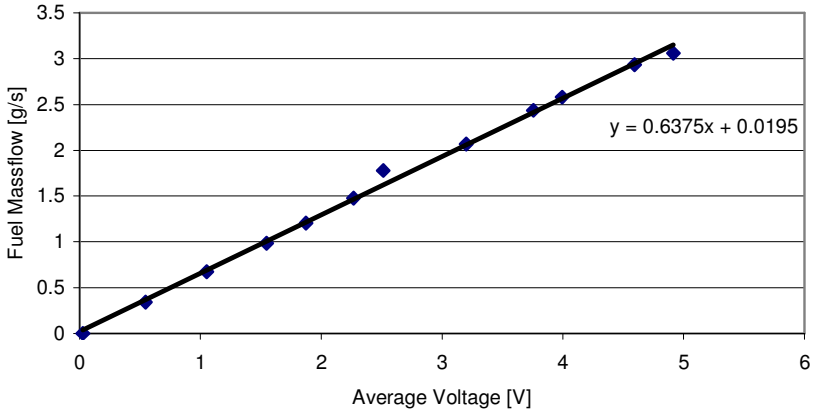


Figure 30: Fuel Flow Calibration

A.2 Dynamometer Calibration

- Mass pieces are suspended from the static torque arm of the dynamometer.
- The input voltage to the data acquisition system from the load cell is measured. Note that an amplifier voltage of 5 Volts is used.
- This process is repeated for increasing and decreasing loads, from which an average voltage is determined.
- The length of the torque arm is established to be 0.4003 meters from which the actual torque is calculated.
- Torque versus Average Voltage is plotted and a linear curve is fitted to the data.

Table 7: Dynamometer Calibration data

Mass (kg)	Weight (N)	Torque (Nm)	Voltage UP (V)	Voltage down (V)	Avg. Voltage (V)
0.00	0.00	0.00	3.422	3.417	3.42
0.62	6.08	2.43	3.423	3.483	3.45
1.62	15.86	6.35	3.702	3.795	3.75
2.62	25.67	10.28	4.029	4.089	4.06
2.89	28.37	11.36	4.125	4.217	4.17
3.89	38.18	15.28	4.442	4.528	4.49
4.89	47.96	19.20	4.761	4.827	4.79
5.16	50.62	20.26	4.854	4.842	4.85
6.16	60.40	24.18	5.172	5.249	5.21
7.16	70.12	28.11	5.489	5.542	5.52
7.43	72.92	29.19	5.576	5.655	5.62
8.43	82.73	33.12	5.889	5.956	5.92
9.43	92.51	37.03	6.205	6.254	6.23
9.71	95.23	38.12	6.289	6.357	6.32
10.70	105.01	42.03	6.599	6.654	6.63
11.70	114.82	45.96	6.914	6.945	6.93
11.85	116.25	46.54	6.968	7.017	6.99
14.12	138.56	55.46	7.669	7.706	7.69
15.12	148.37	59.39	7.984	8.003	7.99
16.12	158.15	63.31	8.293	8.293	8.29

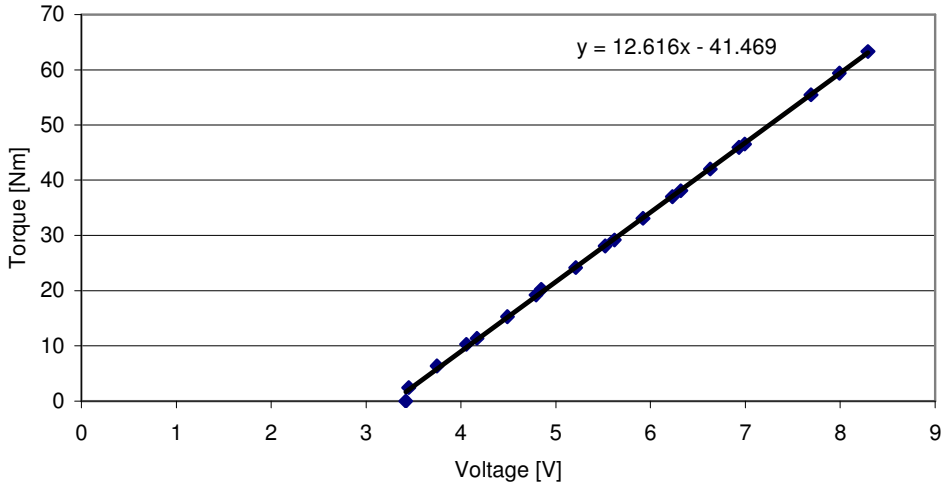


Figure 31: Dynamometer Calibration Curve

A.3 Speed Calibration

Table 8: Speed Calibration Data

Speed (rpm)	Voltage (V)
0	0.009
546	1.842

Using 2.5 as the offset then the value for m can be calculated:

$$m = \frac{(546 + 2.5)}{1.842} = 297.77$$

A.4 Air Flow Calibration

- With the engine running take pressure readings across the orifice plate. These values will be displayed in millimetres of water.
- Voltage readings are to be taken from the data acquisition system.
- The results are tabulated and then plotted. A linear curve is fitted to the data so as to determine the calibration constants.

Table 9: Airflow Calibration Data

Pressure (mm H_2O)	Voltage (V)
25.7	1.349
44.6	2.231
54.9	2.752
58.9	2.990
56.6	3.286
74.7	3.745
78.9	3.963
85.9	4.308

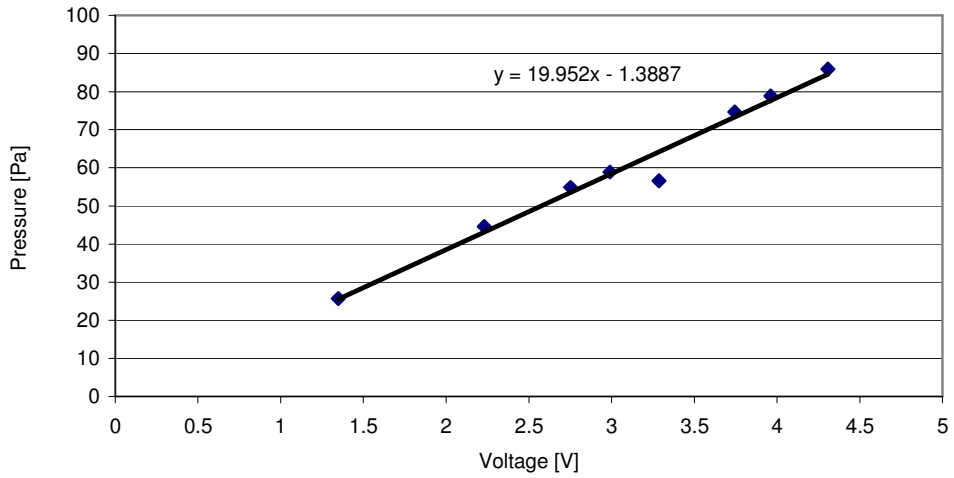


Figure 32: Airflow Calibration Curve

A.5 Ambient Air Thermocouple Calibration

- The calibration procedure for the thermocouple is identical.
- The thermocouples are placed in a beaker of water, which is gradually being heated up.
- The voltage output is read off the data acquisition system and the corresponding temperature is read of a hand held multi-meter.
- The results are tabulated and then plotted. A linear curve is fitted to the data so as to determine the calibration constants.

Table 10: Ambient Air Thermocouple Calibration Data

Temp (°C)	Voltage (V)
13.2	0.152
15.7	0.173
27.1	0.338
35.1	0.355
46.0	0.470
55.0	0.583
66.2	0.684
75.3	0.773
85.0	0.879
93.1	0.962
94.6	0.971
94.7	0.972

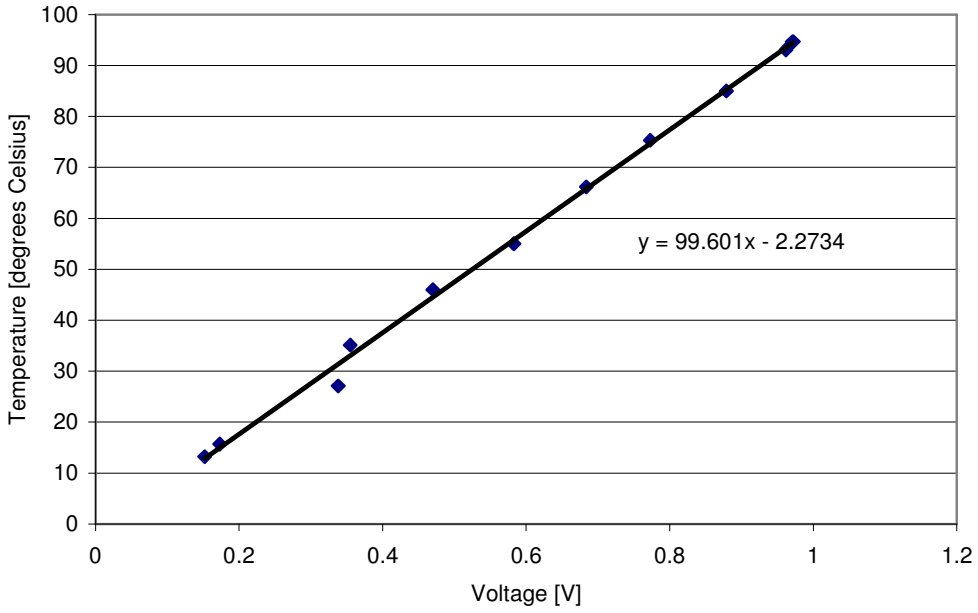


Figure 33: Ambient Air Thermocouple Calibration Curve

A.6 Air Intake Thermocouple Calibration

Table 11: Air Intake Thermocouple Calibration Data

Temp (°C)	Voltage (V)
13.1	0.172
16.2	0.195
25.0	0.294
35.0	0.393
45.0	0.499
55.0	0.596
65.0	0.698
67.8	0.722
69.2	0.737
75.0	0.804
85.0	0.898
94.5	0.986

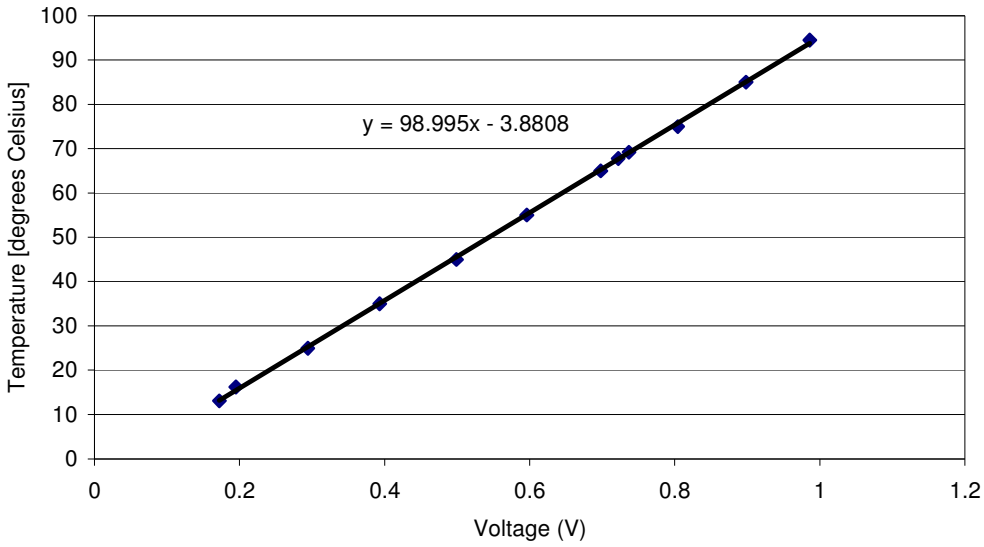


Figure 34: Air Intake Thermocouple Calibration Curve

A.7 Injector Needle Lift Sensor Calibration

Table 12: Injector Needle Lift Sensor Calibration Data

Needle Lift (mm)	Voltage (V)	Needle Lift (mm)	Voltage (V)
0.0	-13.95	3.9	-0.07
0.1	-13.56	4.0	0.28
0.2	-13.24	4.1	0.67
0.3	-12.91	4.2	1.07
0.4	-12.63	4.3	1.44
0.5	-12.25	4.4	1.79
0.6	-11.97	4.5	2.20
0.7	-11.62	4.6	2.57
0.8	-11.23	4.7	2.98
0.9	-10.89	4.8	3.33
1.0	-10.57	4.9	3.74
1.1	-10.23	5.0	4.12
1.2	-9.89	5.1	4.49
1.3	-9.56	5.2	4.87
1.4	-9.22	5.3	5.24
1.5	-8.85	5.4	5.59
1.6	-8.49	5.5	5.94
1.7	-8.16	5.6	6.32
1.8	-7.81	5.7	6.65
1.9	-7.43	5.8	7.03
2.0	-7.05	5.9	7.37
2.1	-6.67	6.0	7.72
2.2	-6.30	6.1	8.09
2.3	-5.94	6.2	8.44
2.4	-5.62	6.3	8.79
2.5	-5.26	6.4	9.13
2.6	-4.89	6.5	9.48
2.7	-4.52	6.6	9.83
2.8	-4.17	6.7	10.17
2.9	-3.83	6.8	10.53
3.0	-3.46	6.9	10.87
3.1	-3.10	7.0	11.23
3.2	-2.72	7.1	11.58
3.3	-2.33	7.2	11.9
3.4	-1.98	7.3	12.24
3.5	-1.61	7.4	12.55
3.6	-1.22	7.5	12.87
3.7	-0.85	7.6	13.20
3.8	-0.46	7.7	13.42

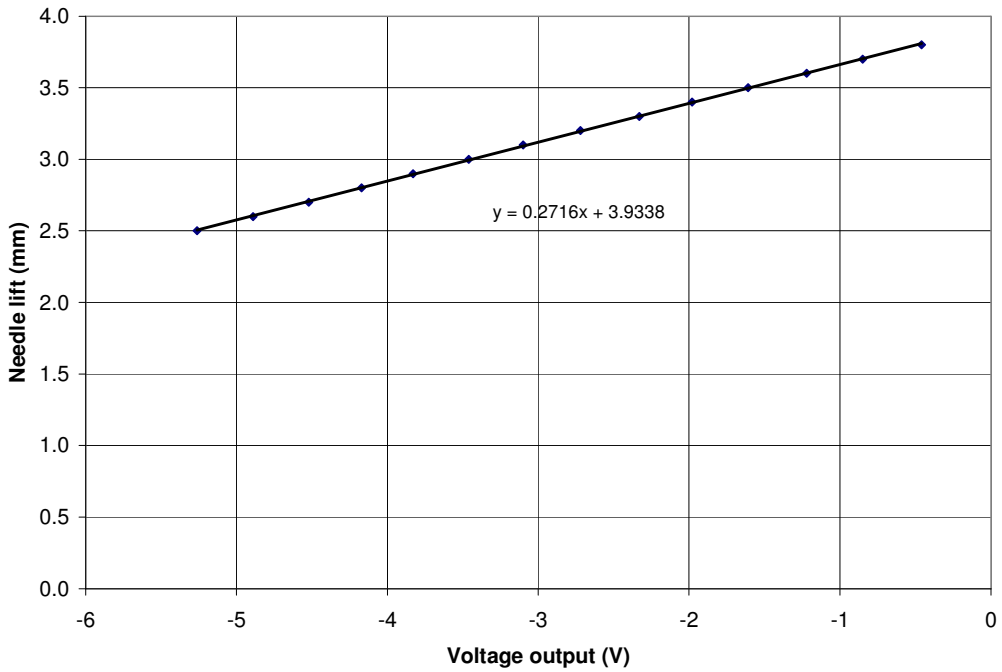


Figure 35: Injector Needle Lift Sensor Calibration Curve

A.8 Equipment Specification

The specifications of the equipment used in the Low Pressure Rig are described in this section.

- Compressor; the compressor is a 1.5 kW Honda unit with a 12 VDC electrical mechanical clutch. The unit is driven by a 3 kW 3-phase motor.
- Temperature Thermocouple; the specifications are shown in Table 13 below.

Table 13: Thermocouple Specifications

Manufacturer	Pyrotec
Model	RTXL
Range	0 - 100°C
Type	PT100

- Pressure Transducer; the specifications are shown in Table 14 below.

Table 14: Pressure Transducer Specification

Manufacturer	Wika
Series	891.23.510
Range	0 – 25 bar
Current	4 – 20 mA
Volts	10 – 30 VDC
Part No	2114567

- Rotameters; the specifications are shown in Table 15 below.

Table 15: Rotameter Specifications

Manufacturer	Fischer Porter
Fuel flow rotameter	FP 1/8 – 25 – G – 5/81
System output rotameter	FP 1/4 – 20 – G – 5/81

The data acquisition and control card used is an “Intelligent Instrumentation”, PCI-20428K-1, Multi-Function Board Kit (with Termination Panel).

1. 16 channels of Analogue Inputs with DMA, of either 0-5V, 0-10V ±5V, or ±10V
2. 12-Bit Resolution (1 part in 4096)
3. Gains of 1,10 and 100
4. 2 Channels of Analogue Output of either 0-5V, 0-10V ±5V, or ±10
5. Master Link C/C++ Drivers and Windows DLL’s plus ‘SYSCHECK’ diagnostics.
6. 100KHZ Analogue Throughput
7. 8 Digital Inputs, 8 Digital Outputs
8. One 16-bit high-Speed Counter
9. Two Rate-Generators with 8 MHz Crystal Time-base
10. Termination Panel - This panel plugs directly into the I/O connector of the board, providing connection to all of the above-mentioned inputs and outputs.

B Appendix – Signal Gas Analyser Procedure

The procedures to follow are for the Signal Series III Analyser. For each test session these procedures have to be performed to ensure good working order of the analyser [15].

Note: THC emission tests could not be performed during this project however procedures involving THC set-up have been included for future reference.

B.1 Start up Procedure

1. Switch on the main power supply at the wall plug. The pumps will start up, the oven lights will burn and the fans will turn on.
2. Switch on all the analyser units (CO, CO_2, NO_X, THC and cooler/dryer). The switches to these analysers are on the front panels of each unit.
3. All the display panels (LCD) will now be lit up and go into standby mode.
4. A Status warning will show on all the LCD displays of the analyser units.
5. Press the STATUS button and then press the PAGE DOWN button twice. Do this for all the analyzer units.
6. The window being displayed at this stage on all of the units should be the “Health Check Window”, which gives the operating status of the analyzer by listing all the operating variables. A flashing variable alerts the user to a problem with that specific variable. Upon start up, usually temperature, pressure and/or the flow variables will be flashing.
7. Allow all units to stand as they are for about 45 minutes to an hour, to allow the temperatures in the NO_X (oven and converter temperatures) and THC (oven and catalyst temperatures) analysers to reach the operating temperatures required. The variables will stop flashing to indicate operating status.
8. The THC unit has a FLAME temperature that will only increase to operating temperature when the gas bottle for “fuel” is opened, and the THC analyzer is in SAMPLE mode (procedure to follow).

B.2 Analyser Requirements and Gas Cylinder Contents

Table 16: Gas Cylinder Contents

Analyser	Cylinder Label	Cylinder Contents	Description
THC	Span	1000 ppm Methane (CH_4) in air	Large
	Fuel	40 % H_2 in Helium	Large
NO_X	Zero	99.9 % Nitrogen	Large
	Span	3030 ppm NO in N_2	Large
CO	Zero	99.9 % Nitrogen	Large
	Span	8.0 % in air	Large
CO_2	Zero	99.9 % Nitrogen	Large
	Span	15.6 % CO_2 in air	Large

B.3 Calibration Procedure

1. Once the NO_X oven and converter and the THC oven and catalyst temperatures have reached their required levels (i.e. no longer flashing), then the next phase can begin. Double check to see that the above four temperature variables on the LCD panels are not flashing.
2. Now press the ESC (Escape) button on all the analysers.
3. Press the SAMPLE button (the button below the LCD screen aligned with SAMP on the screen) on all the analysers. This will change the analyser units from STANDBY to SAMPLE mode.
4. Open the THC FUEL and the NO_X ZERO (nitrogen) gas cylinders. **NB:** Do not turn the regulator dials. All the cylinders have regulators that have been pre-set because of the flows and pressures required by each analyser. The main cylinder valve is the one to be opened.
5. Open the laboratory's supply of compressed air by turning the valve halfway (45^O). The compressed air passes through three filters, namely particulate, water and oil.
6. The CO_2, CO and NO_X analysers should now be in SAMPLE mode without any STATUS warnings.

7. The THC analyzer will give a STATUS FAIL warning, as the analyzer prepares for SAMPLE and FLAME temperature is still low. Press the STATUS button and then press the PAGE DOWN button twice to go back to the “Health Check” window. During this phase the Gas Flow is zero. Once the analyzer is in SAMPLE mode, the Gas flow value will no longer be zero and the FLAME temperature would have been reached.
8. The THC analyzer will try (5) times to light the flame and increase the FLAME temperature. If all five tries have elapsed and the flame temperature is still flashing, then press ESC to exit the “Health Check” window. Now press STOP and then SAMPLE to commence the igniting process again.
9. Once the FLAME temperature on the THC analyzer is ready, calibration may begin.
10. When calibrating, each analyser is calibrated separately, first starting with the THC, then the NO_X, followed by the CO_2 and lastly the CO analyser.
11. Open a single SPAN cylinder corresponding to the analyser to be calibrated. Now press CAL button (the button below the LCD screen aligned with CAL on the screen) on the analyser, and wait for the calibration process to complete before moving onto the next analyser.
12. The calibration process on the analyser first processes ZERO calibration and then proceeds to SPAN calibration, the analyser then reads “SAMPLE SETTLING” on the LCD screen, after which it returns to SAMPLE mode. Once this is done, the calibration process is complete.
13. If a STATUS WARNING is given after the calibration, one or some of the variables have not reached their required status for calibration. Proceed to the “Health Check” window and establish which variables are flashing.
14. Most often it is the gas flow variables which flash, this means insufficient gas is flowing through the analyser. **NB:** Adjust the regulator knobs on the gas cylinder until the variable stops flashing. Do this carefully. ***This is the only time that the regulator knobs should be turned otherwise not.*** Re-calibrate the analyser.
15. After calibration of a single analyser the SPAN cylinder should be shut. Only the ZERO and FUEL cylinders remain open throughout until testing is complete.
16. Now check to see that the calibration process was successful. This is done by pressing the STATUS button, and then the PAGE DOWN button once. The effective range should lie between –100% and +100% for all the analyser units.
17. *Note: If the STATUS WARNING appears, due to N_2 gas flow on the CO or CO_2 while calibration occurs is because N_2 is used by both CO and CO_2 at the same time, it should stop flashing after calibration, if it does not the regulator knob should be adjusted until it stops on both analysers.*

18. If all the preceding procedures have been completed, refer to the table which follows to check that all the variables on the 'Health Check Window' are within the given ranges.

B.4 Variable Ranges For Each Analyser

If the variable values are not within range, the analyzer will give a "STATUS WARNING" error message.

Table 17 - Variable Ranges for CO_2 Analyser

Analyser	Variable	Normal Reading	Upper Limit Reading	Lower Limit Reading
CO_2 7000 M	Amb. Temp.	40 °C	58 °C	0 °C
	Sens. Status	GOOD	FAULT [1]	
	P. S. Status	GOOD	FAULT [1]	
	N_2 Pressure	0.14 bar	Check footnote # **2**	
	Gas Flow	0.7 l/m	1.0 l/m	0 l/m
	Measure 147.9 POH			

Table 18 - Variable Ranges for CO Analyser

Analyser	Variable	Normal Reading	Upper Limit Reading	Lower Limit Reading
CO 7000 M	Amb. Temp.	38 °C	58 °C	0 °C
	Sens Status	GOOD	FAULT [1]	
	P. S. Status	GOOD	FAULT [1]	
	N_2 Pressure	0.18 bar	Check footnote # **2**	
	Gas Flow	0.5 l/m	1.0 l/m	0 l/m

Table 19 - Variable Ranges for THC Analyser

Analyser	Variable	Normal Reading	Upper Limit Reading	Lower Limit Reading
THC 3000 HM	Oven Temp.	191 °C	281 °C	201 °C
	Cat. Temp.	636 °C	680 °C	584 °C
	Amb. Temp.	40 °C	58 °C	0 °C
	Flame Temp.	380 °C	Check footnote # **3**	
	P. S. Status	GOOD	FAULT [1]	
	H. T. Status	GOOD	FAULT [1]	
	Fuel Pressure	0.88 bar	1.1 bar	0.6 bar
	Ref. Pressure	0.45 bar	0.5 bar	0.4 bar
	Gas Flow	1.7 l/m	3.0 l/m	0.5 l/m

Table 20 - Variable Ranges for NOx Analyser

Analyser	Variable	Normal Reading	Upper Limit Reading	Lower Limit Reading
NO_X 4000 VM	Oven Temp.	195 °C	205 °C	175 °C
	Conv. Temp.	383 °C	400 °C [4]	360 °C
	Amb. Temp.	39 °C	60 °C	0 °C
	P. S. Status	GOOD	FAULT [1]	
	H. T. Status	GOOD	FAULT [1]	
	O_3 Pressure	1.06 bar	1.25 bar [5]	0.75 bar
	Vac. Pressure	0.05 bar	0.05 bar	0.01 bar
	Gas Flow	1.9 l/m	5.0 l/m	0.5 l/m

NOTE: IN THE ABOVE TABLES, THE NORMAL READING FOR ALL THE VARIABLES INDICATES PERFECT OPERATION, HOWEVER SHOULD THE VARIABLE READINGS VARY SLIGHTLY BUT ARE STILL WITHIN RANGE; NO ERROR MESSAGES WILL APPEAR.

B.5 Notes

1. The analyser will give a “FAULT” warning, refer to the manual for help or contact a Signal technician.
2. The user manuals do not specify upper and lower limits. If a STATUS WARNING appears on the LCD display then it means insufficient N_2 is flowing through the analyser. Page down to the “Health Check Window” and the N_2 gas flow variable will be flashing. Adjust the regulator on the N_2 gas cylinder until the N_2 variable on the “Health Check Window” stops flashing, check that this is achieved on both the CO and CO_2 analyser.
3. Flashing of this variable will commence, which indicates the temperature is too high or too low.
4. This value is not given in the operating manuals.
5. The optimum O_3 pressure is 1.00 bar and 1.25 bar is an estimated Upper limit.

B.6 Problems With Calibration

Should any problems occur with the calibration of the analyser, a CAL WARNING error message will appear on the LCD screen. The following procedure should be used.

- On the front panel of the analyser, with the error message, press the STATUS button and then the PAGE DOWN button once. The effective range for any of the variables should lie between –100% and +100%. The error message will have appeared if one or more of the variables lie outside the –100% and +100% limits. Find out which of these is causing the fault.
- Check to see that the SPAN/ZERO main valve on the cylinder for that variable is open. If it is closed, open it and recalibrate.
- If the valve is open already, then place the analyser in the correct the correct mode to read the value of the cylinder contents. To get the analyser in this mode, while in the sample mode screen, press the PAGE DOWN button once and notice on the LCD screen, the SPAN and ZERO will appear on the bottom of the screen.
- If the SPAN is giving the problem, press SPAN and wait for the analyser to read the contents of the SPAN of the cylinder. Once this value has been established, adjust the potentiometer on the inside of the analyser front panel (see user manual for location).
- By adjusting the potentiometer, the value being read by the analyser can be adjusted to read the value of the cylinder.
- Once this has been done, close the front panel, place the analyser back into SAMPLE mode and recalibrate.

B.7 Shut Down

- Once testing is completed for the day, remove the heated line from the exhaust connection.
- Allow the analyser to “air out” for 30 minutes to an hour.
- Press STOP on the front panels of all the analyser units. The analyser units will now begin to purge themselves (120 seconds).
- When this is complete, the units will all be in STANDBY mode.

- Now close all the cylinder main valves and do not tamper with the regulator valves.
- Turn off the air supply.
- Switch off the front panel power switches.
- Switch off the wall plug power.

C Appendix - Data Acquisition Procedure

C.1 Performance Data Set-up

The following procedure outlines the steps involved in setting up the directories to which the test data should be stored in the *Windows 95* software package such that they may be analysed further.

1. Once *Windows* has started up, point the cursor to the *Windows Taskbar*, click *Start*, move down the list and point to *Explorer,* displaying the installed files. Click on the *Data* file and then on *PH2W*.
2. Create a relevant folder into which the test data should be saved, e.g. c*:\PH2\Sept2005\25Nm.* The test data will be saved as a *.DAT* file.
3. In *Windows* double click on the *Engine Test* shortcut icon. This will open the *Engine Test* program.
4. In this window click on the *File* button on the menu bar and point the cursor to *Test Data Directory.* A window displaying the directory path is displayed. Select the appropriate data directory where the test data is to be saved. **NB: Always manually add a backslash after the path name since there is a fault in the program.**
5. In the *Engine Test* program window select the *Settings* button on the menu bar and toggle down to *Test Settings*. This will open the *Speedwave Channel Settings* window.
6. On the menu bar click on the *Open File* shortcut button. This will allow you to retrieve the relevant file for the various test rigs. For example to open the file for the Petter engine, *C:/Program Files/TLC/Engine Test/PH2.*
7. On the menu bar of the *Speedwave Channel Settings* window select the *Test Settings* label. The storage option should be set to M*ulti Event* and the saving method changed to *DOS Compatible*.
8. Enter the relevant path for the data to be captured and then click on the *Ok* button. The *Test Filename* is to be set as the *file location*, *fuel type, date and test number*. The codes for the fuel types are listed below.
9. Select the *Steady State Channels* and enter the applicable calibration constants into this window. Remember that for the *Calibration* value a value of *–c* has to be entered and for the *Conversion* value only *m* needs to be entered into the relevant column.

10. Similarly the *High Speed Channels* have to be set.
11. Save the changes in its directory.
12. Select the 'lightning bolt' icon to arm the *Speedwave Channel Settings* with changed parameters. The program is ready to acquire a set of tests.

Table 21 - Fuel Type Coding Description

Fuel Type	Code
diesel	di
Dimethyl Ether (DME)	dm
Methanol/DME	md
Ethanol/DME	ed
Motoring	mo

Once the data sets have been captured, the results are ready to be accessed and interpreted by the Heat and Combustion Analysis (HRCA) program. The following procedure is to be followed when opening a file in HRCA [16].

1. Click on the *Open File* icon at the top of the screen in HRCA. This will open up a *Data Acquisition Wizard*.
2. Select the path and filename and press *Enter.*
3. Choose between *Motoring* and *Firing* modes for the test data. In all instances above, *Firing* was chosen as the option.
4. Select the type of fuel being used for the test. When DME is selected, the fuelflow reading and overflow reading must be entered.
5. Select the number of cycles over which the data must be averaged. The maximum number of cycles is nine with the default being one.
6. The *Data Summary* window should now be displayed.
7. Various graphs can be plotted automatically by choosing the Summary window and clicking on *Plots*. A number of options will appear which can then be selected.
8. The *Data Summary* can be exported to Microsoft Excel by clicking on the Excel icon that is visible at the top of the window. The results will then be saved as a comma separated variable file in Excel in the drive as selected by the user.

C.2 Emissions Data Set-up

Once the PC has been started up in Windows and the Analyser unit has been calibrated then the software programme may be set up to capture the test data. The programme used is Signal and this measures the emissions of the engine in a graphical mode by calculating the average concentration of the emissions and plotting the results as the test is being performed. If anything were to go wrong during a test then one would immediately notice this by the change in pattern of the graphs being plotted. The emissions measured are the Nitric Oxide (NO_X), Unburnt total hydrocarbons (THC), Carbon monoxide (CO) and Carbon dioxide (CO_2).

The following procedure briefly outlines the steps involved whilst performing tests with emissions.

1. Double click on the **Signal** icon (torch flame picture) to open the **Signal Exhaust Analyser Software** operating window.
2. Click the **Test** button on the menu bar scroll to click the **Start New Test** button. This will then open the **Start New Test Information Window.**
3. Here the test name is entered as before and the operator can select the number of data points. For this research project 50 points were chosen.
4. The **Reading Interval** was set at every **1 second.**
5. Clicking the icon with the little folders on it can choose the directory, to which the data is to be saved. Here select the path C:\SignalProgam\Signaldata\{Folder}. The entry {Folder} is to be replaced with whichever folder the data is to be stored in. This is usually the date of the test and the reading number, eg. 270900, which reads 27th of September and reading 00.
6. The operating window shows all concentrations graphically and numerically as the test is being run.
7. For each new test, the new test name needs to be re-entered in order to be stored for further use.
8. The captured data may be viewed in Notepad at a later stage for further use.

D Appendix – Low Pressure DME Rig Procedure

1. Ensure that the 12 VDC power cable for the Low Pressure DME Rig is connected to the engine battery.
2. Ensure that the control termination card is plugged into its corresponding card mounted in the Low Pressure DME Rig control computer.
3. Switch on the Low Pressure DME Rig control computer.
4. Open the file named *DME LP Fuel Sys.dgm* in the program called Visual Designer. The program flow code can be seen in Appendix E.
5. Ensure that the black control box is supplied with 12 VDC power from the 500 mA power supply. A yellow LED on the side of the box will indicate that the box is supplied with power.
6. Click the yellow arrow button in the Visual Designer program to run the control program.
7. Toggle the fan button on the screen and note whether the fan on the evaporator turns on. This is done to ensure communication between the equipment and the PC.
8. Turn on the DME supply cylinder.
9. Ensure that the pressure release valve is closed and set to release at approximately 15 bar.
10. Ensure that the pressure release overflow pipe is connected to the valve and the end is placed outside the window.
11. Ensure that the fuel supply pipe to the three-way valve is connected.
12. Ensure that the fuel outlet rotameter is closed.
13. Switch on the compressor
14. Turn on the power to engage the mechanical clutch on the compressor.
15. Trigger the *DME Supply* button on the PC screen to allow DME to enter the system.
16. Monitor the 'HP Pres' reading on the screen. When it reaches 7.5 bar, click the *DME Supply* button to turn off the DME Supply.
17. Monitor the 'HP Pres' reading on the screen. When it reaches approximately 10.5 bar or stabilises, click on the green *START* button on the screen. This will turn the system into automatic mode.
18. Slightly open the fuel outlet rotameter. When the ball inside the sight glass falls, the fuel line to the three-way valve is charged.
19. Monitor the graph on the screen and when all values have stabilised the system is ready to supply fuel to the engine.

E Appendix – Program Flow Diagram

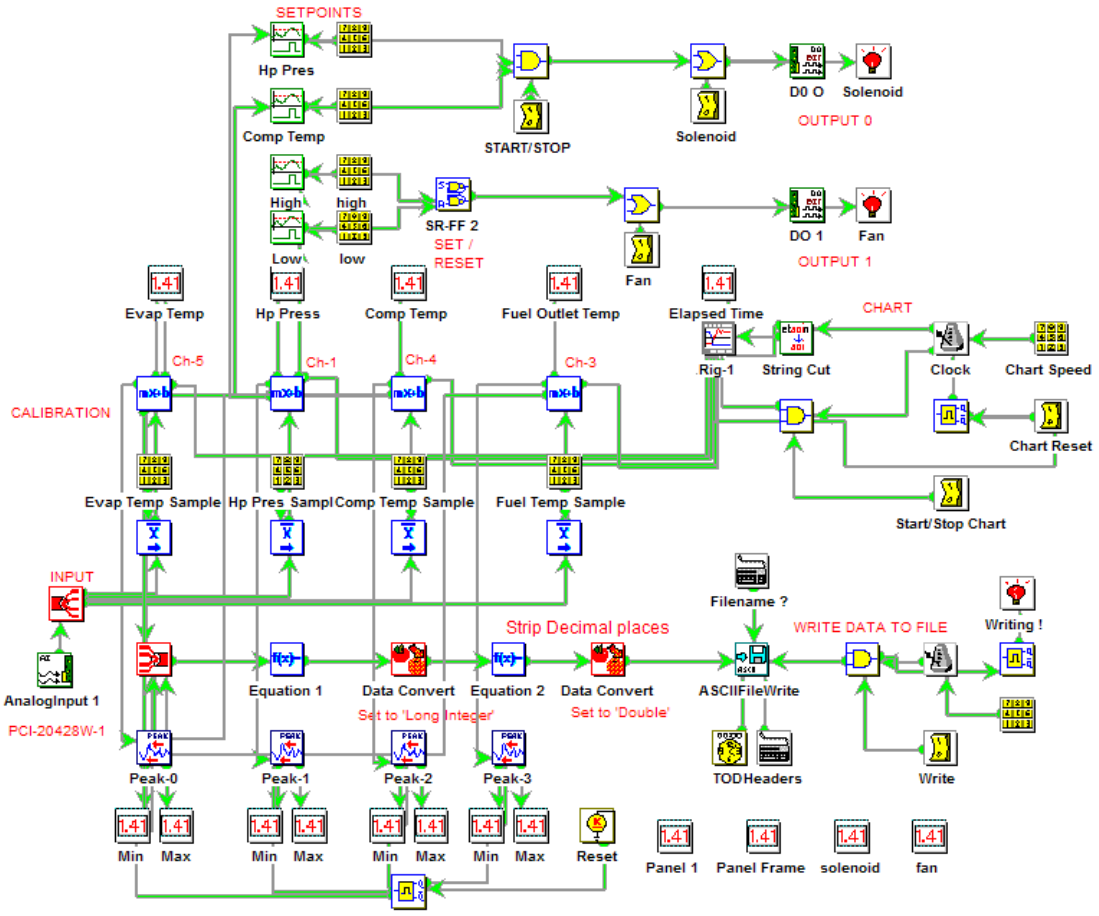


Figure 36: Controller program flow diagram

F Appendix – Raw Data

F.1 DME Data

In this section the "RefProp" computer program was used to generate the data displayed in Table 22 and Table 23. In Table 22 the temperature range and pressure were chosen in order to simulate the conditions of the DME in the "low pressure DME rig". The temperature range and pressure for Table 23 were chosen in order to simulate what the density and bulk modulus of DME would be at a higher pressure.

Table 22: DME Physical Properties at a Low Pressure and Varying Temperature Range

Temperature (K)	Pressure (MPa)	Density (kg/m³)	Enthalpy (kg/m³)	Entropy (kJ/kg-K)	Adi. Bulk Modulus (MPa)	Isothrm. Bulk Modulus (MPa)
278	12.5	710.48	75.205	0.22081	821.16	550.07
279	12.5	709.15	77.461	0.22891	812.27	543.87
280	12.5	707.83	79.720	0.23699	803.45	537.71
281	12.5	706.50	81.981	0.24505	794.69	531.60
282	12.5	705.17	84.245	0.25310	785.98	525.54
283	12.5	703.83	86.512	0.26112	777.34	519.51
284	12.5	702.50	88.782	0.26913	768.75	513.53
285	12.5	701.16	91.055	0.27712	760.22	507.60
286	12.5	699.81	93.331	0.28509	751.75	501.71
287	12.5	698.47	95.609	0.29304	743.34	495.86
288	12.5	697.12	97.891	0.30097	734.99	490.06

Table 23: DME Physical Properties at a High Pressure and Varying Temperature Range

Temperature (K)	Pressure (MPa)	Density (kg/m³)	Enthalpy (kJ/kg)	Entropy (kJ/kg-K)	Adiabatic Bulk Modulus (MPa)	Isothermal Bulk Modulus (MPa)
278	35	735.31	91.817	0.16869	1111.70	768.28
303	35	707.04	147.09	0.35905	899.94	620.85
308	35	701.32	158.30	0.39574	861.82	594.45
313	35	695.57	169.57	0.43203	825.02	569.02
318	35	689.81	180.89	0.46792	789.53	544.51

Table 24: DME Physical Properties at Increasing Pressure

Temperature (K)	Pressure (MPa)	Density (kg/m³)	Enthalpy (kJ/kg)	Entropy (kJ/kg-K)
305	24	691.01	144.03	0.40073
305	25	692.35	144.68	0.39813
305	26	693.68	145.34	0.39556
305	27	694.98	146.01	0.39303
305	28	696.27	146.68	0.39052

F.2 Injector Lift Data

The injector lift data in this section was gathered by generating the relevant plots of injector needle lift vs crank angle in the "HRCA" computer program for all of the tests gathered at a specific engine speed setting. The relevant data was then taken off of the plots for each test. The data was then averaged, and the results are displayed in Table 25, Table 26, Table 27 and Table 28 below. Table 29 and Table 29 display the percentage difference of Injector Needle Lift Duration and Start of Injector Needle Lift between DME and diesel for 25 N.m and 35 N.m torques.

Table 25: Injector Lift Data for diesel at 25 N.m

diesel 25 N.m							
Speed (rpm)	Bottom (mm)	Peak (mm)	Total Lift (mm)	Start (deg.)	Finish (deg.)	Duration (deg.)	Peak (deg.)
1100	0.000	0.23575	0.23575	343.15	372.90	29.75	358.925
1200	0.000	0.23780	0.23780	343.50	375.06	31.56	359.440
1300	0.000	0.23000	0.23000	344.58	377.00	32.42	360.120
1400	0.000	0.22620	0.22620	344.74	378.10	33.36	359.840
1500	0.000	0.23250	0.23250	343.55	381.50	37.95	360.650
1600	0.002	0.23640	0.23440	343.88	383.90	40.02	362.000
1700	0.003	0.24000	0.23700	344.66	386.53	41.86	363.400
1800	0.002	0.23925	0.23725	345.02	389.85	44.82	363.850

Table 26: Injector Lift Data for diesel at 35 N.m

diesel 35 N.m							
Speed (rpm)	Bottom (mm)	Peak (mm)	Total Lift (mm)	Start (deg.)	Finish (deg.)	Duration (deg.)	Peak (deg.)
1100	0.0010	0.2230	0.2220	342.46	372.42	29.96	357.84
1200	0.0032	0.2436	0.2404	342.82	374.34	31.52	358.84
1400	0.0040	0.2490	0.2450	343.44	378.84	35.40	361.20
1500	0.0020	0.2426	0.2406	343.92	380.70	36.78	361.48
1600	0.0000	0.2426	0.2426	343.66	384.44	40.78	362.66
1700	0.0020	0.2430	0.2410	344.14	386.06	41.92	362.76
1800	0.0070	0.2396	0.2326	346.38	387.58	41.20	363.80

Table 27: Injector Lift Data for DME at 25 N.m

DME 25 N.m							
Speed (rpm)	Bottom (mm)	Peak (mm)	Total Lift (mm)	Start (deg.)	Finish (deg.)	Duration (deg.)	Peak (deg.)
1100	0.0016	0.1902	0.1886	355.18	383.82	28.64	369.28
1200	0.0020	0.2152	0.2132	354.24	384.64	30.40	368.48
1300	0.0020	0.2178	0.2158	353.21	386.86	33.65	368.86
1400	0.0000	0.2254	0.2254	353.34	390.28	36.94	370.24
1500	-0.0020	0.2270	0.2290	353.76	394.06	40.30	371.28
1600	-0.0004	0.2208	0.2212	355.96	397.96	42.00	373.60
1700	0.0000	0.2192	0.2192	355.88	399.54	43.66	374.68
1800	0.0000	0.2181	0.2181	357.71	401.40	43.68	376.08

Table 28: Injector Lift Data for DME at 35 N.m

DME 35 N.m							
Speed (rpm)	Bottom (mm)	Peak (mm)	Total Lift (mm)	Start (deg.)	Finish (deg.)	Duration (deg.)	Peak (deg.)
1100	0.0020	0.2372	0.2352	356.06	389.90	33.84	374.64
1200	0.0020	0.2432	0.2412	354.84	390.58	35.74	373.64
1300	0.0032	0.2460	0.2428	352.86	391.80	38.94	373.64
1400	-0.0010	0.2445	0.2455	351.75	392.90	41.15	372.05
1500	-0.0030	0.2476	0.2506	353.16	398.30	45.14	374.52
1600	-0.0026	0.2432	0.2458	353.06	398.66	45.60	375.24
1700	-0.0010	0.2410	0.2420	354.18	401.64	47.46	377.08
1800	0.0000	0.2410	0.2410	355.95	403.72	47.77	378.85

Table 29: Percentage Differences in Injector Needle Lift Duration and Start of Injector Needle Lift at 25 N.m for the two fuels

	Duration (deg.)			Start (deg.)		
Speed (rpm)	diesel 25 N.m	DME 25 N.m	% diff	diesel 25 N.m	DME 25 N.m	% diff
1100	29.75	28.64	0.96	343.15	355.18	1.04
1200	31.56	30.40	0.96	343.50	354.24	1.03
1300	32.42	33.65	1.04	344.58	353.22	1.03
1400	33.36	36.94	1.11	344.74	353.34	1.02
1500	37.95	40.30	1.06	343.55	353.76	1.03
1600	40.02	42.00	1.05	343.88	355.96	1.04
1700	41.87	43.66	1.04	344.67	355.88	1.03
1800	44.83	43.69	0.97	345.03	357.71	1.04
Average			1.03			1.03

Table 30: Percentage Differences in Injector Needle Lift Duration and Start of Injector Needle Lift at 35 N.m for the two fuels

	Duration (deg.)			Start (deg.)		
Speed (rpm)	diesel 35 N.m	DME 35 N.m	% diff	diesel 35 N.m	DME 35 N.m	% diff
1100	29.96	33.84	1.13	342.46	356.06	1.04
1200	31.52	35.74	1.13	342.82	354.84	1.04
1400	35.40	41.15	1.16	343.44	351.75	1.02
1500	36.78	45.14	1.23	343.92	353.16	1.03
1600	40.78	45.60	1.12	343.66	353.06	1.03
1700	41.92	47.46	1.13	344.14	354.18	1.03
1800	41.20	47.78	1.16	346.38	355.95	1.03
Average			1.15			1.03

Table 31: Percentage Differences in Injector Needle Lift for the same fuel at different torques

	Total Lift (mm)			Total Lift (mm)		
Speed	Di 25 Nm	Di 35 Nm	% diff	DME 25 N.m	DME 35 N.m	% diff
1100	0.23575	0.2220	0.94	0.1886	0.2352	1.25
1200	0.23780	0.2404	1.01	0.2132	0.2412	1.13
1400	0.22620	0.2450	1.08	0.2254	0.2455	1.09
1500	0.23250	0.2406	1.03	0.2290	0.2506	1.09
1600	0.23440	0.2426	1.03	0.2212	0.2458	1.11
1700	0.23700	0.2410	1.02	0.2192	0.2420	1.10
1800	0.23725	0.2326	0.98	0.2181	0.2410	1.10
Average			1.01			1.13

F.3 Injector Pressure Data

The injector pressure data in this section was gathered by generating the relevant plots of injector pressure vs crank angle in the "HRCA" computer program for all of the tests gathered at a specific engine speed setting. The relevant data was then taken off of the plots for each test. The data was then averaged, and the results are displayed in Table 31, Table 33, Table 33 and Table 35 below. Table 35 and Table 37 display the percentage difference of Injector Pressure Difference and Start of Injector Pressurisation between DME and diesel for 25 N.m and 35 N.m torques.

Table 32: Injector Pressure Data for diesel at 25 N.m

diesel 25N.m									
Speed (rpm)	Bottom (MPa)	Peak (MPa)	Start (deg.)	Finish (deg.)	Duration (deg.)	Peak (deg.)	dP (MPa)	d(CrankAngle) (deg.)	dP/d(CrankAngle) (MPa/deg.)
1100	0.10	17.05	328.775	359.85	31.075	344.20	16.95	15.425	1.10
1200	0.05	18.40	330.360	360.48	30.120	345.22	18.35	14.860	1.23
1300	0.05	19.18	330.940	360.36	29.420	346.04	19.13	15.100	1.27
1400	0.05	19.54	331.040	360.52	29.480	346.60	19.49	15.560	1.25
1500	0.05	19.45	330.825	360.45	29.625	346.72	19.40	15.900	1.22
1600	0.04	19.90	330.640	361.00	30.360	347.20	19.86	16.560	1.20
1700	0.00	20.37	331.030	361.67	30.630	348.00	20.37	16.970	1.20
1800	0.05	20.75	331.100	362.45	31.350	348.82	20.70	17.725	1.17
Average									1.21

Table 33: Injector Pressure Data for diesel at 35 N.m

diesel 35N.m									
Speed (rpm)	Bottom (MPa)	Peak (MPa)	Start (deg.)	Finish (deg.)	Duration (deg.)	Peak (deg.)	dP (MPa)	d(CrankAngle) (deg.)	dP/d(CrankAngle) (MPa/deg.)
1100	0.05	17.00	328.20	357.96	29.76	344.24	16.95	16.04	1.06
1200	0.05	17.80	328.72	359.88	31.16	344.16	17.75	15.44	1.15
1300	0.05	18.22	329.18	361.00	31.82	344.28	18.17	15.10	1.20
1400	0.05	18.75	329.32	361.35	32.02	344.80	18.70	15.47	1.21
1500	0.05	19.18	330.02	361.72	31.70	346.02	19.13	16.00	1.20
1600	0.10	19.40	330.26	361.32	31.06	346.68	19.30	16.42	1.18
1700	0.10	20.18	329.98	361.40	31.42	347.10	20.08	17.12	1.17
1800	0.05	20.80	330.94	362.52	31.58	348.78	20.75	17.84	1.16
Average									1.17

Table 34: Injector Pressure Data for DME at 25 N.m

DME 25N.m									
Speed (rpm)	Bottom (MPa)	Peak (MPa)	Start (deg.)	Finish (deg.)	Duration (deg.)	Peak (deg.)	dP (MPa)	d(CrankAngle) (deg.)	dP/d(CrankAngle)
1100	-0.30	10.34	332.68	365.92	33.24	357.52	10.64	24.84	0.43
1200	-0.10	10.74	333.08	365.68	32.60	354.24	10.84	21.16	0.51
1300	-0.20	11.28	333.32	365.82	32.50	355.65	11.48	22.33	0.51
1400	0.00	11.72	334.26	366.74	32.48	356.54	11.72	22.28	0.53
1500	-0.10	12.26	334.14	367.74	33.60	357.26	12.36	23.12	0.53
1600	-0.10	11.86	335.02	368.24	33.22	358.58	11.96	23.56	0.51
1700	0.20	11.98	334.86	369.00	34.14	358.48	11.78	23.62	0.50
1800	0.45	11.93	336.03	370.84	34.81	359.54	11.48	23.51	0.49
Average									0.50

Table 35: Injector Pressure Data for DME at 35 N.m

DME 35N.m									
Speed (rpm)	Bottom (MPa)	Peak (MPa)	Start (deg.)	Finish (deg.)	Duration (deg.)	Peak (deg.)	dP (MPa)	d(CrankAngle) (deg.)	dP/d(CrankAngle)
1100	-0.200	10.60	332.52	372.32	39.80	358.90	10.80	26.38	0.41
1200	-0.350	10.62	332.90	372.76	39.86	357.60	10.97	24.70	0.44
1300	-0.150	11.26	333.56	372.72	39.16	355.98	11.41	22.42	0.51
1400	-0.300	11.25	333.92	371.40	37.47	356.12	11.55	22.20	0.52
1500	-0.003	11.44	334.12	370.64	36.52	357.42	11.44	23.30	0.49
1600	-0.200	11.08	334.72	370.32	35.60	357.06	11.28	22.34	0.50
1700	0.000	11.66	335.74	451.32	35.60	358.66	11.66	22.92	0.51
1800	0.000	12.00	335.77	372.60	36.82	360.05	12.00	24.27	0.49
Average									0.49

Table 36: Percentage Differences in the Injector Pressure Difference and Start of Injector Pressurisation at 25 N.m for the two fuels

	dP (MPa)			Start (deg.)		
Speed	diesel 25 N.m	DME 25 N.m	% diff	diesel 25 N.m	DME 25 N.m	% diff
1100	16.95	10.64	0.63	328.78	332.68	1.01
1200	18.35	10.84	0.59	330.36	333.08	1.01
1300	19.13	11.48	0.60	330.94	333.32	1.01
1400	19.49	11.72	0.60	331.04	334.26	1.01
1500	19.40	12.36	0.64	330.83	334.14	1.01
1600	19.86	11.96	0.60	330.64	335.02	1.01
1700	20.37	11.78	0.58	331.03	334.86	1.01
1800	20.70	11.48	0.55	331.10	336.03	1.01
Average			0.60			1.01

Table 37: Percentage Differences in the Injector Pressure Difference and Start of Injector Pressurisation at 35 N.m for the two fuels

	dP (MPa)			Start (deg.)		
Speed	diesel 35 N.m	DME 35 N.m	% diff	diesel 35 N.m	DME 35 N.m	% diff
1100	16.95	10.80	0.64	328.20	332.52	1.01
1200	17.75	10.97	0.62	328.72	332.90	1.01
1300	18.17	11.41	0.63	329.18	333.56	1.01
1400	18.70	11.55	0.62	329.33	333.93	1.01
1500	19.13	11.44	0.60	330.02	334.12	1.01
1600	19.30	11.28	0.58	330.26	334.72	1.01
1700	20.08	11.66	0.58	329.98	335.74	1.02
1800	20.75	12.00	0.58	330.94	335.78	1.01
Average			0.61			1.01

F.4 Performance Data

The performance data in this section was gathered by processing all of the tests gathered at a specific engine speed setting using the "HRCA" computer program. The data was then averaged for each speed setting, and the results are displayed in Table 38, Table 39, Table 39 and Table 41 below.

Table 38: Overall Performance Data for diesel at 25 N.m

Diesel_25N.m								
Speed (rpm)	1100	1200	1300	1400	1500	1600	1700	1800
Load (Nm)	24.78	24.96	24.78	25.06	25.03	24.38	25.53	25.23
Brake Power (W)	2858.83	3136.04	3377.92	3672.46	3926.15	4086.48	4545.60	4750.55
Ind Work/Cycle (J)	428.95	437.92	453.76	450.98	456.20	472.62	501.47	495.80
Indicated Power (W)	7865.65	8760.94	9842.54	10520.38	11394.78	12609.98	14231.17	14863.63
imep (kPa)	645.00	658.50	682.34	678.16	686.00	710.70	754.03	745.53
bmep (kPa)	234.43	235.74	234.18	236.74	236.35	230.32	240.87	238.28
Equivalence Ratio	0.57	0.52	0.52	0.53	0.55	0.51	0.52	0.54
Air/Fuel Ratio	26.20	28.58	28.82	28.03	27.03	29.43	28.67	27.86
Air Flow (g/s)	11.36	11.98	12.31	12.76	13.61	15.60	15.47	16.11
Fuel Flow (g/s)	0.43	0.42	0.42	0.46	0.50	0.53	0.54	0.58
Additive Flow (g/s)	0.00	0.00	0.00	0.00	0.00	0.00	0.00	0.00
Percentage DME (%)	0.00	0.00	0.00	0.00	0.00	0.00	0.00	0.00
Fuel Conv Eff (%)	15.15	17.20	18.14	18.54	17.88	17.68	19.30	18.83
isfc (kg/J)	0.00	0.00	0.00	0.00	0.00	0.00	0.00	0.00
bsfc (kg/J)	0.00	0.00	0.00	0.00	0.00	0.00	0.00	0.00
Injection (°)	347.80	345.30	346.10	346.70	346.80	347.30	348.10	348.90
Ignition (°)	350.90	351.18	352.18	352.14	354.05	352.26	353.10	353.25
Ignition Delay (°)	3.10	5.88	6.08	5.44	7.25	4.96	5.00	4.35
Injection Temp. (K)	826.00	791.20	848.60	894.40	911.50	857.00	912.00	974.25
Ignition Temp. (K)	849.25	834.00	956.80	1009.80	1265.00	910.60	968.00	1031.50
Patm (kPa)	82.50	82.50	82.50	82.50	82.50	82.48	82.40	82.40
Exhaust Temp (°C)	395.58	427.12	435.96	446.84	460.53	470.32	482.37	494.55
Max Pressure (kPa)	7216.30	6988.76	6965.30	7015.10	7040.48	7122.48	7068.10	7041.65
Pos of Pmax (°)	364.25	365.16	365.64	365.52	365.20	365.52	366.73	367.25
Max Temperature (K)	1879.50	1912.46	2030.68	2095.04	2136.75	2019.12	2207.30	2239.10
Pos of Tmax (°)	370.90	371.80	373.44	371.92	372.75	373.52	375.00	375.50
Mech Effic (%)	36.38	35.80	34.36	34.94	34.53	32.46	31.93	31.98
ITE (%)	41.63	47.92	52.88	53.00	51.88	54.56	60.53	58.95
BTE (%)	15.15	17.20	18.14	18.54	17.88	17.68	19.30	18.83
Volumetric Eff (%)	93.15	90.04	85.32	82.26	81.93	87.94	81.97	80.80

Table 39: Overall Performance Data for diesel at 35 N.m

Diesel_35N.m								
Speed (rpm)	1100	1200	1300	1400	1500	1600	1700	1800
Load (Nm)	35.20	34.98	35.34	35.12	35.02	34.84	35.06	34.88
Brake Power (W)	4054.56	4396.18	4821.64	5142.30	5500.92	5838.80	6250.80	6575.98
Ind Work/Cycle (J)	450.72	437.68	434.94	392.68	397.82	393.54	357.92	343.10
Indicated Power (W)	8264.94	8756.86	9441.28	9153.50	9944.24	10505.72	10157.72	10293.08
imep (kPa)	677.76	658.22	654.06	590.50	598.28	591.80	538.22	515.95
bmep (kPa)	332.50	330.44	334.02	331.72	330.96	328.90	331.22	329.62
Equivalence Ratio	0.54	0.65	0.71	0.68	0.60	0.55	0.60	0.70
Air/Fuel Ratio	27.54	23.07	21.10	22.09	25.03	27.26	24.84	21.34
Air Flow (g/s)	11.20	11.78	12.13	12.62	13.44	15.51	15.25	15.85
Fuel Flow (g/s)	0.41	0.51	0.58	0.57	0.54	0.57	0.61	0.74
Additive Flow (g/s)	0.00	0.00	0.00	0.00	0.00	0.00	0.00	0.00
Percentage DME (%)	0.00	0.00	0.00	0.00	0.00	0.00	0.00	0.00
Fuel Conv Eff (%)	22.88	19.74	19.22	20.66	23.48	23.54	23.34	20.28
isfc (kg/J)	0.00	0.00	0.00	0.00	0.00	0.00	0.00	0.00
bsfc (kg/J)	0.00	0.00	0.00	0.00	0.00	0.00	0.00	0.00
Injection (°)	344.34	344.26	346.06	323.78	346.10	346.78	347.18	348.93
Ignition (°)	351.26	351.10	351.26	328.82	351.34	353.14	352.54	353.57
Ignition Delay (°)	6.92	6.84	5.20	5.04	5.24	6.36	5.36	4.63
Injection Temp. (K)	763.20	804.60	947.80	831.00	962.40	936.60	1034.20	1116.00
Ignition Temp. (K)	905.60	955.20	985.40	861.40	1006.00	1177.40	1179.80	1249.17
Patm (kPa)	82.80	82.80	82.80	82.74	82.70	82.70	82.70	82.70
Exhaust Temp (°C)	449.44	447.20	446.26	471.36	487.44	497.42	515.32	526.95
Max Pressure (kPa)	7065.20	7153.08	7164.80	7230.20	7261.44	7446.02	7367.86	7479.37
Pos of Pmax (°)	365.00	364.64	364.48	364.00	364.24	364.40	364.32	365.60
Max Temperature (K)	1887.48	1961.90	2066.52	2079.88	2135.20	2017.32	2157.28	2233.48
Pos of Tmax (°)	372.16	371.72	372.36	368.56	371.24	370.08	368.72	368.60
Mech Effic (%)	49.06	50.26	51.10	56.22	55.42	55.60	61.68	63.88
ITE (%)	46.58	39.36	37.64	36.72	42.46	42.36	37.96	31.77
BTE (%)	22.88	19.74	19.22	20.66	23.48	23.54	23.34	20.28
Volumetric Eff (%)	91.84	88.54	84.02	81.42	80.88	87.36	80.80	79.47

Table 40: Overall Performance Data for DME at 25 N.m

DME_25N.m								
Speed (rpm)	1100	1200	1300	1400	1500	1600	1700	1800
Load (Nm)	24.80	24.86	25.08	25.18	25.02	25.02	25.20	24.87
Brake Power (W)	2853.16	3134.26	3424.13	3693.50	3933.40	4203.36	4492.30	4697.00
Ind Work/Cycle (J)	250.88	248.64	231.28	239.08	233.86	230.88	228.30	218.01
Indicated Power (W)	4596.60	4982.54	5024.72	5584.86	5849.26	6170.80	6479.20	6553.19
imep (kPa)	377.28	373.90	347.80	359.52	351.68	347.18	343.32	327.84
bmep (kPa)	234.16	235.20	236.98	237.76	236.48	236.48	238.04	234.96
Equivalence Ratio	0.38	0.36	0.36	0.36	0.36	0.33	0.35	0.35
Air/Fuel Ratio	26.49	27.93	27.97	27.74	27.61	30.59	28.79	29.21
Air Flow (g/s)	11.66	12.29	12.60	13.24	13.92	16.26	15.93	16.49
Fuel Flow (g/s)	0.44	0.44	0.45	0.48	0.50	0.53	0.55	0.56
Additive Flow (g/s)	0.00	0.00	0.00	0.00	0.00	0.00	0.00	0.00
Percentage DME (%)	0.00	0.00	0.00	0.00	0.00	0.00	0.00	0.00
Fuel Conv Eff (%)	22.82	25.06	26.73	27.20	27.44	27.82	28.54	29.26
isfc (kg/J)	0.00	0.00	0.00	0.00	0.00	0.00	0.00	0.00
bsfc (kg/J)	0.00	0.00	0.00	0.00	0.00	0.00	0.00	0.00
Injection (°)	357.62	354.26	355.70	356.58	357.34	358.66	358.78	359.59
Ignition (°)	358.46	357.70	357.50	358.70	358.90	360.42	360.82	363.81
Ignition Delay (°)	0.84	3.44	1.80	2.12	1.56	1.76	2.04	4.23
Injection Temp. (K)	822.00	876.60	956.33	995.20	1024.40	930.40	1032.60	1061.86
Ignition Temp. (K)	826.80	886.40	1004.33	1120.20	1092.00	985.00	1044.80	1179.57
Patm (kPa)	82.84	82.82	82.82	82.80	82.80	82.80	82.80	82.80
Exhaust Temp (°C)	324.18	331.88	333.17	344.50	349.30	355.78	371.80	379.36
Max Pressure (kPa)	5468.58	5651.20	5808.73	5796.70	5593.60	5243.96	5124.82	4888.93
Pos of Pmax (°)	369.56	368.88	368.50	368.80	368.44	370.12	369.64	366.60
Max Temperature (K)	1516.30	1609.98	1724.28	1788.06	1787.60	1585.66	1725.76	1705.86
Pos of Tmax (°)	375.32	374.16	373.40	374.12	376.00	377.00	378.24	378.74
Mech Effic (%)	62.12	63.34	68.33	66.22	67.36	68.18	69.82	72.21
ITE (%)	36.74	39.82	39.22	41.18	40.82	40.84	41.16	40.83
BTE (%)	22.82	25.06	26.73	27.20	27.44	27.82	28.54	29.26
Volumetric Eff (%)	95.70	92.24	87.20	85.20	83.66	91.48	84.40	82.50

Table 41: Overall Performance Data for DME at 35 N.m

DME_35N.m								
Speed (rpm)	1100	1200	1300	1400	1500	1600	1700	1800
Load (Nm)	35.10	34.82	35.26	35.03	35.18	35.50	35.10	35.10
Brake Power (W)	4055.90	4372.20	4806.82	5146.35	5530.18	5953.66	6264.04	6628.62
Ind Work/Cycle (J)	359.64	326.26	368.84	325.00	332.26	323.70	320.06	334.78
Indicated Power (W)	6612.50	6521.76	8005.64	7598.28	8310.58	8636.10	9088.68	10060.16
imep (kPa)	540.80	490.58	554.68	488.75	499.66	486.78	481.30	503.46
bmep (kPa)	331.72	328.90	333.00	331.03	332.48	335.58	331.72	331.74
Equivalence Ratio	0.39	0.39	0.46	0.43	0.45	0.42	0.53	0.56
Air/Fuel Ratio	26.25	25.67	24.72	23.00	22.33	23.48	18.35	17.34
Air Flow (g/s)	11.38	11.97	12.23	12.86	13.49	15.80	15.57	16.14
Fuel Flow (g/s)	0.44	0.47	0.50	0.56	0.60	0.67	0.85	0.93
Additive Flow (g/s)	0.00	0.00	0.00	0.00	0.00	0.00	0.00	0.00
Percentage DME (%)	0.00	0.00	0.00	0.00	0.00	0.00	0.00	0.00
Fuel Conv Eff (%)	32.94	32.98	32.02	32.40	32.22	31.12	25.98	25.04
isfc (kg/J)	0.00	0.00	0.00	0.00	0.00	0.00	0.00	0.00
bsfc (kg/J)	0.00	0.00	0.00	0.00	0.00	0.00	0.00	0.00
Injection (°)	358.94	357.66	355.34	356.20	357.46	357.54	358.70	360.02
Ignition (°)	359.38	358.98	355.98	356.25	358.42	358.22	360.54	360.42
Ignition Delay (°)	0.44	1.32	0.64	0.05	0.96	0.68	1.84	0.40
Injection Temp. (K)	857.40	905.40	1022.00	1022.00	1132.20	1014.00	1107.00	1200.40
Ignition Temp. (K)	863.00	967.20	1033.60	1024.50	1199.40	1057.60	1182.20	1202.20
Patm (kPa)	82.90	82.80	82.80	82.80	82.80	82.80	82.80	82.80
Exhaust Temp (°C)	426.72	426.16	437.90	437.78	457.52	483.30	498.50	546.22
Max Pressure (kPa)	5372.90	5454.90	6014.44	5854.33	5697.08	5537.88	5355.26	5169.74
Pos of Pmax (°)	371.48	370.36	368.12	368.65	368.88	369.40	369.84	370.24
Max Temperature (K)	1693.94	1684.14	1898.94	1863.13	1888.02	1694.78	1782.04	1827.94
Pos of Tmax (°)	380.36	378.68	376.84	376.40	377.48	378.60	379.08	380.12
Mech Effic (%)	61.44	67.10	60.70	67.73	66.62	69.06	69.12	65.96
ITE (%)	53.60	49.18	52.38	47.78	48.38	45.14	37.66	38.00
BTE (%)	32.94	32.98	32.02	32.40	32.22	31.12	25.98	25.04
Volumetric Eff (%)	93.12	90.08	84.70	82.70	81.10	89.08	82.46	80.76

F.5 Specific Fuel Flow Data

Figure 24, Figure 25 and Figure 26 were created using data from reference 19. The data appears in tabulated form in Appendices F.6, F.7 and F.8.

Table 42: Average Specific Fuel Flow and Ratio between Averages

Fuel Supply	Average Specific Fuel Flow (g/s/W)		
	25 Nm	35 Nm	45 Nm
Di	0.000157	0.000141	0.00012290
HP DME	0.000173	0.000154	0.00011715
LP DME	0.000151	0.000180	0.00017047

Average LP/Average HP Ratio	0.88	1.17	1.46
Average LP/Average Di Ratio	0.97	1.28	1.39

F.6 Low Pressure DME

The following data was taken from reference 19.

Table 43: Overall Results for 25 Nm LP DME

25 Nm LP DME		25 Nm							
		1100 rpm	1200 rpm	1300 rpm	1400 rpm	1500 rpm	1600 rpm	1700 rpm	1800 rpm
Speed	(rpm)	1091.56	1202.30	1304.40	1404.44	1503.60	1600.80	1701.84	1802.94
Load	(Nm)	24.74	25.46	25.18	24.80	24.88	25.02	24.94	24.96
Brake Power	(W)	2826.86	3202.66	3441.08	3649.24	3919.64	4195.74	4446.16	4715.32
Ind. work per Cycle	(J)	461.58	432.60	439.52	434.42	425.94	438.62	421.72	445.36
Indicated Power	(W)	8398.26	8668.94	9555.12	10168.74	10674.10	11702.58	11961.52	13382.36
imep	(kPa)	694.14	650.56	660.94	653.28	640.52	659.60	634.14	669.74
bmep	(kPa)	233.66	240.34	238.04	234.42	235.18	236.48	235.72	235.98
Equivalence Ratio		0.35	0.36	0.38	0.44	0.44	0.36	0.48	0.47
Air/fuel ratio		28.86	27.62	26.28	22.72	22.40	23.32	20.60	20.90
Air Flow	(g/s)	11.21	11.94	12.31	12.75	13.64	15.68	15.39	16.01
Fuel Flow	(g/s)	0.39	0.43	0.47	0.56	0.61	0.67	0.75	0.77
Additive Flow	(g/s)	0.00	0.00	0.00	0.00	0.00	0.00	0.00	0.00
Percentage DME	(%)	0.00	0.00	0.00	0.00	0.00	0.00	0.00	0.00
Fuel Conv. Eff.	(%)	25.58	26.06	25.84	22.90	22.64	21.96	20.94	21.66
isfc	(kg/J)	0.00	0.00	0.00	0.00	0.00	0.00	0.00	0.00
bsfcf	(kg/J)	0.00	0.00	0.00	0.00	0.00	0.00	0.00	0.00
Injection	(°CA)	356.34	354.22	354.46	355.34	356.66	358.30	358.02	359.38
Ignition	(°CA)	357.54	355.74	356.14	355.54	356.74	358.95	359.22	360.10
Ignition delay	(°CA)	1.20	1.52	1.68	0.20	0.08	0.52	1.20	0.72
Patm	(kPa)	82.10	82.10	82.04	82.00	82.00	82.00	82.00	82.00
Exhaust Temperature	(°C)	371.82	410.40	416.84	414.14	426.66	463.38	469.44	513.68
Pmax	(kPa)	6088.86	6080.12	6133.82	6008.78	5780.26	5532.22	5397.44	5184.56
Position of Pmax	(°CA)	370.76	369.20	369.68	369.72	370.12	369.96	370.40	371.20
Tmax	(K)	1860.68	1843.78	1967.02	1998.08	1949.76	1821.88	1908.80	1957.44
Position of Tmax	(°CA)	378.64	377.32	378.76	377.80	377.76	380.36	382.00	384.44
Mech Efficiency	(%)	33.78	36.98	36.08	35.90	36.74	35.88	37.24	35.36
ITE	(%)	76.02	70.50	71.76	63.76	61.68	61.22	56.28	61.44
BTE	(%)	25.58	26.06	25.84	22.90	22.64	21.96	20.94	21.66
Volumetric Efficiency	(%)	92.72	89.62	85.16	81.88	81.84	88.36	81.60	80.14
CO	(ppm)	2770.16	4735.60	5118.80	5662.00	6635.80	7507.80	7535.40	7581.40
CO2	(ppm)	52091.04	71602.80	73946.60	69786.00	62494.00	57462.40	50285.20	48101.60
Nox	(ppm)	1466.98	1263.60	1064.40	800.20	500.60	314.60	269.40	236.60
O2	(ppm)	16.83	11.40	10.97	10.77	11.50	12.35	13.23	13.87
Specific CO	(ppm/W)	0.98	1.48	1.49	1.44	1.69	1.79	1.69	1.61
Specific CO2	(ppm/W)	18.43	22.36	21.49	19.12	15.94	13.70	11.31	10.20
Specific Nox	(ppm/W)	0.52	0.39	0.31	0.22	0.13	0.08	0.06	0.05
Specific O2	(ppm/W)	0.01	0.00	0.00	0.00	0.00	0.00	0.00	0.00

Table 44: Overall Results for 35 Nm LP DME

35 Nm LP DME		35 Nm							
		1100 rpm	1200 rpm	1300 rpm	1400 rpm	1500 rpm	1600 rpm	1700 rpm	1800 rpm
Speed	(rpm)	1099.08	1202.30	1304.40	1399.90	1302.20	1605.60	1704.03	1802.45
Load	(Nm)	34.75	35.07	35.17	34.50	34.91	35.20	35.00	34.83
Brake Power	(W)	3996.98	4418.10	4805.40	5057.93	4760.48	5919.20	6245.60	6574.15
Ind. work per Cycle	(J)	468.88	478.40	468.70	465.47	470.86	451.38	458.60	458.35
Indicated Power	(W)	8587.90	9587.13	10188.97	10859.80	10211.97	12079.83	13024.73	13770.08
imep	(kPa)	705.08	719.47	704.80	699.87	708.04	678.80	689.63	689.28
bmep	(kPa)	328.15	331.57	332.40	325.97	329.98	332.63	330.70	329.08
Equivalence Ratio		0.65	0.66	0.62	0.64	0.64	0.62	0.71	0.70
Air/fuel ratio		14.72	14.51	15.59	15.09	15.06	15.48	13.45	13.54
Air Flow	(g/s)	11.50	11.94	12.48	12.93	12.45	16.05	15.87	16.61
Fuel Flow	(g/s)	0.78	0.82	0.80	0.86	0.83	1.04	1.18	1.23
Additive Flow	(g/s)	0.00	0.00	0.00	0.00	0.00	0.00	0.00	0.00
Percentage DME	(%)	0.00	0.00	0.00	0.00	0.00	0.00	0.00	0.00
Fuel Conv. Eff.	(%)	18.00	18.90	21.13	20.77	20.27	20.08	18.63	18.85
isfc	(kg/J)	0.00	0.00	0.00	0.00	0.00	0.00	0.00	0.00
bsfcf	(kg/J)	0.00	0.00	0.00	0.00	0.00	0.00	0.00	0.00
Injection	(°CA)	364.05	354.77	353.23	354.23	354.08	354.35	357.15	358.00
Ignition	(°CA)	367.50	359.03	355.30	357.83	357.39	357.85	358.00	359.50
Ignition delay	(°CA)	3.45	4.27	2.07	3.60	3.31	3.50	0.85	1.50
Patm	(kPa)	83.50	83.43	83.50	83.40	83.44	83.40	83.40	83.40
Exhaust Temperature	(°C)	391.88	416.47	416.63	418.40	417.17	454.28	494.78	510.90
Pmax	(kPa)	6388.38	6626.40	6427.87	6331.80	6462.02	6139.35	5765.80	5668.18
Position of Pmax	(°CA)	368.95	367.40	369.07	369.47	368.64	369.05	370.25	370.00
Tmax	(K)	1840.53	1941.00	1959.13	2026.17	1975.43	1839.80	1927.85	1918.18
Position of Tmax	(°CA)	376.45	374.93	377.27	375.80	376.00	376.55	380.20	380.65
Mech Efficiency	(%)	47.00	46.17	47.23	46.60	46.67	49.03	48.00	47.85
ITE	(%)	38.68	41.00	44.77	44.57	43.44	40.98	38.83	39.48
BTE	(%)	18.00	18.90	21.13	20.77	20.27	20.08	18.63	18.85
Volumetric Efficiency	(%)	94.38	89.57	86.33	83.30	86.40	90.23	84.00	83.18
CO	(ppm)	12357.00	6377.20	2400.80	2002.60	1671.20	2149.80	3364.20	7581.40
CO2	(ppm)	33117.60	80612.00	96099.60	91514.40	84325.20	75859.60	68027.20	61543.00
Nox	(ppm)	1607.60	1700.00	1680.20	1388.00	1121.60	1503.00	597.20	473.75
O2	(ppm)	18.93	14.15	9.63	8.80	9.37	10.20	11.60	13.05
Specific CO	(ppm/W)	3.09	1.44	0.50	0.42	0.35	0.36	0.54	1.15
Specific CO2	(ppm/W)	8.29	18.25	20.00	18.09	17.71	12.82	10.89	9.36
Specific Nox	(ppm/W)	0.40	0.38	0.35	0.27	0.24	0.15	0.10	0.07
Specific O2	(ppm/W)	0.00	0.00	0.00	0.00	0.00	0.00	0.00	0.00

Table 45: Overall Results for 45 Nm LP DME

45 Nm LP DME		45 Nm							
		1100 rpm	1200 rpm	1300 rpm	1400 rpm	1500 rpm	1600 rpm	1700 rpm	1800 rpm
Speed	(rpm)	1101.26	1202.30	1304.40	1406.40	1503.60	1605.60	1706.72	1806.82
Load	(Nm)	38.34	44.76	44.74	45.26	45.18	44.94	44.84	44.72
Brake Power	(W)	4421.68	5638.04	6112.88	6663.10	7110.72	7556.78	8013.12	8462.52
Ind. work per Cycle	(J)	495.96	544.34	542.10	531.26	540.58	541.78	529.46	519.72
Indicated Power	(W)	9102.82	10907.66	11784.68	12452.74	13546.24	14498.88	15060.62	15651.04
imep	(kPa)	745.76	818.54	815.16	798.88	812.88	814.74	796.18	781.56
bmep	(kPa)	362.26	423.10	422.82	427.46	426.68	424.64	423.60	422.58
Equivalence Ratio		0.70	0.79	0.82	0.80	0.78	0.75	0.79	0.82
Air/fuel ratio		13.52	11.79	11.37	11.59	12.08	12.65	11.78	11.34
Air Flow	(g/s)	11.34	11.73	12.18	12.62	13.83	15.65	15.50	16.24
Fuel Flow	(g/s)	0.84	0.99	1.07	1.09	1.15	1.24	1.32	1.43
Additive Flow	(g/s)	0.00	0.00	0.00	0.00	0.00	0.00	0.00	0.00
Percentage DME	(%)	0.00	0.00	0.00	0.00	0.00	0.00	0.00	0.00
Fuel Conv. Eff.	(%)	18.56	19.96	20.08	21.52	21.86	21.50	21.42	20.78
isfc	(kg/J)	0.00	0.00	0.00	0.00	0.00	0.00	0.00	0.00
bsfcf	(kg/J)	0.00	0.00	0.00	0.00	0.00	0.00	0.00	0.00
Injection	(°CA)	366.34	363.10	364.46	365.18	366.50	356.60	358.30	359.30
Ignition	(°CA)	366.90	363.46	367.58	365.42	367.40	356.60	359.45	365.50
Ignition delay	(°CA)	0.56	0.36	3.12	0.24	0.72	2.12	1.44	6.20
Patm	(kPa)	83.10	83.20	83.18	83.10	83.10	83.10	83.10	83.10
Exhaust Temperature	(°C)	458.38	461.76	481.86	506.18	529.76	560.14	579.12	585.18
Pmax	(kPa)	6081.14	6876.12	6745.26	6422.96	6310.70	5962.04	5687.62	5573.36
Position of Pmax	(°CA)	370.60	368.08	368.64	368.48	369.48	370.44	371.40	369.88
Tmax	(K)	1910.06	2133.82	2221.86	2225.98	2150.72	1939.02	2054.68	2071.28
Position of Tmax	(°CA)	379.36	377.72	379.52	380.04	381.92	385.00	386.04	385.32
Mech Efficiency	(%)	48.60	51.72	51.90	53.56	52.50	52.16	53.22	54.10
ITE	(%)	38.20	38.56	38.68	40.22	41.60	41.22	40.24	38.44
BTE	(%)	18.56	19.96	20.08	21.52	21.86	21.50	21.42	20.78
Volumetric Efficiency	(%)	92.92	87.98	84.28	80.94	82.96	87.92	81.96	81.10
CO	(ppm)	19406.75	35808.25	32186.00	26113.50	19241.20	15051.40	13859.50	13978.00
CO2	(ppm)	84741.50	64880.00	72233.20	85829.50	88802.00	87902.20	80576.00	74498.40
Nox	(ppm)	1263.25	1250.50	1186.60	1056.25	929.40	756.60	681.00	542.80
O2	(ppm)	9.30	18.33	12.00	7.73	6.78	7.43	8.85	10.15
Specific CO	(ppm/W)	4.39	6.35	5.27	3.67	2.71	1.99	1.73	1.65
Specific CO2	(ppm/W)	19.17	11.51	11.82	12.88	12.49	11.63	10.06	8.80
Specific Nox	(ppm/W)	0.29	0.22	0.19	0.16	0.13	0.10	0.09	0.06
Specific O2	(ppm/W)	0.00	0.00	0.00	0.00	0.00	0.00	0.00	0.00

F.7 High Pressure DME

The following data was taken from reference 19.

Table 46: Overall Results for 25 Nm HP DME

25 Nm HP DME		25 Nm							
		1100 rpm	1200 rpm	1300 rpm	1400 rpm	1500 rpm	1600 rpm	1700 rpm	1800 rpm
Speed	(rpm)	1105.14	1198.46	1301.46	1399.58	1499.93	1598.84	1702.80	1802.94
Load	(Nm)	25.26	24.74	25.28	25.16	25.20	25.18	24.70	24.72
Brake Power	(W)	2924.98	3107.10	3444.52	3688.42	3955.95	4213.38	4405.08	4664.08
Ind. work per Cycle	(J)	376.24	381.52	377.92	375.00	400.83	398.02	384.90	376.28
Indicated Power	(W)	6929.78	7620.30	8197.36	8747.34	10020.85	10606.06	10924.36	11306.92
imep	(kPa)	565.76	573.72	568.30	563.92	602.78	598.54	578.86	565.84
bmep	(kPa)	238.78	233.92	238.78	237.78	237.98	237.78	233.40	233.40
Equivalence Ratio	()	0.48	0.47	0.48	0.47	0.48	0.44	0.47	0.45
Air/fuel ratio	()	20.41	20.69	20.67	21.21	20.72	22.58	20.92	22.12
Air Flow	(g/s)	11.44	11.82	12.26	12.73	14.05	15.89	15.80	16.57
Fuel Flow	(g/s)	0.56	0.57	0.59	0.60	0.68	0.70	0.76	0.75
Additive Flow	(g/s)	0.00	0.00	0.00	0.00	0.00	0.00	0.00	0.00
Percentage DME	(%)	0.00	0.00	0.00	0.00	0.00	0.00	0.00	0.00
Fuel Conv. Eff.	(%)	18.34	19.10	20.42	21.62	20.55	21.06	20.50	21.88
isfc	(kg/J)	0.00	0.00	0.00	0.00	0.00	0.00	0.00	0.00
bsfcf	(kg/J)	0.00	0.00	0.00	0.00	0.00	0.00	0.00	0.00
Injection	(°CA)	351.82	334.70	353.26	354.50	355.15	355.38	354.98	356.22
Ignition	(°CA)	353.26	335.42	355.02	355.62	357.20	357.54	358.98	358.98
Ignition delay	(°CA)	1.44	0.72	1.76	1.12	2.05	2.16	4.00	2.76
Patm	(kPa)	82.90	82.90	82.90	82.90	82.80	82.80	82.80	82.80
Exhaust Temperature	(°C)	335.84	334.78	335.26	343.82	351.00	355.36	350.36	371.62
Pmax	(kPa)	6679.56	6552.60	6370.94	6082.86	6021.55	5779.12	5559.40	5407.04
Position of Pmax	(°CA)	365.96	366.92	367.28	368.36	368.90	370.00	370.60	370.72
Tmax	(K)	1748.26	1814.82	1880.08	1900.58	1886.15	1777.22	1846.40	1864.00
Position of Tmax	(°CA)	371.68	372.00	372.80	374.92	376.05	378.32	378.60	379.68
Mech Efficiency	(%)	42.24	40.94	42.04	42.18	39.50	39.74	40.48	41.28
ITE	(%)	43.46	46.92	48.60	51.22	52.00	53.00	50.88	53.08
BTE	(%)	18.34	19.10	20.42	21.62	20.55	21.06	20.50	21.88
Volumetric Efficiency	(%)	93.38	89.02	85.04	82.08	84.48	89.66	83.72	82.96
CO	(ppm)	640.20	760.50	689.50	788.50	990.20	1079.40	1136.00	1207.20
CO2	(ppm)	43314.00	71893.50	76309.00	75697.00	69309.20	60617.60	54039.50	53402.80
THC	(ppm)	137.80	143.25	147.00	164.25	199.00	218.40	238.00	247.80
NOx	(ppm)	2317.60	2088.25	1801.25	1319.00	1007.00	785.60	624.25	555.60
O2	(ppm)	9.50	10.27	10.98	12.55	14.00	15.13	15.63	15.47
Specific CO	(ppm/W)	0.22	0.24	0.20	0.21	0.25	0.26	0.26	0.26
Specific CO2	(ppm/W)	14.81	23.14	22.15	20.53	17.52	14.39	12.27	11.45
Specific THC	(ppm/W)	0.05	0.05	0.04	0.04	0.05	0.05	0.05	0.05

Table 47: Overall Results for 35 Nm HP DME

35 Nm HP DME		35 Nm							
		1100 rpm	1200 rpm	1300 rpm	1400 rpm	1500 rpm	1600 rpm	1700 rpm	1800 rpm
Speed	(rpm)	1103.18	1202.30	1299.50	1396.70	1503.60	1600.80	1701.60	1803.92
Load	(Nm)	35.68	35.04	35.32	36.98	34.88	34.84	35.13	34.84
Brake Power	(W)	4121.80	4410.12	4807.26	5409.14	5489.48	5839.78	6260.85	6580.74
Ind. work per Cycle	(J)	418.92	409.48	427.56	427.34	413.03	432.60	438.93	420.92
Indicated Power	(W)	7702.48	8205.42	9260.46	9947.72	10350.20	11541.42	12447.85	12654.48
imep	(kPa)	629.98	615.78	642.96	642.64	621.08	650.52	660.05	632.94
bmep	(kPa)	337.12	330.94	333.78	349.42	329.40	329.14	331.98	329.16
Equivalence Ratio	()	0.61	0.53	0.56	0.58	0.59	0.57	0.59	0.62
Air/fuel ratio	()	15.85	18.20	17.28	17.33	16.28	16.86	16.46	15.39
Air Flow	(g/s)	11.33	11.65	12.01	12.56	14.06	15.52	15.58	16.33
Fuel Flow	(g/s)	0.71	0.64	0.70	0.75	0.86	0.92	0.95	1.06
Additive Flow	(g/s)	0.00	0.00	0.00	0.00	0.00	0.00	0.00	0.00
Percentage DME	(%)	0.00	0.00	0.00	0.00	0.00	0.00	0.00	0.00
Fuel Conv. Eff.	(%)	20.28	24.22	24.32	25.36	22.38	22.32	23.28	21.82
isfc	(kg/J)	0.00	0.00	0.00	0.00	0.00	0.00	0.00	0.00
bsfcf	(kg/J)	0.00	0.00	0.00	0.00	0.00	0.00	0.00	0.00
Injection	(°CA)	354.26	353.82	353.58	355.50	355.85	356.74	331.25	357.14
Ignition	(°CA)	354.58	353.98	353.62	355.98	356.10	357.38	333.40	359.66
Ignition delay	(°CA)	0.32	0.16	0.04	0.48	0.25	0.64	2.15	2.52
Patm	(kPa)	83.30	83.30	83.30	83.30	83.30	83.30	83.30	83.30
Exhaust Temperature	(°C)	417.88	435.30	435.50	446.56	431.80	444.90	466.33	480.02
Pmax	(kPa)	6522.80	6430.00	6488.60	6229.82	6002.50	5911.46	5687.58	5539.34
Position of Pmax	(°CA)	367.68	367.24	366.84	368.36	369.00	370.04	370.10	370.92
Tmax	(K)	1783.12	1849.06	1967.46	1996.80	1893.40	1839.10	1883.23	1911.92
Position of Tmax	(°CA)	373.68	373.60	374.04	375.36	375.50	376.88	379.95	379.24
Mech Efficiency	(%)	53.56	53.80	51.94	54.52	53.13	50.44	50.35	52.10
ITE	(%)	37.90	45.08	46.86	46.56	42.13	44.10	46.23	41.96
BTE	(%)	20.28	24.22	24.32	25.36	22.38	22.32	23.28	21.82
Volumetric Efficiency	(%)	92.66	87.40	83.44	81.18	81.88	87.48	82.63	81.68
CO	(ppm)	3746.91	3681.97	2535.98	2074.77	965.40	871.94	880.77	930.54
CO2	(ppm)	16800.87	64891.33	83954.00	87897.00	85051.00	78213.00	72919.50	66952.20
THC	(ppm)	309.43	268.95	233.12	240.07	233.27	243.31	250.01	251.86
NOx	(ppm)	1821.31	1869.25	1776.27	1614.52	1353.85	1150.28	992.28	897.66
O2	(ppm)	10.60	6.80	7.68	8.60	10.70	11.75	12.88	13.20
Specific CO	(ppm/W)	0.91	0.83	0.53	0.36	0.18	0.15	0.14	0.14
Specific CO2	(ppm/W)	4.08	14.71	17.46	16.25	15.49	13.39	11.65	10.17
Specific THC	(ppm/W)	0.08	0.06	0.05	0.04	0.04	0.04	0.04	0.04

Table 48: Overall Results for 45 Nm HP DME

45 Nm HP DME		45 Nm							
		1100 rpm	1200 rpm	1300 rpm	1400 rpm	1500 rpm	1600 rpm	1700 rpm	1800 rpm
Speed	(rpm)	1104.14	1200.38	1299.50	1399.58	1502.62	1600.80	1705.25	1800.00
Load	(Nm)	46.56	45.12	45.22	45.24	45.32	45.02	44.38	45.38
Brake Power	(W)	5174.56	5673.36	6152.94	6626.30	7127.54	7544.00	7923.75	8553.52
Ind. work per Cycle	(J)	449.02	464.90	467.86	484.16	500.18	498.66	484.55	486.98
Indicated Power	(W)	8262.46	9301.02	10133.38	11294.40	12526.30	13304.10	13770.98	14608.60
imep	(kPa)	675.16	699.08	703.56	728.06	752.16	749.86	728.63	732.24
bmep	(kPa)	422.86	426.42	427.20	427.20	427.98	425.40	419.25	428.72
Equivalence Ratio	()	0.57	0.61	0.59	0.61	0.60	0.55	0.44	0.57
Air/fuel ratio	()	17.06	15.74	16.34	15.76	16.06	17.76	17.06	17.02
Air Flow	(g/s)	10.91	11.29	11.60	12.25	13.51	15.16	15.19	16.05
Fuel Flow	(g/s)	0.64	0.72	0.71	0.78	0.84	0.86	0.89	0.94
Additive Flow	(g/s)	0.00	0.00	0.00	0.00	0.00	0.00	0.00	0.00
Percentage DME	(%)	0.00	0.00	0.00	0.00	0.00	0.00	0.00	0.00
Fuel Conv. Eff.	(%)	28.44	27.82	30.48	29.98	29.82	31.10	31.33	31.90
isfc	(kg/J)	0.00	0.00	0.00	0.00	0.00	0.00	0.00	0.00
bsfcf	(kg/J)	0.00	0.00	0.00	0.00	0.00	0.00	0.00	0.00
Injection	(°CA)	351.58	351.78	353.90	354.54	356.86	358.30	358.35	360.62
Ignition	(°CA)	351.82	351.78	354.98	355.26	358.50	360.42	358.85	362.14
Ignition delay	(°CA)	0.24	0.00	1.08	0.72	1.64	2.12	0.50	1.52
Patm	(kPa)	83.20	83.20	83.18	83.20	83.10	83.10	83.08	83.00
Exhaust Temperature	(°C)	491.86	516.12	530.22	536.98	556.40	548.22	563.48	599.88
Pmax	(kPa)	6778.48	6773.62	6469.86	6369.30	5985.48	5710.04	5520.05	5273.44
Position of Pmax	(°CA)	366.60	366.88	367.32	367.40	369.36	370.72	370.55	371.64
Tmax	(K)	1893.48	2000.86	2078.62	2105.26	2040.92	1921.12	1993.93	1992.90
Position of Tmax	(°CA)	372.96	373.24	374.92	376.36	379.64	381.56	382.78	386.28
Mech Efficiency	(%)	62.66	61.00	60.76	58.72	56.96	56.74	57.58	58.68
ITE	(%)	45.42	45.58	50.20	51.10	52.38	54.86	54.40	54.46
BTE	(%)	28.44	27.82	30.48	29.98	29.82	31.10	31.33	31.90
Volumetric Efficiency	(%)	89.22	84.88	80.54	78.94	81.10	85.40	80.38	80.44
CO	(ppm)	3589.00	3652.75	3143.00	3041.00	2722.50	2625.33	2910.67	2998.67
CO2	(ppm)	56197.75	89831.50	100670.00	105964.67	107165.50	105393.67	100508.00	96723.33
THC	(ppm)	125.00	131.25	141.67	167.33	218.00	234.33	338.50	381.00
NOx	(ppm)	2085.50	1996.25	1910.67	1697.00	1551.50	1355.33	1217.67	1076.33
O2	(ppm)	5.10	6.00	6.80	7.80	9.00	10.20	11.00	11.30
Specific CO	(ppm/W)	0.69	0.64	0.51	0.46	0.38	0.35	0.37	0.35
Specific CO2	(ppm/W)	10.86	15.83	16.36	15.99	15.04	13.97	12.68	11.31
Specific THC	(ppm/W)	0.02	0.02	0.02	0.03	0.03	0.03	0.04	0.04

F.8 Diesel

The following data was taken from reference 19.

Table 49: Overall Results for 25 Nm diesel

25 Nm DIESEL		25 Nm							
		1100 rpm	1200 rpm	1300 rpm	1400 rpm	1500 rpm	1600 rpm	1700 rpm	1800 rpm
Speed	(rpm)	1100.30	1200.40	1305.36	1399.58	1503.60	1600.80	1701.84	1800.00
Load	(Nm)	25.14	24.62	25.04	24.68	25.02	25.18	24.94	24.80
Brake Power	(W)	2896.40	2895.10	3421.42	3620.66	3941.04	4218.50	4441.32	4677.00
Ind. work per Cycle	(J)	299.70	341.72	364.28	333.46	313.70	251.06	249.52	235.46
Indicated Power	(W)	4519.82	6836.58	7925.24	7778.08	7861.36	6698.64	7077.68	7063.80
imep	(kPa)	450.66	513.88	547.80	501.44	471.74	377.54	375.24	354.08
bmep	(kPa)	237.52	232.62	236.48	233.40	236.48	237.76	235.44	252.42
Equivalence Ratio	()	0.74	0.65	0.67	0.62	0.61	0.63	0.64	0.61
Air/fuel ratio	()	20.19	23.21	22.34	24.22	24.56	23.91	23.43	24.68
Air Flow	(g/s)	10.99	11.58	12.02	12.64	14.10	15.45	15.57	16.34
Fuel Flow	(g/s)	0.54	0.50	0.54	0.52	0.58	0.65	0.66	0.66
Additive Flow	(g/s)	0.00	0.00	0.00	0.00	0.00	0.00	0.00	0.00
Percentage DME	(%)	0.00	0.00	0.00	0.00	0.00	0.00	0.00	0.00
Fuel Conv. Eff.	(%)	12.20	14.20	14.58	15.92	15.74	14.98	15.32	16.20
isfc	(kg/J)	0.00	0.00	0.00	0.00	0.00	0.00	0.00	0.00
bsfcf	(kg/J)	0.00	0.00	0.00	0.00	0.00	0.00	0.00	0.00
Injection	(°CA)	350.82	346.46	346.50	346.82	347.10	346.46	347.38	347.78
Ignition	(°CA)	352.78	351.86	353.54	353.50	353.42	351.74	352.98	353.38
Ignition delay	(°CA)	1.96	5.40	7.04	6.68	6.32	5.28	5.60	5.60
Patm	(kPa)	82.58	82.56	82.60	83.10	83.10	83.00	83.00	83.00
Exhaust Temperature	(°C)	368.74	393.54	415.66	421.72	432.32	438.66	452.62	468.36
Pmax	(kPa)	7242.72	7020.08	6950.74	7205.16	7526.46	7660.18	8044.94	7925.78
Position of Pmax	(°CA)	363.92	364.96	365.32	364.32	364.68	363.64	364.84	364.96
Tmax	(K)	1904.10	1935.60	2029.36	2108.00	2119.66	2052.90	2295.24	2303.88
Position of Tmax	(°CA)	366.64	368.00	368.84	367.64	367.80	366.56	367.20	368.12
Mech Efficiency	(%)	52.90	45.30	43.20	46.60	50.22	63.22	63.30	66.66
ITE	(%)	23.12	31.40	33.78	34.22	31.42	23.76	24.42	24.44
BTE	(%)	12.20	14.20	14.58	15.90	15.74	14.98	15.32	16.20
Volumetric Efficiency	(%)	90.14	87.06	83.08	81.46	84.62	87.08	82.58	81.90
CO	(ppm)	60370.00	39445.33	30686.00	30878.25	29565.50	25440.33	20339.00	25440.33
CO2	(ppm)	35000.00	60000.00	66000.00	65000.00	65000.00	62000.00	52500.00	53500.00
THC	(ppm)	2853.00	2930.00	2403.00	2499.00	2428.00	2501.75	1977.00	1511.50
NOx	(ppm)	608.25	818.25	960.00	884.75	755.50	676.00	658.00	693.50
O2	(ppm)	5.13	6.00	6.80	7.80	9.00	10.15	11.00	11.30
Specific CO	(ppm/W)	21.77	12.40	8.93	8.53	7.50	6.94	5.73	4.35
Specific CO2	(ppm/W)	12.00	19.00	19.50	18.00	16.50	14.80	12.00	11.80
Specific THC	(ppm/W)	1.03	0.92	0.70	0.69	0.62	0.59	0.45	0.32

Table 50: Overall Results for 35 Nm diesel

35 Nm DIESEL		35 Nm							
		1100 rpm	1200 rpm	1300 rpm	1400 rpm	1500 rpm	1600 rpm	1700 rpm	1800 rpm
Speed	(rpm)	1104.14	1201.34	1304.40	1401.50	1497.74	1600.80	1698.96	1800.00
Load	(Nm)	34.86	34.82	34.75	35.00	34.58	35.23	34.78	35.06
Brake Power	(W)	4031.00	4379.24	4748.20	5131.95	5421.34	5906.95	6188.26	6607.54
Ind. work per Cycle	(J)	366.56	356.20	426.80	420.03	396.92	507.40	494.96	494.46
Indicated Power	(W)	6745.20	7132.10	9278.70	9811.40	10057.90	13538.03	14014.84	14833.14
imep	(kPa)	551.20	535.66	641.83	631.63	605.90	763.03	744.30	743.52
bmep	(kPa)	329.42	328.88	328.43	330.38	326.58	332.90	328.62	331.20
Equivalence Ratio	()	0.95	0.86	0.80	0.82	0.82	0.77	0.75	0.74
Air/fuel ratio	()	15.74	17.45	18.86	18.41	18.27	19.34	20.00	20.13
Air Flow	(g/s)	11.29	11.64	12.26	12.56	13.72	15.66	15.64	16.40
Fuel Flow	(g/s)	0.72	0.67	0.65	0.68	0.75	0.81	0.78	0.81
Additive Flow	(g/s)	0.00	0.00	0.00	0.00	0.00	0.00	0.00	0.00
Percentage DME	(%)	0.00	0.00	0.00	0.00	0.00	0.00	0.00	0.00
Fuel Conv. Eff.	(%)	12.88	14.98	16.73	17.25	16.56	16.70	18.14	18.60
isfc	(kg/J)	0.00	0.00	0.00	0.00	0.00	0.00	0.00	0.00
bsfcf	(kg/J)	0.00	0.00	0.00	0.00	0.00	0.00	0.00	0.00
Injection	(°CA)	351.14	340.98	345.35	347.15	348.02	346.10	346.42	347.50
Ignition	(°CA)	351.18	341.68	352.40	353.70	352.66	353.30	352.38	355.46
Ignition delay	(°CA)	0.04	0.76	7.00	6.55	4.64	7.23	5.96	7.96
Patm	(kPa)	82.60	82.60	82.60	82.60	82.60	83.00	83.00	83.04
Exhaust Temperature	(°C)	385.76	402.68	413.75	435.90	455.22	460.30	478.14	496.56
Pmax	(kPa)	7383.42	7495.72	7161.43	7141.85	7353.10	7327.90	7228.54	7132.88
Position of Pmax	(°CA)	363.76	363.24	365.30	365.70	365.00	366.65	366.38	367.04
Tmax	(K)	1876.26	1996.66	2058.63	2150.40	2151.60	2091.68	2184.80	2221.80
Position of Tmax	(°CA)	368.40	366.96	370.55	370.60	369.92	374.75	374.44	374.88
Mech Efficiency	(%)	59.82	61.54	51.23	52.38	53.94	43.68	44.00	44.62
ITE	(%)	19.74	24.48	32.75	32.95	30.70	38.35	41.14	41.74
BTE	(%)	12.88	14.98	16.73	17.25	16.56	16.70	18.14	18.60
Volumetric Efficiency	(%)	92.26	87.40	84.78	80.85	82.68	88.28	83.08	82.24
CO	(ppm)	20339.00	63652.00	49088.00	39218.75	34576.25	30395.70	27097.33	20336.96
CO2	(ppm)	8389.70	35578.40	49112.00	61251.50	64077.00	63903.00	62066.00	57929.60
THC	(ppm)	8170.13	6235.01	4611.75	3310.46	2734.72	2414.52	2113.17	1776.13
NOx	(ppm)	993.17	962.43	1036.07	1031.73	962.60	818.84	761.36	690.27
O2	(ppm)	6.05	5.23	6.33	7.75	9.05	10.23	10.83	11.08
Specific CO	(ppm/W)	19.94	14.40	10.13	7.64	6.27	5.16	4.84	3.09
Specific CO2	(ppm/W)	2.05	8.05	10.13	11.92	11.61	10.85	10.04	8.79
Specific THC	(ppm/W)	1.99	1.41	0.95	0.64	0.50	0.41	0.34	0.27

Table 51: Overall Results for 45 Nm diesel

45 Nm DIESEL		45 Nm							
		1100 rpm	1200 rpm	1300 rpm	1400 rpm	1500 rpm	1600 rpm	1700 rpm	1800 rpm
Speed	(rpm)	1104.14	1202.30	1299.50	1400.58	1503.60	1602.72	1702.80	1800.98
Load	(Nm)	46.22	45.64	44.48	45.40	44.74	44.80	45.24	44.70
Brake Power	(W)	5344.16	5744.12	6056.82	6659.42	7042.28	7520.32	8067.46	8430.12
Ind. work per Cycle	(J)	447.26	426.78	469.02	472.16	431.74	421.94	409.46	345.66
Indicated Power	(W)	8231.26	8552.42	10158.06	11021.18	10819.58	11271.56	11620.06	10374.80
imep	(kPa)	672.58	641.82	705.30	710.00	649.24	634.52	615.70	519.76
bmep	(kPa)	436.68	431.04	420.52	428.98	422.58	423.34	427.46	422.32
Equivalence Ratio	()	0.97	1.06	0.89	0.95	0.89	0.85	0.95	0.97
Air/fuel ratio	()	15.43	14.12	16.77	15.82	16.77	17.63	15.70	15.40
Air Flow	(g/s)	11.15	11.43	11.91	12.43	13.57	15.16	15.06	15.99
Fuel Flow	(g/s)	0.72	0.81	0.71	0.79	0.81	0.86	0.96	1.04
Additive Flow	(g/s)	0.00	0.00	0.00	0.00	0.00	0.00	0.00	0.00
Percentage DME	(%)	0.00	0.00	0.00	0.00	0.00	0.00	0.00	0.00
Fuel Conv. Eff.	(%)	16.96	16.26	19.58	19.44	19.96	20.04	19.28	18.60
isfc	(kg/J)	0.00	0.00	0.00	0.00	0.00	0.00	0.00	0.00
bsfcf	(kg/J)	0.00	0.00	0.00	0.00	0.00	0.00	0.00	0.00
Injection	(°CA)	351.18	351.78	345.50	347.86	345.94	346.18	346.50	346.94
Ignition	(°CA)	351.26	351.82	352.58	352.62	352.54	352.46	352.34	353.78
Ignition delay	(°CA)	0.08	0.04	7.08	4.76	6.60	6.28	5.84	6.84
Patm	(kPa)	83.20	83.20	83.14	83.10	83.10	83.10	83.10	83.10
Exhaust Temperature	(°C)	445.28	467.06	476.06	472.74	486.10	491.10	515.70	501.30
Pmax	(kPa)	7616.36	7400.54	7473.78	7459.12	7162.24	7282.36	7443.44	8097.72
Position of Pmax	(°CA)	364.16	364.20	364.80	365.40	365.60	364.52	364.64	363.60
Tmax	(K)	2000.12	2061.42	2205.44	2276.06	2151.86	2068.06	2215.38	2356.98
Position of Tmax	(°CA)	371.00	369.88	371.64	372.16	372.56	372.12	372.20	366.52
Mech Efficiency	(%)	64.98	67.28	59.68	60.46	65.08	66.74	69.54	81.52
ITE	(%)	26.12	24.28	32.84	32.18	30.66	30.06	27.80	22.88
BTE	(%)	16.96	16.26	19.58	19.44	19.96	20.04	19.28	18.60
Volumetric Efficiency	(%)	91.06	85.78	82.70	80.10	81.38	85.34	79.78	80.14
CO	(ppm)	73653.40	58126.40	45780.40	37172.25	31215.80	28415.60	26207.20	28342.20
CO2	(ppm)	8389.70	35578.40	49112.00	61251.50	64077.00	63903.00	62066.00	43156.80
THC	(ppm)	5999.60	5296.75	4100.33	3956.75	2941.80	2659.80	2742.60	3712.00
NOx	(ppm)	1005.50	1251.00	1569.80	1497.25	1665.00	1658.80	1604.80	1476.20
O2	(ppm)	3.03	3.55	5.60	6.93	7.98	8.17	9.40	10.25
Specific CO	(ppm/W)	13.78	10.12	7.56	5.58	4.43	3.78	3.25	3.36
Specific CO2	(ppm/W)	1.57	6.19	8.11	9.20	9.10	8.50	7.69	5.12
Specific THC	(ppm/W)	1.12	0.92	0.68	0.59	0.42	0.35	0.34	0.44